Chapter 11
Biomaterial–Cell Tissue Interactions in Surface Engineered Carbon-Based Biomedical Implants and Devices

N. Ali, Y. Kousa, J. Gracio, G. Cabral, A. Sousa, T. Shokufar, E. Titus, J.C. Madaleno, W. Ahmed and M.J. Jackson

Abstract Implantable prosthesis and medical devices are subjected to several interacting forces whenever they come in contact with the physiologic systems (blood, immune, musculoskeletal, nervous, digestive, respiratory, reproductive and urinary) and organs of the human body. These interactions include the effects of core body temperature (and/or variable temperatures in the oral cavity), the body physiologic fluids containing several ions and biomolecules, proteins and cells of various progeny and functions. This chapter focuses on cell tissue–implant interactions and how carbon-based implants are being developed for next-generation implantable devices.

11.1 Introduction to Surface Engineered Carbon-Based Materials

Pathological diseases of the arteries and the heart that cause life-threatening blood flow restrictions, for example can be treated either by open heart surgery intervention, by implantation of intracoronary stents and/or by use of artificial devices like artificial heart valves in heart valve pathologies. However, in spite of considerable advances in improving the mechanical properties of stents, advances in

N. Ali · Y. Kousa · J. Gracio · G. Cabral · A. Sousa · T. Shokufar · E. Titus · J.C. Madaleno
University of Aveiro, Aveiro, Portugal

W. Ahmed
School of Medicine, University of Central Lancashire, Preston, UK

M.J. Jackson (✉)
Kansas State University, Salina, KS, USA
e-mail: jacksonmj04@yahoo.com

W. Ahmed and M.J. Jackson (eds.), *Surgical Tools and Medical Devices*,
DOI 10.1007/978-3-319-33489-9_11

implants techniques, and advances in antithrombosis therapy, the use of stents and heart valves are still complicated by substantial cases of thrombotic occlusions/stenosis and restenosis [1–4] due to platelet activation resulting from the release of metallic particles/ions (in metallic stents), shear forces and blood contacting of the metallic surface [5–8]. Likewise, thromboembolism (valve thrombosis and systemic embolism) remains as the major draw back in the management of implanted mechanical heart valve prostheses [9, 10]. Patients with these implanted prostheses are faced with life-threatening bleeding problems because they are kept under life-long anticoagulant therapies in order to reduce the risk of thromboembolism. Platelet aggregation in these prostheses is the key factor in thrombus formation and dissemination as emboli which can be life threatening, if not promptly managed. In order to reduce the risk of platelet aggregation/thromboembolism and complications following the life-long course(s) of anticoagulants, the biomaterials need to be improved in order to achieve better biocompatibility/hemocompatibility [11–13].

Apart from thrombosis, other problems associated with the failure of medical implants and devices that need to be overcome are problems of mechanical failure, wear, tear and/or fatigue; the problem of chemical degradation, corrosion and oxidative degeneration; the problem of calcification and the problem of excessive immune response and/or infection as triggered by these biomaterial implants. Metallic implants may have good fatigue life and may be cheap (stainless steel for example) but they can release metallic ions and wear debris into the surrounding tissues leading to osteolysis, loosening and/or failure of the implants. All these problems encountered with implanted prostheses and medical devices could be solved with carbon thin film surface coating modifications using appropriate, durable and biocompatible biomaterial.

The passive nature of carbon in tissues has been known since ancient times. Charcoal and lampblack were used for ornamental and official tattoos by many. Other forms of carbon have been studied for possible use for biomedical applications stimulated primarily by Gott's original studies [14]: artificial graphite, vitreous or glassy carbons, carbon fibres, pyrolytic carbons, composites, and vacuum vapour-deposited carbon coatings [15]. The fundamental nature of these carbon materials and their interactions with the living tissues needs to be explored therefore. Likewise, pyrolytic carbon-coated heart valve leaflets have been successfully applied as artificial clinical heart valves [16]. Pyrolytic carbon has the major advantage of being resistant to thrombus formation, which was the biggest limitation to the earlier generation of stainless steel artificial heart valves. There was always a need to use anticoagulant drugs by patients who had the earlier stainless steel heart valves to prevent clot formation on the stainless steel, but this had the potential to suppress the beneficial effect of the natural blood clotting mechanism in patients. Pyrolytic carbon is an artificial material made of carbon microcrystals with a high-density turbostatic structure, originally engineered for use in nuclear reactors and may not be readily available for large-scale use. When pyrolytic carbon is alloyed with silicon, it shows excellent thromboresistance [16]. Pyrolytic carbon

has also been used as a coating on different types of implant prostheses, such as dental implants, percutaneous devices and tendon tracheal replacements. This chapter tends to report the state of the art in the potential of a more readily available synthetic carbon-based thin film coatings (DLC and its doped hybrids) for thromboresistant applications and various biomedical applications as stated below.

Surface coating modification is essential because it is now known that the outermost layer of a biomaterial (few nanometre scale range) is most crucial in its interfacial interaction in vivo. Baier et al. [17] have shown that exposure of an organic-free surface to fresh flowing blood for as little as 5 s leads to its complete coating by a very uniform, tenaciously adherent proteinaceous thin film. The biomaterial's outer surface dictates the configuration of this attached protein film that in turn plays an important role in determining the fate of the biomaterial in the host via a series of cascade interactions. Thus intensive research has been focused on DLC over the last few decades due to the ability of forming ultrathin films of DLC and due to the promising characteristics of DLC-like attractive tribological, electrical, chemical and optical properties. The issue of biocompatibility and hemocompatibility of DLC when used as implants and medical devices will no doubt be expected to stem from possibly favourable tissue–biomaterial surface and interactions. Generally, two main pathways could be feasible, in an effort to create a biocompatible material: creating a material with surfaces that are bioactive (like the host tissue) that can actively support the body's control mechanisms; and/or creating materials that are 'inert or passive' to the body's control mechanism in order to avoid triggering an adverse reaction (though there being nothing exactly like absolute inertness in a hostile physiological environment [18]). Moreover, it is impossible to exaggerate though, that among a large number of events occurring during the process of blood coagulation (including perhaps thrombus formation and possible thromboembolism) and decoagulation, the physicochemical adsorption is virtually the main reaction that can be readily regulated unless a bioactive material is used [19]. Thus the present chapter reports on researches into the use of DLC thin films (and its doped hybrids) as an approach to modify the physicochemical properties of biomaterials and to create a material that may be 'passive' and/or 'bioactive' in the tissue.

The endothelial lining has been reported to be the best non-thrombogenic surface [20, 21]. According to Herring et al. [22, 23] various methods including improvement of physicochemical properties, pretreatment with proteins and incorporation of negative charges have been proposed in order to reduce the surface thrombogenicity of vascular prostheses. Pesakova et al. [24, 25] have also stated that the biocompatibility of materials can be influenced by factors such as surface charge, hydrophobicity and topography. It has been reported by Ahluwalia et al. [26, 27] based on surface potential measurements using the vibrating Kelvin probe method, that positively charged surfaces enhance cell adhesion in comparison to neutral or negatively charged surfaces. The hydrophyllic or hydrophobic nature of a surface has also been associated with extent of cell interactions with the surface [26, 28]. Altankov and Groth [28] have reported that wettable (hydrophilic)

surfaces tend to be more conducive for cell adhesion. Grinnell [29] also reported observing cell adhesion to occur preferentially to water wettable surfaces. Van Wachem et al. [30, 31] carried out investigation of in vitro interaction of human endothelial cells (HEC) with polymers of different wettabilities in culture, and reported observing optimal adhesion of cells with moderately wettable polymers. The biocompatibility and hemocompatibility of Diamond-Like Carbon (DLC) films has been investigated in the literature [32–40]. Jones et al. [33] deposited DLC coatings prepared by PECVD on titanium substrates and tested them for hemocompatibility, thrombogenicity and interactions with rabbit blood platelets, and reported that the DLC coatings produced no haemolytic effect, platelet activation or tendency towards thrombus formation and that platelet spreading correlated with the surface energy of the coatings. Cytotoxicity tests have also been carried out on DLC coatings by [41–43] amongst others, and they all reported observing no negative effects by DLC coatings on the viability of cells which showed normal metabolic activities like cell adhesion and spreading. Mouse fibroblasts grown on DLC coatings for 7 days showed no significant release of lactate dehydrogenase [44], an enzyme that catalyses lactate oxidation, often released into the blood when tissue is damaged, compared to control cells, indicating no loss of cell integrity. It has also been reported by Allen et al. [45, 46] that mouse macrophages, human fibroblasts and human osteoblast-like cells grown on DLC coatings on various substrates exhibited normal cellular growth and morphology, with no in vitro cytotoxicity.

Szent-Gyorgyi [47, 48] suggested that proteins may have an electronic structure similar to that of semiconductors. Eley et al. [49] reported semiconductivity in certain proteins. This was later corroborated by works from others like that of Postow and Rosenberg [50]. Bruck in 1973 suggested that intrinsic semiconduction and electronic conduction may be involved in blood compatibility of polymeric systems [51–54], instead of mere ionic interaction, after the compatibility of the blood with surfaces has been associated chiefly with ionic charges, based on the observation that endothelial wall, platelets, and plasma proteins carry net ionic charges in normal physiologic conditions. Bruck [51, 52] observed clotting times six to nine times longer than those observed with non-conducting polymers and also observed little or no platelet aggregation in electroconducting polymers, when compared to non-conducting control samples based on his study with pyrolytic polymers. Bruck concluded that ‘it is possible that electroconduction and semi-conduction is involved in the interaction of surfaces with plasma proteins in the activation of the Hageman factor and the platelets by an unknown mechanism’ [53].

Since changes in surface energy [27], surface charge conditions [26] and electronic conduction [52] have all been suggested to have an effect on the biocompatibility and hemocompatibility of materials, the present investigation is directed to understanding the effect of the above-identified factors in DLC biomaterials on especially the human microvascular endothelial cell compatibility, the platelet interaction (thrombus formation) and the cytotoxicity of various cell lines

(eg. retinal pericytes, V79, L132, etc). These factors were changed by modifying the DLC films by doping with Si, N, for example which is known to alter the surface energy, surface charge condition and electronic conduction in DLC films. This investigation has the final aim of assisting with furthering the understanding of the underlying physics of material interactions in a biological environment, and the potential to develop Si-DLC as a more readily available alternative to pyrolytic carbon and to discover and exploit the fundamental role of the electrical property and the surface energy of DLC biomaterial, so as to use it as a key to turn the potential biocompatibility and hemocompatibility of DLC into any desirable (particular) biomedical application. Surface topography is another important factor in biomaterial–cell tissue interaction. Surface engineered and patterned surfaces are now commonly created and used model for studying biomaterials–cell tissue interaction. This philosophy is based on the spatial distribution/extension of cellular appendages (cell spreading) and cell–cell/cell–material interactions based on this communication channels as one of the cell signalling modalities. Cell–cell interactions and cell–material interactions are thought to be physicochemical and electrochemical.

The physicochemical surface properties of the outermost interface of bacteria, for example and other particles as well as phagocytic cells, can essentially be of only two kinds: (a) interfacial tension and (b) electrical surface potential [55]. When a foreign surface, solid, liquid or gas, is brought into contact with the body tissue fluid/protein solution, a certain amount of the dissolved protein will be adsorbed to the surface. This process is consistent with the Gibbs theory of surface energy and may be described by the adsorption isotherm of Freudlich or Langmuir. The amount of protein adsorbed and the characteristics of the protein monolayer depend mainly on the nature of the foreign surface and the structure and the concentration of the proteins in solution [56]. The protein needs to first approach a distance to the foreign surface that will allow interaction between the molecular forces associated with the foreign surface and the protein—this is governed by diffusion. Then the characteristics of the foreign surface determine the nature of bonds or the type of changes that takes place in the configuration of the protein and the biologic molecule present.

In this chapter the biocompatibility and hemocompatibility of carbon-based thin film materials is reviewed and categorised based on certain models already existing as well as models being proposed by the author, under specific interaction with various proteins and cells due to possible differences in particular cell behaviour, and also taking into consideration whether the cells used for the test is human or animal cells and if the test is in vitro, ex vivo and or in vivo. These tests can equally be categorised under direct cell–biomaterial interactions to estimate the number of cells adherent (cell adhesion and/or cell aggregation for platelets), cell characteristics on the surfaces (cell spreading for example) and assays to determine the level of enzymes from the intracellular compartment. It is to be noted that some cells that actually exist in the blood when used for toxicity test or examined for cellular proliferation on the biomaterial are actually a test of biocompatibility rather than

hemocompatibility, although almost all hemocompatibility tests may equally be used to assess degree of biocompatibility, biocompatibility tests may not be used to assess hemocompatibility.

11.2 Potential Biomedical Applications of DLC

Very well adherent and appropriate DLC coating could be chemically inert and impermeable to liquids. They could therefore protect biological implants against corrosion as well as serve as diffusion barriers. DLC films are considered for use as coatings of metallic as well as polymeric biocomponents to improve their compatibility with body fluids [57–59]. The potential biomedical applications of DLC and modified DLC include protection of surgical prostheses of various kinds: intracoronary stents [60, 61]; prosthetic heart valves [9, 10, 42, 62, 63]. The new prosthetic heart valve designed by FII Company and Pr. Baudet is composed of a Ti6Al4V titanium alloy coated with DLC [42]. When artificial heart organ polymers used for making heart organs are compared to DLC-coated polymers, these polymers seem to show higher complement activation compared to DLC counterpart (Polycarbonate substrates coated with DLC, PC-DLC compared with Tecoflex, polyurethane) [64]. DLC and modified DLC can be used in blood contacting devices, e.g. rotary blood pump [65]. DLC is now being investigated for anti-Prion protective coating on surgical instruments and as well as anti-MRSA bug in hospital utensils where appropriate due to its known hydrophobic and low surface energy properties.

DLC is equally being investigated as a template/model surface for DNA writing and immobilisation for biochemical sensor applications. Specific biomolecules could be easily immobilised on the DLC. Surface immobilisation of DNA was reported to have several advantages: (1) Minimising the amount of DNA needed to achieve a desired effect and enhancing effective concentration vector; (2) Preventing DNA/vector aggregation; (3) reducing toxicity and degradation of delivered particles and (4) Delivering DNA to specific cellular sites [66]. DLC-Ag-Pt nanocomposites were reported to exhibit significant antimicrobial efficacy against staphylococcus bacteria, and to exhibit low corrosion rates at the open-circuit potentials in a PBS electrolyte [67].

In orthopaedics DLC can be used for coating orthopaedic pins [57] and coating of hip implants (e.g. femoral heads) [68–70]. DLC can reduce the wear of the polyethylene cup by a factor of 10–600 when used on metal implants to form a DLC-on-DLC sliding surface. The wear (and the amount of particles causing a foreign body reaction) is 10^5–10^6 lower compared to metal on metal pairs. The corrosion of a DLC-coated metal implant can be 100000 times lower than in an uncoated one. DLC can diminish the bone cement wear by a factor of 500, which can improve the bone cement to implant bonding [69–71].

In urological dialysis (hemodialysis), DLC-coated microporous polycarbonate and DLC-coated dialysis membranes show that DLC imparted an enhanced enzyme electrode performance [72, 73]. DLC has also been reported to do well in both

organ [74] and cell culture [75] when compared to the materials conventionally used for this purpose. DLC can be used as active barrier against attack by microorganisms and against biodeterioration of advanced technological devices operating in closed spaces of satellites, aircrafts and submarines, for examples [76] and as good protectors against environmental pollutants and atmospheric wastes [77]. In addition nanocrystallite copper-modified DLC has been reported to have a fungicidal effect [78].

11.3 Definitions and General Aspects of Biocompatibility

Biocompatibility can be defined as 'the ability of a material to perform with an appropriate host response in a specific application' [18]. Four components of biocompatibility have been identified:

1. The initial events that take place at the interface, mainly including the adsorption of constituents of tissue fluids onto the material surface [79];
2. Changes in the material as a result of its presence in the tissues, usually described under the headings of corrosion or degradation [80];
3. The effects that the material has on the tissue, the local host response [81];
4. The sequelae of the interfacial reaction that are seen systematically or at some remote sites [82].

Possible tests useful for evaluation of biocompatibility are listed below:

Level I:

- Initial Screening and Quality Control of Polymers
- Agar overlay response of materials
- Agar overlay response of materials extracts
- Inhibition of cell growth by water extracts of materials
- Intradermal irritation test for materials extract and leachable components.

Level II:

- Initial Evaluation of Novel Biomaterial
- Tissue culture test on materials
- Tissue culture test on materials extracts
- Cell growth in contact with test materials
- Hemolytic activity test
- Intramuscular implantation of material
- Test of osmotic fragility of erythrocytes
- In vitro mutagenicity test
- Test of material extracts by perfusion of isolated rabbit heart.

11.3.1 Specie Differences

1. The dog model is relatively inexpensive and convenient, but may lack relevance to humans;
2. The baboon model is relatively expensive and unavailable, but is relevant to humans and
3. Similarity of platelet function, the concentration and activity of clotting factors, and the hematocrit should be the primary determinants for deciding which species are most relevant to humans.

11.3.2 Cell Specificity

It is important to note that different cells perform different functions and thus their interactions with same biomaterial may differ. Specific biomaterial–cellular interaction can be compared with that of another cell line if the cell type, origin and function are very similar.

11.4 Blood

The blood is a fluid connective tissue with a matrix called plasma. The plasma proteins are in solution unlike the other connective tissues that occur in insoluble forms like fibres, thus the proteins in solution in the plasma make the plasma slightly denser than water. The blood is composed of plasma (46–63 %) and formed elements (37–54 %). The plasma is composed of water (92 %), plasma proteins (7 %) and other solutes (1 %). The formed elements of blood are composed of red blood cells 99.9 %, and the remaining 0.1 % platelets and white blood cells. The water 'dissolves' and transports organic and inorganic molecules, formed elements and heat from one part of the body to the other. The plasma proteins are composed of albumins (60 %), globulins (35 %, transports ions, hormones, lipids; immune function), fibrinogen (4 %) and regulatory proteins (<1 %: enzymes, proenzymes, hormones). Other solutes of blood are composed of electrolytes (major ones are Na^+, K^+, Ca^{2+}, Mg^{2+}, Cl^-, HCO_3^-, HPO_4^{2-}, SO_4^{2-}), organic nutrients (lipids: fatty acids, cholesterol, glycerides; carbohydrates mainly glucose; and amino acids) and organic wastes (eg., urea, uric acid, creatinine, bilirubin, ammonium ions). Albumin is the major contributor to osmotic pressure of plasma and transport lipids and steroid hormones. Fibrinogen is an essential component of blood clotting system that can be converted to insoluble fibrin [83].

11.4.1 Definitions and General Aspects of Hemocompatibility

The European Society for Biomaterials Consensus Conference following the considerations of the Macromolecule Division of the International Union of Pure and Applied Chemistry (IUPAC) thought that definition of blood compatibility should take into account the following [81]:

- The activation of the blood coagulation system at the blood–material interface;
- The response of the immune system induced after the blood–material contact;
- Other tissue responses which appear as consequences of the blood–material contact.

At the conference they proposed to define four properties characteristic of the biomaterial's blood compatibility:

- Thrombogenicity
- Antithrombogenicity
- Complement activation ability
- Complement inhibition ability.

The understanding of the process of coagulation occurring during injury to the blood vessel wall like a cut may give some background idea of the events that may apply to the blood–material interaction. The process of haemostasis, the cessation of bleeding and establishment of a framework for tissue repair consists of three phases: the vascular phase, the platelet phase and the coagulation phase, all of which occurring in a chain reaction. The vascular and platelet phases occur within a few seconds after the injury, but the coagulation phase does not start until 30 s or more after the vessel wall has been damaged. When the blood vessel wall is cut in an injury, for example contraction of the vessel's smooth muscle is triggered locally (vascular spasm) and this decreases the diameter of the vessel wall. This vascular spasm and constriction helps to stop the loss of blood and lasts for about 30 min—a period known as the vascular phase. During this phase also changes occur in the local vessel endothelium: the endothelial cells contract and expose the underlying basement membrane to the blood stream; the endothelial cells begin releasing chemical factors and local hormones (e.g. ADP, tissue factor, prostacyclin, endothelins); and then the endothelial cell membranes become 'sticky'. Platelets now begin to attach to the sticky endothelial surfaces, to the basement membrane, and to the exposed collagen fibres. This attachment marks the start of the platelet phase of the haemostasis—platelet adhesion, activation, platelet aggregation and the formation of a platelet plug. Platelet aggregation begins within 15 s after an injury occurs. As the platelets arrive at the injury site, they become activated, change shape, become spherical and develop cytoplasmic processes that extend towards adjacent platelets. The platelets begin releasing ADP (stimulates platelet

aggregation and further secretion from the platelets), thromboxane A2 and serotonin which stimulate vascular spasm, clotting factors, PDGF (platelet-derived growth factor, a peptide that promotes vessel repair) and calcium ions (required for platelet aggregation and by several steps in clotting process). The platelet phase proceeds rapidly, because the ADP, thromboxane and calcium ions that each arriving platelet releases stimulate further platelet aggregation. Finally, the blood coagulation occurring during the coagulation phase involves a complex sequence of steps that leads to the conversion of circulating fibrinogen into the insoluble protein fibrin which forms a growing network that covers the surface of the platelet plug [83]. Listed below are various hypotheses proposed for blood–biomaterial interactions by several authors.

The interfacial blood–biomaterial interactions: some 'conventional wisdom' and some 'unresolved hypotheses' **are** adapted partly from [84–86]:

11.4.2 General Hypothesis

The overall process of in vivo thrombogenesis, thromboembolization and subsequent endothelialisation on a foreign surface is dominated by surface properties rather than hemodynamics (or by hemodynamics rather than by surface properties).

11.4.3 Material

1. A material with a critical surface tension of about 25 dyn/cm will have a low thrombogenic potential.
2. A small negative surface charge lowers material thrombogenicity.
3. High water content materials have a low thrombogenic potential due to the lowered free energy of the hydrated interface.
4. High water content materials may continually expose a fresh foreign interface, leading to a high thrombogenic potential; however, they also tend to exhibit low thromboadherance due to their low interfacial free energy.
5. H-bonding group in a surface lead to strong interactions with biological species and therefore endow a surface with a high thrombogenic potential.
6. A surface with a high apolar/polar ratio is desirable for low thrombogenic potential.
7. Thrombus is nucleated in regions of the surface where a specific spatial distribution of specific chemical (electrostatic) groups is present.
8. Flexible (as opposed to stiff) polymer chain ends and loops in the material interface lower the thrombogenic potential of the foreign surface.

11.4.4 Material and Hemodynamics

1. Thrombi will always be generated at surface imperfections due to flow disturbances, surface compositional differences and/or trapped gas bubbles.
2. Smooth surfaces in arterial flow conditions may release thromboemboli before they grow too large to be dangerous (corollary: high shear rates can detach thromboemboli before they have grown too large).
3. Certain rough and textured surfaces may form and retain fibrin, thrombus, leading to a 'passivated' surface.

11.4.5 Hemodynamics

1. Thrombi will always be generated in regions of low flow or flow separation.
2. Low shear rates can lead to regional accumulation of activated protein coagulation factors and subsequent thrombogenesis on a nearby surface.
3. High shear rates can be destructive to blood cells (e.g. shear rates can initiate platelet activation and lead to thrombogenesis).
4. In a tubular flow field, the platelets tend to accumulate preferentially near the wall and the red cells near the central core (Corollary: the red cells enhance the rate of collision of platelets with the wall).

11.4.6 Erythrocytes and Leucocytes

1. The role of leucocytes in thrombogenesis may be related to their ability to recognise a particular biomaterial surface as 'foreign' after certain proteins and/or platelets have adhered to that surface.
2. Red blood cells may play only a minor role in the thrombogenic process.

11.4.7 Blood Cells and Protein Surface Tensions

Surface tensions of cells and proteins can be measured by a variety of techniques.

Surface tension of cells and proteins are relatively high, they tend to be hydrophilic in their natural state [87].

11.4.8 Heparinised Surfaces and Drugs

1. The natural endothelium is non-thrombogenic because endothelial cells produce the powerful antiplatelet aggregation agent prostacyclin (PGI_2).
2. There may be synergistic interaction between specific drug therapies and specific biomaterials such that reduced drug regimens may be indicated in combination with the use of specific biomaterials in devices or implants.
3. Heparinised surfaces must leach heparin to be non-thrombogenic. (General corollary: 'immobilised' antithrombogenic drugs are ineffective unless they leach into the flowing blood.)
4. Heparinised surfaces that bind antithrombin III do not need to leach heparin to be non-thrombogenic.

11.4.9 Calcification

1. Calcification may be initiated at points of high mechanical strain in a foreign material (such as blood pump diaphragm).
2. Calcification in foreign materials is a biological process; γ-carboxy glutamic acid is a necessary amino acid in one key protein involved in this process.

11.4.10 Surface Charges

1. Under normal conditions, the blood vessel wall and blood cells are negatively charged (potentials across the blood vessel wall were measured using Ag–AgCl reference electrodes: under normal conditions the inner electrode was negative with respect to the outer electrode) [88].
2. Injury to the blood vessel wall reduces the magnitude of the negative charge density and very often even causes a reversal in the sign of the surface charge (injury is generally accompanied by thrombus formation) [89].
3. 3. A decrease in pH reduces the negative charge density of the blood vessel wall and of blood cells. The isoelectric point occurs at pH $\sim$4.7 (The pH of the electrolyte has a significant effect on the surface charge of the blood vessel walls. At pH $\sim$4.7 the blood vessel wall has zero surface charge and below this pH the blood vessel wall is positively charged) [90].
4. Antithrombogenic drugs increase the magnitude of the negative charge density, whereas thrombogenic drugs have the opposite effect and in many cases even reverse its signs (electrophoresis measurements conducted on RBC and WBC in

the presence and absence of antithrombogenic and coagulant drugs show similar actions of these drugs on both blood cells and blood vessel wall) [91].

5. Positively charged prosthetic materials are thrombogenic whereas negatively charged surfaces tend to be non-thrombogenic—the higher and the more uniform the negative charge density, the better is the chance of the material being non-thrombogenic (tubes of various metals were implanted in the canine thoracic aorta or the canine thoracic inferior vena cava—metals which have negative standard electrode potential tended to function longer in dogs than those which registered positive potential; with insulator materials using streaming potential to determine surface charge characteristics and using untreated, chemically treated and electrically treated Teflon tubes, the more negative the surface the more useful the material) [92].

11.5 Cell Culture/Seeding Peculiar to Each Cell

11.5.1 Human Microvascular Endothelial Cells (HMEC-1)

Human Microvascular Endothelial Cells (HMEC-1) were recovered from the molecular biology departmental bank of the University of Ulster. Cell cultures were maintained in MCDB-131 supplement with L-glutamine (200 mM), 10 % foetal Calf Serum (FCS), epidermal growth factor (EGF) (10 ng/ml) and Penicillin (20 IU/ml), streptomycin (20 µg/ml). Cells were grown as mono layers in tissue culture flasks at 37 °C under 5 % CO_2/95 % air. Proteins are removed with two washings of phosphate-buffered saline (PBS: 8.2 g/l NaCl, 3.1 g/l Na_2HPO_4. $12H_2O$, 0.2 g/l $NaH_2PO_4.2H_2O$; pH 7.4). Harvesting of cells for subculturing or testing was performed with a trypsin solution (0.05 % trypsin/0.02 % EDTA), shortly afterwards, the trypsin was inactivated with the culture media and by centrifugation supernatants were separated from the cells. Cells were used when cells were about to confluent under exponential growth phase. The samples were sterilised with 70 % ethanol before they are taken into the hood and given sufficient time to dry inside the hood for the experiment and afterwards rinsed with PBS or distilled water. Every normal culturing sterility precaution was taken throughout the experiment. Approximately, 4.0×10^5 cells/ml were seeded on top of the silicon wafers (placed inside the Petri dishes) of the a-C:H samples. About 5.5×10^5 cells/ml were seeded into the rest of the samples, and about 1×10^3 cells/ml were seeded into the wells of 96 well culture plates that were coated with a-C:H and Si-DLC. The uncoated samples were used as control. For the MTT assay some control wells were also created and marked blank by the computer program. The MTT assay was carried on for about 56 h, some of the test using silicon wafer substrates were carried on for up to about 36 h, and the rest for 6 h (length of time indicated as the case may be).

11.5.2 Human Platelets

Whole blood was taken from normal healthy individuals into a standard tube with anticoagulant (3.8 % sodium citrate). Centrifugation at 1200 rpm for 5 min to get PRP (platelet rich plasma) and at 3000 rpm for 10 min to get PPP (Platelet poor plasma) was done as soon as possible. The platelet number in the PRP was diluted with PPP to $\sim 1 \times 10^8$ cells/ml by mixing PRP with PPP. The samples were sterilised with 70 % ethanol before they were taken into the hood and given sufficient time to dry inside the hood. Every normal culturing sterility precaution was taken throughout the experiment. About 1×10^8 cells/ml were seeded on top of the a-C:H and Si-DLC samples placed inside the Petri dish. Incubation was done at 37 °C under 5 %CO_2/95 % air for the 15, 30 and 75 min. Afterwards proteins were removed with two washings of phosphate buffered saline (PBS) before the fixation. The cells on the silicon wafer substrates were fixed with 2.5 % glutaraldehyde in 0.1 M phosphate solution, followed by 1 % osmium tetraoxide in 0.1 M phosphate solution. The samples were dried with increasing concentrations of ethanol successively and finally with hexamethyldisiloxane (HMDS).

11.5.3 Pericytes Cell Line

The cells are normal bovine retinal pericytes isolated from the eye at the University of Ulster biomedical science department (see appendix for procedure). The cells used for the test was of passage number 4 (not to exceed passage number 6 in this particular cell line). The media used for cell culturing was made up with DMEM (500 ml), FCS (100 ml), fungizone (5 ml) and Pen/Strept (2 ml). Cells were grown as mono layers in tissue culture flasks at 37 °C under 5 % CO_2/95 % air. Proteins are removed with two washings of phosphate buffered saline (PBS: 8.2 g/l NaCl, 3.1 g/l $Na_2HPO_4.12H_2O$, 0.2 g/l $NaH_2PO_4.2H_2O$; pH 7.4). Harvesting of cells for subculturing or testing was performed with a trypsin solution (0.05 % trypsin/0.02 % EDTA), shortly afterwards, the trypsin was inactivated with the culture media and by centrifugation supernatants were separated from the cells. Cells were used when cells were about to confluent under exponential growth phase. About 1–2 $\times 10^3$ cells/ml were seeded into various 96 well plates (coated with a-C:H, or Si-DLC, or uncoated control TCPS) for MTT assay. The samples were sterilised with 70 % ethanol before they are taken into the hood and given sufficient time to dry inside the hood for the experiment. Every normal culturing sterility precaution was taken throughout the experiment.

11.5.4 Human Embryonic Lung, L132 Cell Lines

The cell line originally purchased from ATCC (CCL-5), is epithelial and normal but with Hela characteristics. The passage number is important so the passage number (P33) of the cells used for the test was under the normal passage number. The culture media was composed of MEM (500 ml, with L-glutamine), FCS (50 ml), sodium pyruvate (5 ml), Penicillin/streptomycin (5 ml) and non-essential amino acids, NEAA (5 ml). Cells were grown as mono layers in tissue culture flasks at 37 °C under 5 % CO_2/95 % air. Proteins are removed with two washings of phosphate buffered saline (PBS: 8.2 g/l NaCl, 3.1 g/l $Na_2HPO_4.12H_2O$, 0.2 g/l $NaH_2PO_4.2H_2O$; pH 7.4). Harvesting of cells for subculturing or testing was performed with a trypsin solution (0.05 % trypsin/0.02 % EDTA), shortly afterwards, the trypsin was inactivated with the culture media and by centrifugation supernatants were separated from the cells. Cells were used when cells were about to confluent under exponential growth phase. The samples were sterilised with 70 % ethanol before they are taken into the hood and given sufficient time to dry inside the hood for the experiment, and afterwards rinsed with PBS or distilled water. Every normal culturing sterility precaution was taken throughout the experiment. About 12×10^3 cells/ml were seeded into various 96 well plates (coated with a-C:H, or Si-DLC, or uncoated control TCPS) for MTT assay.

11.5.5 V79 Cell Lines

The Chinese hamster fibroblast like normal cell line (V79) was originally bought from ATCC (V79-4; CCL-93). The culture media was composed of DMEM (500 ml), FCS (50 ml), Penicillin/streptomycin (5 ml), NEAA (5 ml) and sodium pyruvate (5 ml). Cells were grown as mono layers in tissue culture flasks at 37 °C under 5 % CO_2/95 % air. Proteins are removed with two washings of phosphate buffered saline (PBS: 8.2 g/l NaCl, 3.1 g/l $Na_2HPO_4.12H_2O$, 0.2 g/l $NaH_2PO_4.2H_2O$; pH 7.4). Harvesting of cells for subculturing or testing was performed with a trypsin solution (0.05 % trypsin/0.02 % EDTA), shortly afterwards, the trypsin was inactivated with the culture media and by centrifugation supernatants were separated from the cells. Cells were used when cells were about to confluent under exponential growth phase. About $1–2 \times 10^3$ cells/ml were seeded into various 96 well plates (coated with a-C:H, or Si-DLC, or uncoated control TCPS) for MTT assay. The samples were sterilised with 70 % ethanol before they are taken into the hood and given sufficient time to dry inside the hood for the experiment. Every normal culturing sterility precaution was taken throughout the experiment.

11.6 Statistics and Counting of Cells

11.6.1 Cell Fixation and Drying

The cells on the silicon wafer samples were fixed with 2.5 % Glutaraldehyde in 0.1 M phosphate solution for 5 min, followed by 1 % Osmium Tetraoxide in 0.1 M phosphate solution for 5 min. The samples were successively dried with increasing concentrations of ethanol and finally with hexamethyldisiloxane (HMDS).

11.6.2 Gold–Platinum Coating for Charging Compensation

The samples in silicon wafer substrates were coated with a conducting material (gold–platinum), after cell fixation and drying, to about 30 nm thickness, using Polaron E5000 SEM coating unit, in order to reduce charging and obtain a better contrast during scanning electron microscope (SEM) imaging.

11.6.3 SEM Imaging of Cells

A low-vacuum SEM Hitachi S-3200 N was used for the observation of the cells interaction with the Si-DLC (a-C:H:Si) films on silicon substrates. The conditions for SEM imaging were high secondary electron (HSE), aperture 3 (#3), 0°-tilt, scan-4, 5.0 kV, and $\times$200 magnification.

11.7 Stereological Investigations

The cells number counting over an area of 600 μm $\times$ 400 μm on the SEM image of various samples were performed using the UTHSCSA, ImageTool program developed in the department of dental diagnostic science at the University of Texas Health Science Center, San Antonio, by Wilcox et al. [93].

11.7.1 Stereological Investigation and Statistical Analysis (Endothelial and Other Cells)

Human microvascular endothelial cells (HMEC-1) were obtained from the molecular biology department of the University of Ulster at Jordanstown, Northern Ireland. Cell cultures were maintained in MCDB-131 supplement with L-glutamine

(200 mM), 10 % foetal calf serum (FCS), EGF (10 ng/ml) and Penicillin (20 I. U/ml), streptomycin (20 μg/ml). Cells were grown as monolayers in tissue culture flasks at 37 °C under 5 %CO_2/95 % air. Proteins were removed with two washings of PBS. Harvesting of cells for subculturing or tests was performed with a trypsin solution. Shortly afterwards, the trypsin was inactivated with the culture media and by centrifugation supernatants were separated from the cells. Cells were used when they were about to confluent and under exponential growth phase. The samples were sterilised with 70 % ethanol before they were taken into the hood and given sufficient time to dry inside the hood (and afterwards rinsed with PBS or distilled water). Every normal culturing sterility precaution was taken throughout the experiment. Approximately, 4×10^5cells/ml were seeded on top of the DLC and Si-DLC samples placed inside the petri dishes, and about 1×10^3cells/ml were seeded into the wells of 96 well culture plates that were coated with DLC and Si-DLC.

The uncoated samples were used as control. For the MTT assay some control wells were also created and marked blank. The cells for the MTT assay were seeded for a total of about 56 h. The cells on the silicon wafer substrates were fixed with 2.5 % glutaraldehyde in 0.1 M phosphate solution for 5 min, followed by 1 % osmium tetraoxide in 0.1 M phosphate solution for 5 min. The samples were dried with increasing concentrations of ethanol successively and finally with HMDS.

11.7.2 Stereological Investigations and Statistical Analysis (Platelets)

The cell number counting over an area of 600 μm × 400 μm on the SEM image of various samples was performed using the ImageTool program [93]. In order to cover a statistically reasonable large area of the tested film area, several ×200 (higher magnifications cover only very small sample area) images of the SEM were acquired (the SEM stage with the mounted samples was moved ≥ 2 mm in both *X* and *Y* directions before SEM was acquired in order to avoid scanning same area twice) for counting the number of platelet aggregates. This is because platelets are numerous ($\sim$300,000 cells/μl) and the average size of platelets is very small ($\sim$2 μm). In estimating the number of adherent platelets, high magnification (×1500) is used to enable visibility of platelet-full morphology and counting. However, at such high magnifications, the sample areas covered by the SEM scan become so small that the estimation of the number of adherent platelets may become subjective if several images were not taken at different spots for each sample and the analysis of these painstakingly recorded and averaged. The effect of silicon doping on the mean of the number of platelet aggregates counted on the films examined was tested using a two-tailed heteroscedastic *t*-test to compare group means for the undoped and silicon-doped films that had an unequal variance in the number of platelet aggregates counted. Statistical significance was defined as a *p*-value of <0.05.

11.8 Photo-Fluorescent Imaging of Cells/Tissues

In photo-fluorescent imaging, fluorophores (fluorescent compounds: eg fluoroscein, rhodamine, luminol) are incorporated to the cell/tissue to be examined in order to label the sample. Fluorophores naturally absorb light at one wavelength and emit at a longer wavelength following some energy transitions. A fluorophore on absorbing a photon has its outer shell of electron excited from a ground to an excited energy level, this energy can be released as a thermal radiation (with the electron returning to the ground state) or part of this energy can be transferred to the molecular environment (e.g. cell/tissue) with the remainder photon energy emitted (photon with less energy and longer wavelength). This absorption and emission of photons creates contrasts which can be utilised in the imaging process to image structures at a molecular level in either live or fixed cells/tissues. The temperature and the micro-molecular environment do affect the fluorescent process, making different molecules of the same fluorophore to release different amounts of energy and creating a range of emission spectrum. These days, the molecular structure of the fluorescent material can be modified to target specific regions or molecules within a cell or tissue in order to study the entity of interest. Thus the chosen photo-fluorescent molecule can be used to label specific proteins and/or transfect (genetically alter) cells in order to insert, for example a fluorescent peptide called green fluorescent protein (GFP) in the native protein of the cell.

11.8.1 Typical Sample Preparation for Photo-Fluorescent Microscopy

Place samples in 6 well plate in triplicate and seed with 1×10^5 cells (3 ml media) and incubate at 37 °C and 5 % CO_2 for 24 h. Fix cells using a solution of 4 % paraformaldehyde and 2 % sucrose in PBS for 20 min; bovine serum albumin (BSA) in PBS and then permeabilise using buffered 0.5 % Triton X-100 (0.5 % Triton supplemented with 20 mM Hepes buffer, 300 mM sucrose, 50 mM NaCl and 3 mM $MgCl_2$) by chilling to 0 °C for 5 min. Wash samples again with 1 % BSA/PBS. Add TRITC-conjugated phalloidin solution at a concentration of 10 μg/ml, in 1 % BSA/PBS, for 20 min at room temperature. Then remove the phalloidin, wash samples and mounte on microscope slides with glycerol. Observe samples with, for example a Confocal laser scanning microscope (CLSM). Finally, analyse cell shape factor and cell spreading area from the micrographs. The software calculates the shape factor using the formula 4π (area/perimeter)^2 which gives a value between zero and one, a value of one being a perfect circle.

11.9 Biocompatibility and Hemocompatibility Models

Several models for assessing biocompatibility and haemocompatibility of materials in vitro exist (Fig. 11.1). These models are used in an attempt to find a platform for explaining what actually goes on at the material-biointerfaces. Interestingly, all these are influenced by electron and ionic exchanges at these interfaces. The balance (ratio) of non-adhesive to adhesive proteins, for example say albumin–fibrinogen ratio is thought to depict how these models tend to overlap and therefore all together may be important in interpreting material-biointerfacial interactions.

11.9.1 Proteins-Adhesive and Non-adhesive Proteins

This model is based on adhesive verses non-adhesive protein interactions on surfaces, and/or Vroman effect of protein adsorption, where proteins and the adhesion molecules compete for specific binding sites. It is now known that proteins either present in serum or secreted by the cells play a key role in the adhesion and spreading of the cells on the substrate biomaterial. The existing hypotheses are as follows [84–86]:

1. Protein adsorption comprises the initial interaction of a foreign material with blood (only the outermost $\sim$1 nm range of the surface is involved in the interfacial interaction). Exposure of an organic-free surface to fresh flowing

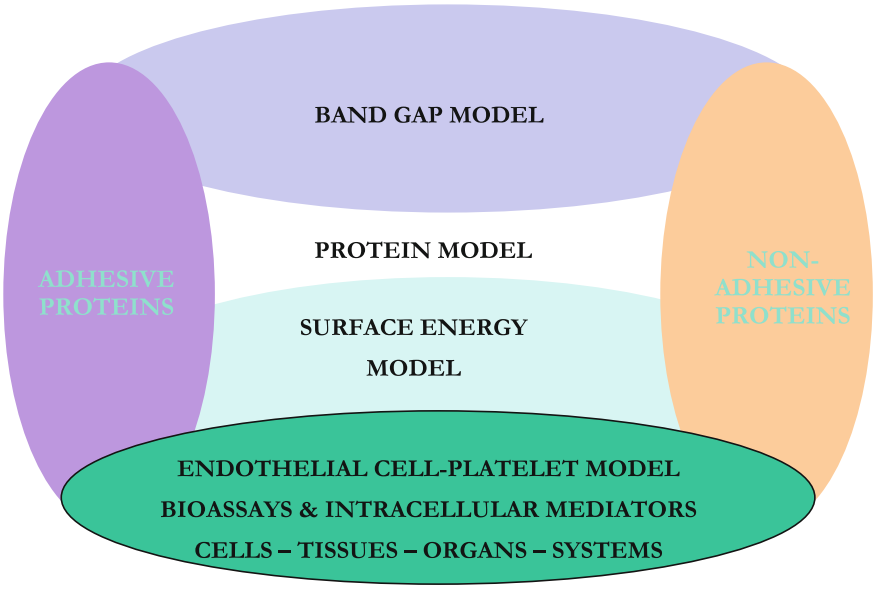

Fig. 11.1 Overlapping models for assessing material-biointeractions

blood for as little as 5 s, leads to its' complete coating by a very uniform, tenaciously adherent proteinaceous film. Thus the focus of attention has shifted from the substrate as the inducers of thrombogenicity, to the substrate as the dictators of a special configuration of adsorbed protein molecules that will favour or inhibit the subsequent events, including activation of the clotting mechanism and adhesion of platelets [94, 95].

2. The composition and organisation of the initial protein layer are determined by the surface properties of the material.
3. The composition and organisation of the initial protein layer mediates subsequent platelet interactions in vivo, and may also determine long-term effects.
4. In vitro protein adsorption studies are relevant to in vivo behaviour in humans.
5. The heat evolved on adsorption of proteins can lead to their denaturation on the surface; the magnitude of the heat evolved may be determined by the surface composition.
6. Hydrophobic surfaces will tend to adsorb protein more 'strongly' than hydrophilic surfaces, leading to greater denaturation of proteins on the hydrophobic surfaces.
7. Fibrinogen dominates the initial protein layer on most foreign materials and fibrinogen adsorption leads to high thrombogenic potential for that surface.
8. A layer of adsorbed albumin reduces in vitro platelet adhesion; materials that preferentially adsorb albumin will be antithrombogenic in vivo.
9. Certain other specific proteins may also adsorb and have a significant influence on subsequent events (e.g. CIG, or fibronectin, VWF, complement factors, high molecular weight kininogen, lipoproteins, etc.)
10. The various carbohydrate components of adsorbed glycoproteins may play an important role in the recognition of the biomaterial as foreign and in the subsequent events leading to thrombus deposition.

11.9.2 Surface Energy Model

Materials surface energy (and/or contact angle) is known to influence protein and cellular interactions on these surfaces. The actual interaction superseding depends on the properties of the surface and/or the biomolecule(s) arriving on the surface. Some of the existing hypothesis is stated above (Sect. 11.4), for example: 'a material with a critical surface tension of about 25 dyn/cm will have a low thrombogenic potential'. It is important to know that that the contact angle based of single liquid cannot give a good or accurate indication of the material's surface chemistry. There is need to use more than one liquid for measuring the contact angle, essentially a polar liquid on one hand and a dispersive liquid on the other. Surface energy of the material can be calculated from the contact angles values obtained using more than one liquid if the appropriate equations are applied. The calculated surface energy can equally be resolved into the surface energy components (by the use of appropriate equation/method, e.g. DLVO (Derjaguin–Landau–Verwey–Overbeek), Owens–Wendt, Van Oss–Chaudhry–Good): the Lifshitz-van

der Waals dispersive, the polar and the acid–base components. Equally the hydrophobic and the hydrophilic forces can be assigned. It may be possible to relate the biocompatibility of various materials to the appropriate surface energy components (and/or the total surface energy), the hydrophobic or hydrophilic energies and to determine the major contributing component in the biocompatibility behaviour.

11.9.3 Band Gap Model

Both materials' surfaces and the interacting biomolecules have got some electronic properties and more so when the two different interacting surfaces come into close ranges/contact. The band gap of the biomaterial under investigation can be related to that of the interacting biomolecule or protein. It is possible to predict the biomaterial–biomolecule interactions based on the distribution of electrons (or density of states, DOS), or contact potential difference (CPD), work function (WF) and/or band gap. The complexity and dynamic nature of these interactions have to be taken into account. If some electrons move from their occupied valence band level in the biomolecule to the free state of the biomaterials surface, it is expected that the biomolecules morphology could change or denature. This is only possible where the energy gap at the biomaterial–biomolecule interface allows a charge transfer. Chen et al. [96] studied the hemocompatibility of $Ti(Ta^{+5})O_2$ and reported an improved biocompatibility based on the band gap of $Ti(Ta^{+5})O_2$ being 3.2 eV compared to 1.8 eV of fibrinogen arriving on the surface. Thus because the band gap of fibrinogen is within that of $Ti(Ta^{+5})O_2$, it is not possible to affect electron transfer from the protein to the materials surface, and less amount of fibrinogen become adherent on the surface, which subsequently led to less adherent platelets.

11.9.4 Surface Topography, Roughness and Patterning

Surface topography, roughness and patterning have been implicated in altering protein adhesion and conformational changes. Studies creating various patterns on surfaces have indicated the implication of having various features of shape, size and depth dimensions on the surfaces to the degree of information gained on cellular and developmental biology [97]. It is almost impossible to change surface pattern without changing the chemical, physical and biological interactions. The author is of the opinion that this parameter is important in understanding the processes of developmental biology rather than directing dictation biocompatibility interactions. The experimental data presented in this chapter by the author is based on using samples with same and similar ultrasmooth surfaces having a non-statistically different surface topography, roughness and patterns.

11.9.5 Endothelial-Platelet Model

The seeding of bovine thoracic endothelial cells on cellulose surfaces with increasing hydrophobicity resulted in increased endothelial cell adhesion and proliferation and decreased migration [98]. Investigation on endothelial-specific cell adhesion to peptide sequences on different extra cellular matrix (ECM) molecules grafted on to various surfaces reveal that the arg-glu-asp-val (REDV) sequence from fibronectin was selective for the adhesion of endothelial cells but not fibroblasts, smooth muscle cells, or activated platelets where other sequences like arg-gly-asp (RGD), tyr-ile-ser-gly-arg (YISGR) or pro-asp-ser-gly-arg (PDSGR) were implicated [99]. The material–microvascular endothelial cellular interaction could be related inversely to those of platelets (in vitro and in vivo) since increased platelets aggregation/adhesion on a material could be associated with increased potential of a material to induce clotting [36], whilst increased endothelial–material adhesion could be associated on the other hand with an increased potential of a material not to induce clotting [40] (Fig. 11.2). Further detail of this model is implied in the discussions below [35, 36, 39, 40].

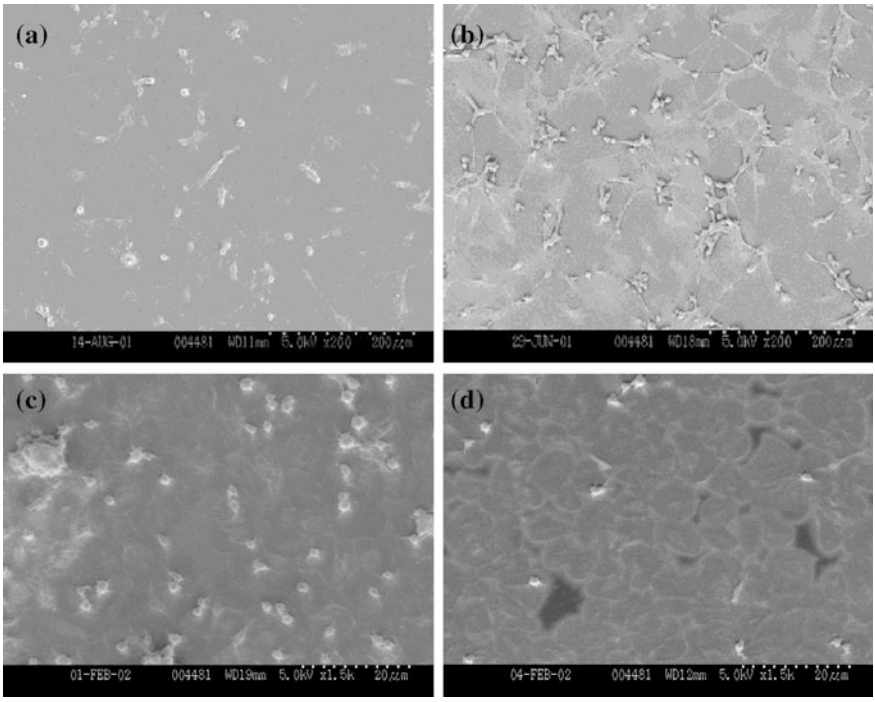

Fig. 11.2 Endothelial-Platelet model: **a** endothelial cells on DLC, **b** endothelial cells on Si-DLC, **c** platelets on DLC and **d** platelets on Si-DLC thin films

11.10 Carbon-Based Materials Interaction with Selected Proteins and Cells

When a cell is coming in contact with a biomaterial the degree of interaction can generally be taken as adsorption, contact, attachment and or spreading [29]. For activated platelets five stages of spreading can be described according to the increasing degree of activation [100]:

1. Round or discoid with no pseudopodia;
2. Dendritic, early pseudopodial with no flattening;
3. Spread-dendritic, intermediate pseudopodial with one or more flattened pseudopodia, but with no spreading of the cell body;
4. Spreading, late pseudopodial with the cell body beginning to spread;
5. Fully spread morphology, the cell is well spread with no distinct pseudopodia.

11.11 DLC Interactions with Fibroblasts In Vitro

The body's connective tissues can be classified as proper connective tissue (subdivided into loose and dense connective tissue proper), fluid connective tissues (subdivided into blood and lymph) and supporting connective tissues (subdivided into the cartilage and the bone). Fibroblasts are the most abundant permanent residents of the connective tissue proper and are the only cells always present in it. Fibroblasts secrete hyaluronans (a polysaccharide derivative) and proteins, both of which interact in the extracellular fluid to form proteoglycans that make ground substances viscous. They also secrete protein subunits that interact to form large extracellular fibres which could create loose/open framework or densely packed framework.

11.11.1 Human Fibroblasts

Dowling et al. [101] carried out a cell adhesion test on a DLC (obtained by saddle beam deposition) partially coated 2.8 cm diameter stainless steel disc using human fibroblast cell line and reported a very good cell adhesion and good spreading of the cells on the coated as well as the non-coated surfaces of the disc [101].

Allen et al. [102] tested DLC-coated polysterene (coating obtained by the low temperature dual ion beam technique using a saddle field source) and control uncoated polysterene tissue culture plates with primary cultured human synovial fibroblast (HSFs) and reported that there was no statistically significant difference in the cell growth on both samples [102]. The LDH assay of the fibroblasts also indicate that DLC has not caused any significant level of cell toxicity when compared to the uncoated samples [102].

Mouse fibroblasts

Hauert et al. [103] examined the interaction of mouse fibroblast (3T3 cell line) with a-C:H:Si (0.2–22.5 at.% silicon addition) obtained with PACVD system and reported that the cells proliferated well on the coated culture dishes, that no influence like any toxic effect was observed from the Si–C bonds present on the surface to the growth and proliferation of the cells after 2 days of incubation [103]. Hauert et al. [103] concluded that the toxic effect described by Allen et al. [104] is caused by bulk Si-C not present in the a-C:H:Si thin film.

McColl et al. [105] and **Parker et al**. [106, 107] studied the interaction of DLC with 3T3-1 mouse fibroblasts in vitro. The 3T3-1 cell viability in inserts Millicell-PCF membrane with DLC coating and without coating were determined in their study by Trypan Blue dye exclusion and reported that the cells grew well in both control membrane inserts and DLC-coated sample hich implies that DLC is not cytotoxic to the growing 3T3-1 cells.

Thomson et al. [108] following exposure of mouse fibroblast (C3H10T1/2 cell line) to DLC-coated 24 well culture plate obtained by saddle field source (using acetylene, butane or propane source gas) over a period of 7 days, reported that there was no significant difference in release of lactate dehyrogenase (LDH) in any of the coated samples and the uncoated control sample. Also their photomicrographic morphological examination confirmed that there was no cellular damage in the coated samples when compared to the uncoated control samples [108].

Murine fibroblast

Dowling et al. [101] did a cytotoxicity study using murine fibroblast to examine DLC-coated alloy, titanium alloy and a plastic sample using SEM after 6-, 24- and 48-h incubation period. According to Dowling et al. [101] there was good cell morphology, adhesion, density and spreading observed on both the DLC-coated alloy and on the plastic, but the tinanium alloy surface exhibited many cell death, thus the DLC coating acts as a barrier between the titanium alloy and the murine fibroblast cell line and demonstrates a low level of cytotoxicity.

11.11.2 DLC Interaction with Osteoblasts In Vitro

Osteoblasts are the bone forming cells and have major role in mineralisation leading to osseointegration of a prosthesis.

Allen et al. [109] investigated the effect of DLC coatings (obtained by fast atom bombardment from a hexane precursor) deposited on polystyrene 24-well tissue culture plates on two osteoblast-like cell lines cultured on the uncoated and DLC-coated plates for periods of up to 72 h and by measuring the production of three osteoblast-specific marker proteins: alkaline phosphatase, osteocalcin and type I collagen. According to Allen et al. [109] there was no evidence that the presence

of the DLC coating had any adverse effect on any of these measured parameters which are indicative of metabolic processes in these osteoblast-like musculoskeletal system cells.

Schroeder et al. [110] evaluated a new surface coating for bone-related implants by combining the hardness and inertness of a-C:H (DLC, obtained by a combination of radio frequency plasma and DC magnetron sputtering deposition techniques) films with the biological acceptance of titanium. They incorporated different amounts of titanium (7–24 atm.%) into a-C:H films by a combined radio frequency (RF) and magnetron sputtering set-up. Their X-ray photoelectron spectroscopy (XPS) of air-exposed a-C:H/titanium.
(a-C:H/Ti) films revealed that the films were composed of TiO_2 and TiC embedded in and connected to an a-C:H matrix. They performed cell culture tests using primary adult rat bone marrow cell cultures (BMC) to determine effects on cell number and on osteoblast and osteoclast differentiation. According to Schroeder et al. [110] addition of titanium to the carbon matrix, leads to cellular reactions such as increased proliferation and reduced osteoclast-like cell activity, while these reactions were not seen on pure a-C:H films and on glass control samples, thus they concluded that a-C:H/Ti could be a valuable coating for bone implants, by supporting bone cell proliferation while reducing osteoclast-like cell activation.

Du et al. [74] reported based on their study of interaction between osteoblasts (isolated from 4-day-old Wistar rats) and DLC as well as CN (carbon nitride) thin films (obtained by IBAD technique), that the osteoblasts attach, spread and proliferate on both DLC and CN sample surfaces without apparent impairment on the cell physiology [74].

Allen et al. [102] have also reported that DLC interact well with human 'osteoblast-like' cell line SaOS-2. When they compared the growth of human osteoblasts in both the DLC-coated and non-coated polysterene plates, they found out that there was similar level of growth observed in both samples, and the osteoblasts adhered well to the DLC samples and produced extensive filopodia when viewed under the SEM. The LDH assay of the osteoblast-like cells also indicated that DLC has not caused any significant level of cell lysis/toxicity when compared to the uncoated samples [102].

11.11.3 DLC Interaction Kidney Cells In Vitro

Human embryonic kidney (HEK-293) cells

Lu et al. [111] observed the interaction of DLC (obtained by ion beam assisted deposition) with HEK-293 cells using a haemocytometer for cell counting and Trypan Blue dye exclusion for assessing HEK-293 cell viability in DLC-coated P-35 dishes. According to Lu et al. [111] HEK-293 cells grew well, there was no delay attachment to the DLC-coated dishes compared to the control and that both

the cells growing in the DLC-coated and the control dishes had cell viability of 60 % at the first day of incubation which increased to >90 % at the second day of incubation.

Baby hamster kidney cells

Evans et al. [112] examined the interaction of DLC obtained using saddle field source and baby hamster kidney cells and reported good cell adhesion on the coated surfaces indicating good cell compatibility.

11.11.4 Mutagenicity Evaluation of DLC

Dowling et al. [101] performed a mutagenicity test (Ames test) on DLC coatings on stainless steel samples coated on both sides and uncoated samples using five strains of *Salmonella typhimurium* bacteria (TA-98, TA-100, TA-1535, TA-1537, TA-102) with and without metabolic activation in accordance with the method originally reported by Ames et al. [113]. According to Dowling et al. [101] both the DLC and the stainless steel samples were not mutagenic as they induced no significant increase in the number of revertants of the five strains of *Salmonella typhimurium* tested.

11.11.5 DLC Interaction with Specific Cells (Hemocompatibility)

Bruck [114] has pointed to the importance of specie-related haematological differences of experimental animals in the proper assessment of biomaterials for human use. He pointed out that 'the terms "biocompatibility" and "hemocompatibility" are often used inaccurately to denote the performance of biomaterials based on single or few in vitro tests; these tests frequently ignoring considerations of hemorheological parameters, damages to the reticuloendothelial system, and haematological species-related differences' [114]. DLC, deposited on stainless steel and titanium alloys used for components of artificial heart valves has been found to be biologically and mechanically capable of improving their performance [115]. Devlin et al. [116] has shown improvement of carbon/carbon composite prosthesis by DLC coating [116].

11.11.6 DLC Interaction with Endothelial Cells

Endothelium is nature's haemocompatible surface, and the performance of any biomaterial designed to be haemocompatible must be compared with that of the

endothelium [117]. Endothelial hemocompatibility can be considered under three areas: the interaction between the endothelium and circulating cells (mainly platelets and leucocytes—close interactions between erythrocytes and endothelium are rare); the modulation of coagulation and fibrinolysis by endothelium; and other activities that affect the circulating blood or the vascular wall. Under normal circumstances, platelets do not interact with the endothelial cells—that is platelet adhesion to the vessel wall and the formation of platelet aggregates do not normally take place except when required for haemostasis. Hence, the surface of endothelial cells does not promote platelet attachment [117]. The formation of platelet aggregates in close proximity to the endothelium is also rendered difficult by prostacyclin (PGI2), a powerful inhibitor of platelet aggregation secreted by the endothelial cells. Prostacyclin can be secreted by endothelial cells in culture as well as by isolated vascular tissue [118]. The vascular endothelium is now known to be a dynamic regulator of haemostasis and thrombosis with the endothelial cells playing multiple and active (rather than passive) roles in haemostasis and thrombosis [119, 120]. Many of the functions of the endothelial cells appear to be antithrombotic in nature. Several of the 'natural anticoagulant mechanisms', including the heparin–antithrombin mechanism, the protein C-thrombomodulin mechanism, and the tissue plasminogin activator mechanism, are endothelial-associated. Among the proteins on the endothelial surface is antithrombin III [121] which catalyses the inactivation of thrombin by heparin. Endothelial cells also have heparan sulphate and dermatan sulphate (glycosaminoglycans) on their surfaces [122] which are known to have anticoagulant activity. On the other hand, the endothelial cells also appear to be capable of active prothrombotic behaviour in some extreme conditions of anticoagulation, because endothelial cells synthesise adhesive cofactors such as von Willibrand factor [123], fibronectin and thrombospondin [124]. Endothelial cells are now known to play crucial roles in a large number of physiological and pathological processes [125–134]. Most of these physiopathologic events take place at the microvasculature (capillary beds) which constitutes the vast majority of the human vascular compartment. Thus it becomes vital to conduct hemocompatibility studies using microvascular endothelial cells. This is also vital because not all endothelial cells are alike. Endothelial cells derived from the microvascular structures of specific tissues differ significantly from large-vessel endothelial cells [135–140]. The study of human microvascular endothelial cells has been limited due to the fact that these cells are difficult to isolate in pure culture, are fastidious in their in vitro growth requirements, and have very short life span undergoing senescence at passages 8–10. Ades et al. [141] overcame these problems by the transfection and immortalization of human dermal microvascular endothelial cells (HMEC). These cells termed CDC/EU.HMEC-1 (HMEC-1) do retain the characteristics of ordinary endothelial cells (HMEC) and could be passaged up to 95 times, grow to densities 3–7 times higher than ordinary HMEC and require much less stringent growth medium [141]. HMEC-1 is just like ordinary endothelial cells and exhibits typical cobblestone (or polyhedral) morphology when grown in a monolayer culture.

Van Wachem et al. [142] reported that in their investigation of in vitro interaction of HEC and polymers with different wettabilities in culture, optimal adhesion

of HEC generally occurred onto moderately wettable polymers. Within a series of cellulose type of polymers, the cell adhesion increased with increasing contact angle of the polymer surfaces [142]. Moderately wettable polymers may exhibit a serum and/or cellular protein adsorption pattern that is favourable for growth of HEC [142]. Van Wachem et al. [143] reported that moderately wettable tissue culture poly(ethylene terephthalate) (TCPETP), contact angle of 44° as measured by captive bubble technique, is a better surface for adhesion and proliferation of HEC than hydrophobic poly(ethylene terephthalate) (PETP), contact angle of 65° suggesting that vascular prostheses with a TCPETP-like surface will perform better in vivo than prostheses made of PETP.

11.11.7 Nitrogen-Doped DLC Interaction with Endothelial Cells

This section reports the initial response of atomic nitrogen-doped diamond-like carbon (DLC) to endothelial cells in vitro. The introduction of nitrogen atoms/molecules to the diamond-like carbon structures leads to atomic structural changes favourable to the thriving of human microvascular endothelial cells, thus the bioresponse of ordinary diamond-like carbon could be improved with atomic nitrogen doping. Whilst the semiconductivity and stress-relieving properties of nitrogen in DLC are thought to play a part, the increase in the non-bonded N atoms and N_2 molecules in the atomic-doped species (with the exclusion of the charged species) seems to contribute to the improved bioresponse [39, 40]. The bioresponse is associated with a lower WF and slightly higher water contact angle in the atomic-doped films, where the heavy charged particles are excluded, as confirmed by SIMS analysis. The films used in the study were synthesised by RF PECVD technique followed by post-deposition doping with nitrogen, and afterwards the films were characterised by XPS, Raman spectroscopy, SIMS and Kelvin probe. The water contact angles were measured, and the counts of the adherent cells on the samples were carried out. This study is relevant to improving biocompatibility of surgical implants and prostheses.

The results in Fig. 11.3 show the water contact angle of uncoated, DLC-coated, N-DLC-coated as well as 'SN'-DLC-coated samples. The water contact angle increased with DLC coating when compared with uncoated sample. However, the contact angle value for the N-doped film is slightly lower than that of DLC whereas the values for the doping where the sweep plate (to remove ions) were employed is higher. The adherent endothelial cells are shown in Fig. 11.4. The number of adherent cells seems to be highest for the doped films (where the sweep plates were employed), followed by the doped films including the ionic species, DLC and finally, uncoated sample. This shows that the trend in the endothelial behaviour seems not to be directly related to the degree of hydrophobicity. These preliminary results seem to suggest therefore that hydrophobic films, with additional properties like decreased compressive stress, increased atomic networks and decreased

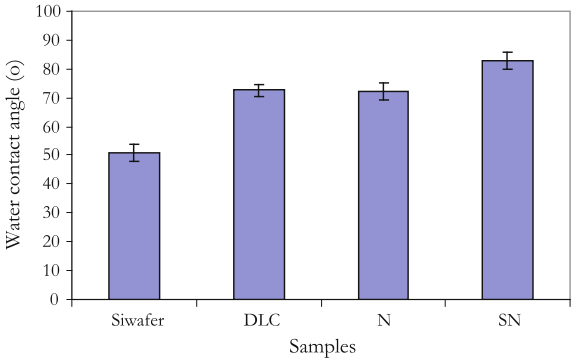

Fig. 11.3 Water contact angle of control silicon wafer, DLC and N-doped DLC obtained by the water drop optical technique

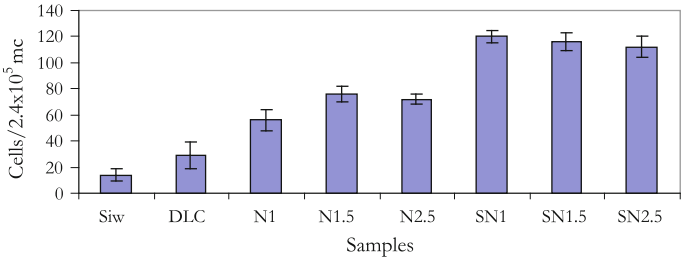

Fig. 11.4 HMEC attachment per 2.4 × 10^5 μ^2 of a-C:H:N (SN1-2.5 h—with use of sweep plate to remove ions, and N-films doped with ions included), a-C:H (DLC) thin films and bare silicon wafer (Siw) control samples

graphitic clusters as well as semiconductivity [36] may be favourable to human microvascular endothelial cellular attachment and proliferation. Other researchers have reported surface properties expressed in terms of hydrophobicity to be the key factor dictating the type and conformation of adsorbed proteins and therefore the cell adhesion. The seeding of bovine thoracic endothelial cells on cellulose surfaces with increasing hydrophobicity resulted in increased endothelial cell adhesion and proliferation and decreased migration [98]. Investigation on endothelial-specific cell adhesion to peptide sequences on different ECM molecules grafted on to various surfaces reveal that the arg-glu-asp-val (REDV) sequence from fibronectin was selective for the adhesion of endothelial cells but not fibroblasts, smooth muscle cells or activated platelets where other sequences like arg-gly-asp (RGD), tyr-ile-ser-gly-arg (YISGR) or pro-asp-ser-gly-arg (PDSGR) were implicated [99]. The material–microvascular endothelial cellular interaction could therefore be related inversely to those of platelets (in vitro and in vivo) since increased platelets aggregation/adhesion on a material could be associated with increased potential of a material to induce clotting [36], whilst increased endothelial–material adhesion

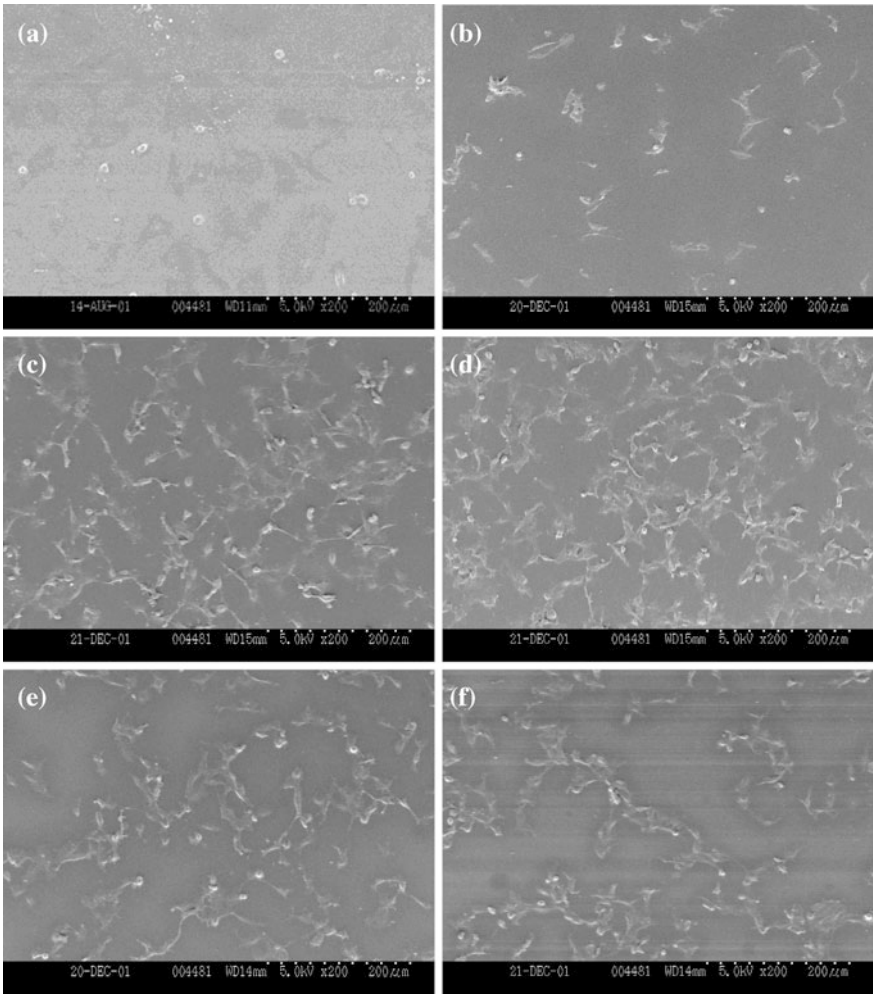

Fig. 11.5 SEM micrographs of endothelial cells attached to a-C:H:N thin films, ×200; **a** Uncoated substrate, **b** DLC-coated substrate, **c** sample 'SN1' (1 h exposure to atomic nitrogen), **d** sample 'SN2.5', atomic species for 2.5 h; **e** 'N1' (1 h, atomic and charged species) and **f** 'N2.5' (2.5 h, atomic and charged species)

could be associated on the other hand with an increased potential of a material not to induce clotting. Figures 11.4 and 11.5 compares directly the cell adhesion results obtained with both types of nitrogen species used for the doping over the duration of ∼1–2.5 h. The doping changes with time seem to be insignificant (1 h compared with 2.5 h). This is not surprising as only a small amount of impurities are usually required to effect a change in the microstructure, and the doping effects seem peak after some time. It seems that the films obtained with the use of sweep plates (to remove ions) encouraged more endothelial growth and proliferation compared

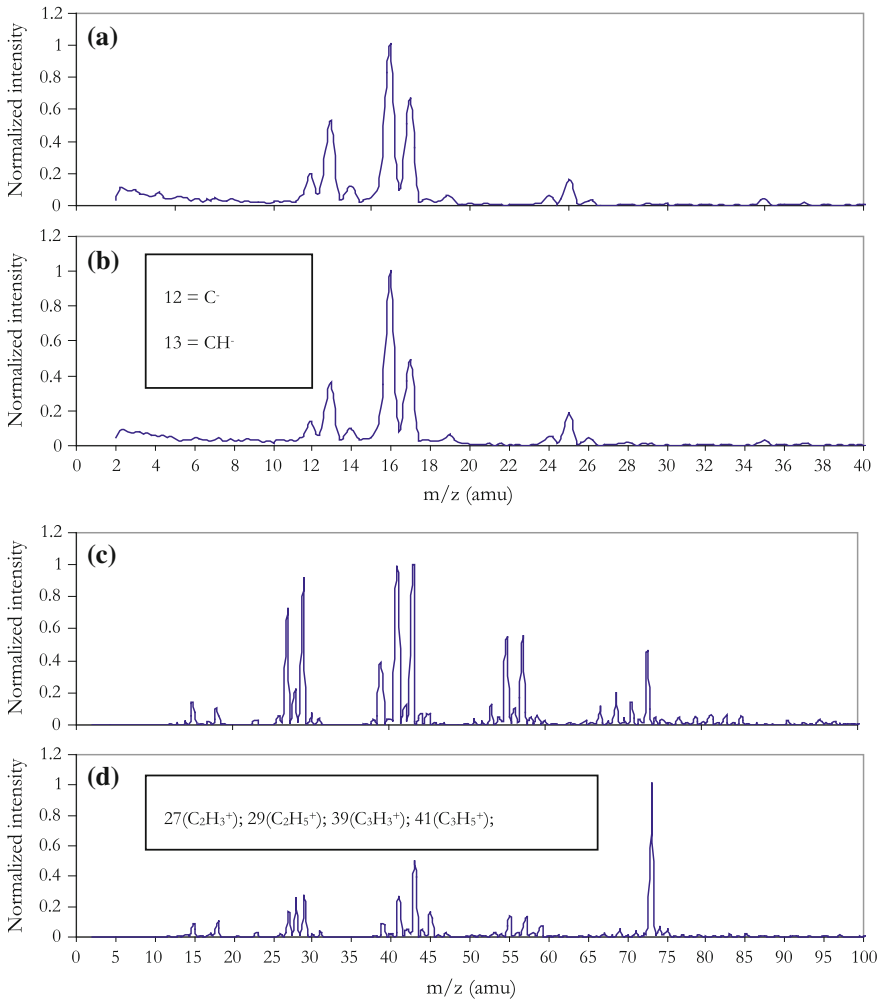

Fig. 11.6 SIMS analysis of nitrogen-doped DLC thin films: negative ions **a** 'N', **b** 'SN'; positive ions, **c** 'N', **d** 'SN'

to its counterpart. This is thought to be due to some changes in the films microstructure and chemical bonding as revealed by XPS and SIMS techniques.

The results of the atomic chemical bonding inferred from the XPS peak assignment suggest an increased atom percentage of the non-bonded N atoms (Peak at 399.6 eV) and N_2 molecules (Peak at 401.1 eV) in the films where the sweep plates were used to remove the ions. The non-bonded N atoms in these films are up to five times ($\times 5$) higher when compared to their counterparts [39].

The SIMS analysis of the films is shown in Fig. 11.6, and is displayed as normalised intensity of mass to charge ratios of various ions detected. The negative

ion scans for both the 'N' and 'SN' type films are very similar. These ions are of low m/z ratio (<25 amu), Fig. 11.6a, b. However, the relative/normalised intensity of the positive ions seems to be different, and the detected ions include heavier particles of higher m/z ratio (Fig. 11.6b, c). The relative intensity of the heavier particles of higher m/z ratio (>25 < 73 amu) seems to be higher in the 'N' type films. The heavier ions associated with higher plasma energies may be important during processing in increasing the films density, and establishing the integrity of the film's surface barrier to gas/moisture percolation, as the peak at 73 [$H_3O(H_2O)_3^+$] seems to be smaller in the 'N' type films (Both films were subjected to deionised water drops that were dried up afterwards, before SIMS analysis). The pattern of the SIMS depth profile with time is shown in Fig. 11.7. The positive ions depth profile was performed to probe for m/z corresponding to 14 (N^+, CH_2^+), 28 (N_2^+, $CHNH^+$, CO^+), and 30 (CH_3NH^+); and the negative ions depth profile for m/z corresponding to 14 (N^-, CH_2^-), 26 (CN^-) and 38 (C_2N^-). The depth profile result shows that the non-bonded N_2 (28 amu) species are relatively more intense and steadily distributed in the 'SN' type films (Fig. 11.7b), compared to its counterpart.

The structural vibration information gained by the Raman spectroscopy shows a slight difference. The Raman D and G peak positions shifted slightly to a higher energy as a result of the inclusion of the ionic species [39]. This may be indicative of an increased sp^3/sp^2 fraction in the film, also suggested by the XPS results [39].

The relative WF of the films as measured by the Kelvin probe technique shows that the relative work functions change from higher values ('N') films to lower values ('SN') films {Au–Au:250 mV, Au–N_2:200 mV, Au–SN2.5:100 mV, Au–SN1:75 mV}, Fig. 11.8. Kaukonen et al. [144] suggested based on their density function theoretical (DFT) calculation that a single N atom substitution at sp^3 or sp^2 site in a-C subsurface layers increases the total density of states (TDOS) below the energy gap resulting in Fermi energy (E_f) level moving down and the WF increasing. Whereas substitution on the sp^1 and sp^2 rings in the outer surface leads to TDOS increase near the conduction band edge with the Fermi level moving up and the WF decreasing. This decrease in the WF is thought to be dependent on the new states formed above the E_f following N substitution and a redistribution of the surface charges resulting in changes in the surface dipoles. Based on this interpretation it seems that N substitution in this study is dominant at the sp^1, sp^2 rings in the outer surface for 'SN' type N-doped films, that is, the 'SN' atomic species substitute preferentially at the sp^1 and sp^2 rings compared to the ionic N species. Nitrogen doping of a-C is known to increase the sp^2/sp^3 ratio and density function theoretical (DFT) calculations [144] suggest that N atoms positioned at an sp^3 site decrease their coordination number with resulting sp^2 N (or N with a non-planar threefold coordination). It therefore seems logical that N atoms positioned at sp^1 or sp^2 sites could increase the coordination number with resulting sp^2 N or sp^3 N, respectively. The Raman and XPS analysis suggest that both sp^3 C and sp^2 C are higher in the 'N' films, with the I_D/I_G ratios being equally higher. Thus its seems that in the 'N' type films where higher energy of the impinging N species are concerned, the more substitutions occur at the sp^3 sites, and thus decreasing the coordination number with resulting sp^2 N. On the other hand, it seems that

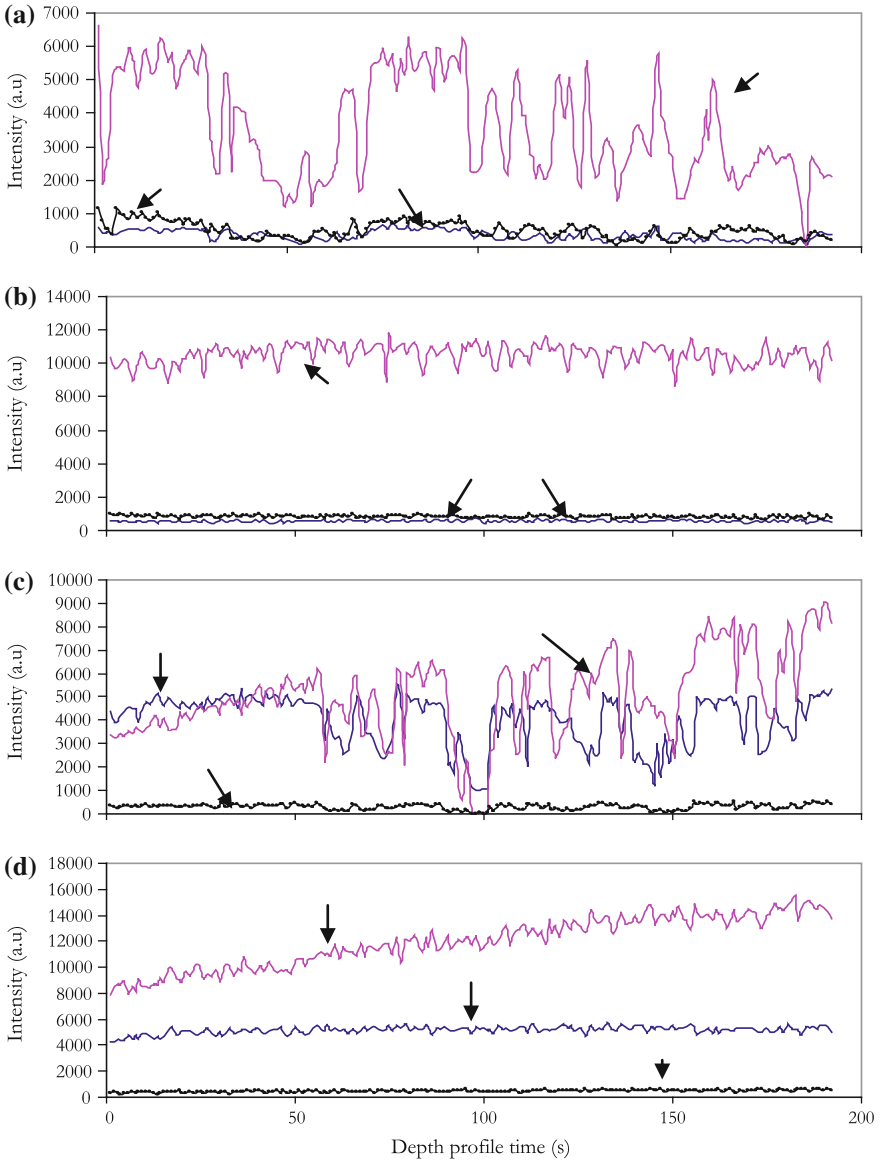

Fig. 11.7 SIMS depth profiling of some positive and negative ions: **a** + ions sample 'N', **b** + ions of sample 'SN'; **c** negative ions of sample 'N' and **d** sample 'SN'

relatively less substitution occurs in the 'SN' films. It is therefore not surprising that nitrogen incorporation into DLC as in the 'N' type species reduces the contact angle (increases the surface energy), whereas the N-neutral specie ('SN') doping increased the contact angle (slightly) in this study (Fig. 11.3).

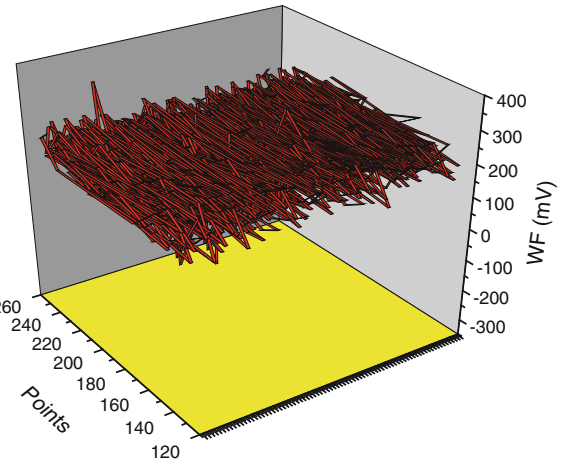

Fig. 11.8 The work function ('N2' film) over a scan area of 60 × 30 μm to 80 × 30 μm as determined by Scanning Kelvin Probe

Typical SEM imaging of the adherent cells on the film surfaces is shown in Fig. 11.5. Figure 11.5a, b shows the endothelial cell attachment on bare (uncoated) substrate and DLC-coated substrate, respectively. The worst bioresponse occurs on the bare substrate (Fig. 11.5a), followed by DLC coatings (Fig. 11.5b) and the best response is seen on the nitrogen-doped counterparts. However, it can be seen from the SEM images that there are better endothelial cell adhesion and proliferation on the 'SN' films (Fig. 11.5c, d) compared to 'N' films (Fig. 11.5e, f). Statistical analysis at 95 % confidence interval with 2-tailed paired sample analysis shows that there is a significant difference between uncoated samples and DLC-coated samples, between DLC and either 'N' or 'SN' type films, as well as between 'N' type and 'SN' type films.

Nitrogen-doped DLC thin films and their interaction with microvascular endothelial cells were examined. The nitrogen-doped DLC seems to have a better bioresponse compared to the undoped DLC thin films even though some of the N-doped films (where the ions were not excluded) have lower contact angle (more hydrophilic). Amongst the nitrogen-doped films, the films synthesised with the exclusion of ions seem to improve the bioresponse compared to its counterpart. The non-bonded N atoms in these films are higher and the contact angles obtained are also higher. Biocompatibility is therefore not simply related to hydrophobicity but may also relate to other materials micro and atomic structural changes induced by atomic nitrogen, like semiconductivity and films stress relieve.

11.11.8 DLC Interaction with Platelets

Platelets are small, granulated bodies 2–4 μm in diameter. They are round to spindle-shaped cytoplasmic fragments containing enzymes and prenzymes but no nucleus. There are about 300,000/μl of platelets in the circulating blood and they

normally have a half-life of about 4 days. The membranes of platelets contain receptors for collagen, vessel wall von Willebrand factor (vWF), and fibrinogen. When a blood vessel wall is severed, platelet adhere to the exposed collagen, laminin and vWF in the wall via intergrins. This process of platelet adhesion, unlike platelet aggregation does not require platelet metabolic activity [145]. However, binding of platelets to collagen initiates platelet activation (this can also be induced by ADP or thrombin). The activated platelets change shape, put out pseudopodia, discharge their granules which attract other platelets to stick to other platelets, a process known as platelet aggregation. The cytoplasm of platelets contains actin, myosin, glycogen, lysosomes and two kinds of granules (dense granules and α-granules) which may be released after platelets are activated. The dense granules contain non-protein substances (includes serotonin, ADP and other adenine nucleotides) that are secreted in response to platelet activation and the α-granules contain secreted proteins other than hydrolases in lysosomes which includes clotting factors and platelet-derived growth factor (PDGF). Released platelet granules generate inflammatory response to injury, the white blood cells (leucocytes) are attracted by selectins and bind to integrins on endothelial cells leading to their extravasation through the blood vessel walls [145].

Platelet adhesion hypothesis:

1. Platelets adhesion on a foreign surface is a necessary precursor to platelet aggregation on that surface.
2. High platelet adhesion on a foreign surface is bad.
3. In vitro platelet adhesion is related directly to in vivo thrombus formation and embolisation on foreign surfaces.
4. Platelets adhere with different strengths on different sites.
5. Platelet adhesion and release reactions at foreign interfaces occur when specific platelet membrane receptor sites ‘recognise’ specific groups on the foreign surface (corollary: platelet adhesion is not a random process).
6. Some platelet release factors (e.g. serotonin and ADP from dense granules) enhance platelet aggregation on foreign surfaces, while the roles of others (platelet factor IV with its heparin neutralising activity, HNA, and β-thomboglobulin from α-granules) remain to be clarified.

Chen et al. [146] varied acetylene to argon flow ratios in the DLC obtained with plasma immersion ion implantation deposition technique in their study. According to Chen et al., the blood compatibility of DLC depends on the sp^3 to sp^2 ratio rather than absolute sp^3 or sp^2 content and that the blood compatibility becomes worse with larger sp^3 to sp^2 ratio [146].

Krishnan et al. [147] did a quantitative analysis of I-125 radio-labelled platelet to examine platelet adhesion (using radiscintigraphy techniques) on titanium and DLC-coated titanium and have shown that DLC-coated titanium exhibited a lower platelet adhesion compared to uncoated titanium [147].

Cui and Li [75] also studied platelet interaction with DLC-coated PMMA intraoccular lens and uncoated PMMA intraoccular lens (IOLs). Their result shows that DLC-coated PMMA-IOLs had a lower platelet adhesion compared to the uncoated sample [75].

Gutensohn et al. [148] studied the interaction of stents coated on both inner and outer surfaces with DLC (obtained by plasma-induced cold deposition technique) and human platelets. In their study they used DLC to achieve a uniform protective coating to reduce the release of metal ion, platelet activation and thrombogenicity. Flow cytometric analyses revealed significantly higher increase of mean channel fluorescence intensity for the platelet activation-dependent antigens CD62p and CD63 in non-coated stents compared to DLC-coated stents ($p < 0.05$). Patients undergoing coronary angioplasty and stenting procedures are known to be at higher risk for reocclusion and restenosis of vessel when plate express increased numbers of activation-dependent antigens [2, 3]. Of all the antigens they analysed that P-selectin (GMP-140) seems to play a key role and appears to be most closely associated with an increase in thrombotic risk [2, 3]. Using atomic adsorption spectrophotometry and inductively coupled plasma mass spectrometry analyses they have shown that there was a significant release of metallic ion in the non-coated stents compared to DLC-coated stents. As a consequence of reduced metal ion release due to DLC coating platelet activation was significantly lower in DLC-coated stents compared to the non-coated stents under otherwise identical experimental conditions [148].

Alanazi et al. [64, 65] evaluated the interaction of polycarbonate-coated DLC (obtained with CVD under varied deposition conditions), segmented polyurethane (SPU, usually used for fabrication of medical devices including artificial heart) and an amphiphilic block copolymer composed of 2-hydroxyethylmethacrylate (HEMA) and styrene (St) (HEMA/St; an excellent non-thrombogenic polymer was used as a negative control) with platelets in whole human blood. They used the parallel plate flow chamber and epifluorescent video microscopy (EVM) using whole human blood containing Mepacrine-labelled platelets perfuse at a wall shear rate of 100 s^{-1} at 1 min intervals for a period of 20 min. In their assessment of the optical penetration of their EVM system and the activation/adhesion of platelets, they concluded that the activation of platelets on PC-DLC compared with the other biomaterials was minimal, the surface roughness before and after the coating applied to blood contacting devices is insignificant (16–23 nm), the contact angle is improved after DLC coating, the contact angle and chemical composition are independent of film thickness, defects of DLC films can be caused by elevated substrate, and blood compatibility depends on deposition conditions [64, 65].

Jones et al. [33] studied interaction between rabbit platelets and components of a Ti-TiN-TiC-DLC multilayer system. They adopted an interlayer approach in order to achieve adequate adhesion between DLC coatings deposited by plasma-assisted CVD and titanium substrate. The substrate, interlayers and DLC were assessed for haemocompatibility and thrombogenicity using a dynamic blood method and interactions with rabbit blood platelets, respectively. The adhesion, activation and morphology of the platelets were determined by stereological techniques using

SEM. The coatings produced no significant haemolytic effect compared to the medical grade polysterene control. In contrast to the DLC coating, all of the interlayers showed a slight tendency towards thrombus formation during the later stages of the incubation [33].

Dion et al. [42] evaluated the in vitro platelet retention of the new prosthetic heart valve that has been designed by FII Company and Pr. Baudet which is composed of Ti6Al4V titanium alloy coated with DLC (obtained by chemical vapour deposition technique). The retention/adhesion of platelets was evaluated by analysing radioactivity on the exposed wall of test or control tubes through which a blood cell suspension containing ^{111}In-labelled platelets had circulated. Their results show that on DLC/Ti6Al4V platelets adhere twice the amount that they do on the reference material (a silicone medical grade elastomer, the behaviour of which in contact with blood is the same as that observed with the NIH recommended polydimethyl siloxane) [42].

Okpalugo et al. [36, 40]
The human blood platelets interaction with a-C:H:Si films has revealed a relation between the microstructure of a-C:H:Si and its level of platelets aggregation. An increase in contact angle (or lowering of surface energy) of a-C:H and a moderate increase in the intrinsic electron conduction (semiconduction)/decrease in WF may lead to decreased platelets aggregation implying an increase in clotting time (decreased rate of clotting), high surface energy (low contact angle), non-conduction (insulating films), and graphitisation seems to lead to an increase in platelet aggregation implying a decrease in clotting time and an increase in the rate of blood clotting. Thus the hemocompatibility and biocompatibility of a-C:H and a-C:H:Si seems to be dependent on its electrical properties as well as the surface energy and the microstructure of the thin film biomaterials.

Silicon-doped films show a much lower level of platelet aggregation [36]. This seems to correlate with the lowering of surface energy, CPD/WF, resistivity and degree/rate of graphitisation due to silicon doping. Bruck [52–54] observed clotting times six to nine times longer than those observed with non-conducting polymers and also observed little or no platelet aggregation on electroconducting polymers, when compared to non-conducting control samples. In this study, thermal annealing of a-C:H below 400 °C led to excellent performance similar to that observed in a-C:H:Si. This is attributed to the increased electroconduction without graphitisation at the lower annealing temperature of a-C:H (Fig. 4.2.1-4). Chen et al. [96] varied acetylene to argon flow ratios during the deposition of a-C:H obtained by plasma immersion ion implantation. According to Chen et al. [96], the blood compatibility of a-C:H depends on the sp^3 to sp^2 ratio rather than absolute sp^3 or sp^2 content and that the blood compatibility becomes worse with larger sp^3 to sp^2 ratio. The results of the surface roughness as obtained with the AFM have shown that all the films analysed have smooth surfaces [40].

The results of the Raman spectroscopy show an increase in the I_D/I_G ratios [34–40] with annealing temperature for the a-C:H films in agreement with earlier reports in the literature [149, 150] and also for the a-C:H:Si thin films. The increase

in I_D/I_G ratio on the annealing of a-C:H has been associated with the growth of crystallites structure in the a-C:H thin film. In the a-C:H films the increase in the I_D/I_G ratio with thermal annealing seems to be linear whereas in a-C:H:Si the increase occurred only at relatively higher annealing temperatures above 300 °C. The I_D/I_G ratio decreases with increasing amount of silicon in the films [34–40].

Physical and chemical changes in carbon materials resulting in graphitisation may occur during thermal annealing of carbon materials. Graphitisation occurred at higher annealing temperatures greater than 400 °C [34–40] as revealed by the bimodal shoulders. Silicon doping seems to lower the degree of graphitisation [34–40]. Graphitisation is associated with increased sp^2 content, while silicon doping seems to increase the sp^3 sites. Shoulder peaks associated with annealing and graphitisation appeared on a-C:H and lightly doped a-C:H:Si (TMS = 5 sccm) at 400–600 °C [34–40]. A much higher annealing temperature is required to give a shoulder on films with higher amounts of silicon. Silicon does not form π-bond and it therefore increases the amount of sp^3 bonds in the film.

Typical XPS chemical analysis for the as deposited and thermally annealed a-C:H and a-C:H:Si films are as indicated [34–40]. The peak binding energies of the films are consistent with those reported in the literature by Dementjev [151, 152], Grill [153], Miyake [154] and Baker and Hammer [155]. There was only a slight change in the values of the binding energies for the silicon-modified films even after annealing to 600 °C. Also in agreement with Demichelis et al. [156] there was an increase in sp^3/sp^2 ratios after peak deconvolution. Silicon does not form π-bonds, thus silicon doping of a-C:H films would be associated with increase in sp^3 bonds and delayed graphitisation observed in a-C:H:Si films annealed between 200 and 600 °C, which is associated with decreased platelet aggregation observed in these a-C:H:Si films. The contact angle measurement results obtained using the optical method and the surface energy measured (and calculated) by the Wilhemy plate technique of films deposited on silicon substrates reveal that silicon doping leads to an increase in the contact angle and a lowering of the surface energy which could be associated with decreased platelet aggregation [36, 40].

The histograms below shows the summary of the result of the platelet aggregation on the a-C:H and Si-a-C:H thin films (as deposited and thermally annealed films) seeded with platelets for 15 min (Fig. 11.9) and 30 min (Fig. 11.10),

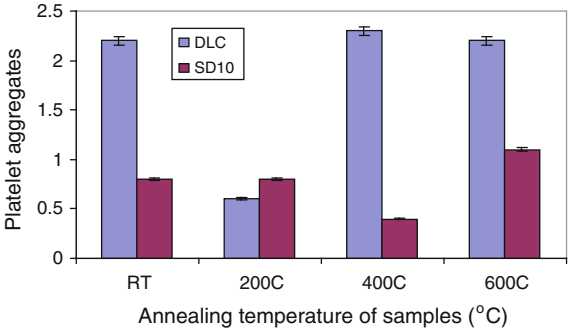

Fig. 11.9 Averaged human platelets aggregates/2.4 × 10^5 μ^2 on a-C:H and a-C:H:Si (as obtained and thermally annealed) samples (seeded for 15 min)

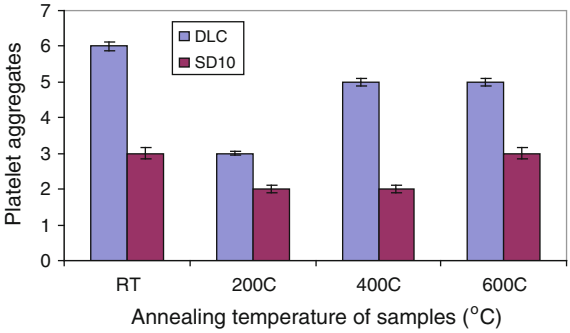

Fig. 11.10 Averaged human platelet aggregates/2.4 × 10^5 μ^2 on a-C:H and a-C:H:Si (as obtained and thermally annealed) samples (seeded for 30 min). RT = Room temperature

respectively. Figure 11.11 shows the SEM image of platelet seeding for 75 min on as deposited DLC and silicon-doped DLC thin films.

The electrical properties of the a-C:H and a-C:H:Si samples as well as the CPDs/WF have shown a correlation with the microstructure of the films as revealed by the Raman spectroscopy and XPS investigation, and the platelet aggregation on the films (Figs. 11.12, 11.13). Typical I–V curves of the metal–semiconductor–metal (MSM) sandwich show that the electrical conduction mechanism is not simple ohmic but semiconducting. The resistivity curve of the as deposited shows that silicon addition to a-C:H lowers the resistivity.

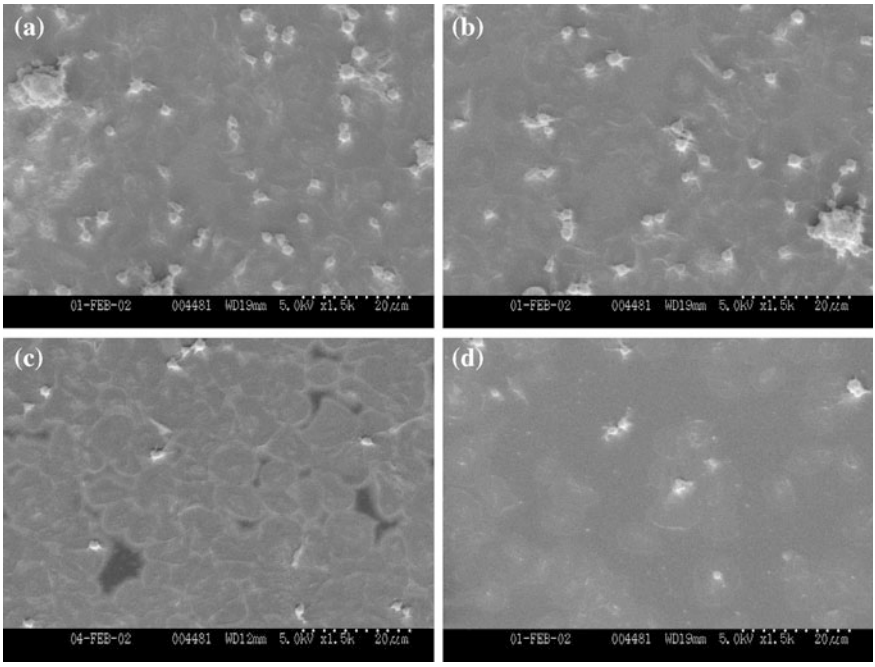

Fig. 11.11 SEM images of platelets seeded for 75 min on as obtained a-C:H (**a**, **b**), SD10 (**c**) and SD5 (**d**); ×1500

Thermal annealing of both a-C:H and a-C:H:Si leads to a decrease in the resistivity (Fig. 11.12, 11.13) which is likely to be associated with microstructural changes monitored by Raman spectroscopy as indicated by the sp^3/sp^2 ratios. At 600 °C of annealing temperature, the conductivity in both a-C:H and a-C:H:Si becomes simple ohmic [38, 40]. This result is consistent with the Raman spectroscopy investigation, which revealed graphitisation at this annealing temperature. Though decreased resistivity and decreased WF resulted in less platelet aggregates, graphitisation leads to increased number of platelet aggregates in the film [35, 36, 38].

The increasing graphitic content of the films at an annealing temperature of 600 °C increases the proportion of delocalised π-bonded electrons and therefore increases the electrical conductivity of the films as well, which hence result in the ohmic behaviour. The CPD and the WF of a-C:H thin films decreased with increasing amount of silicon doping and with increasing annealing temperatures as

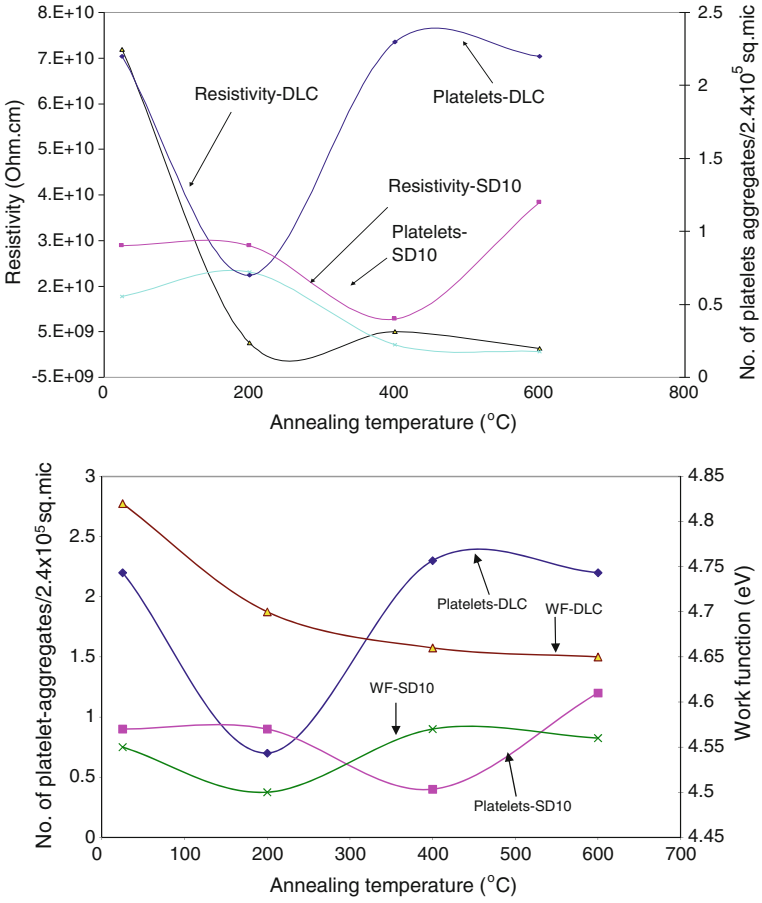

Fig. 11.12 Number of platelets aggregation (Seeded for 15 min) per 2.4×10^5 μ^2 as a function of resistivity and work function of a-C:H (DLC) and a-C:H:Si (SD10) thin films

shown in Figs. 11.12, 11.13. These electrical properties are related to the observed changes in the platelet aggregation on the a-C:H and a-C:H:Si thin films (Figs. 11.12, 11.13).

11.11.9 DLC Interaction with Blood Cells not Involved in the Clotting Process

Going strictly by the definition of hemocompatibility, apart from endothelial cells and platelets that are directly involved in the process of thrombosis and antithrombosis, the other blood cells though present in the blood can only be used to assess biocompatibility instead of hemocompatibility since they are not directly involved in thrombus formation and or prevention of thrombus formation. Thus the interaction of DLC with the other blood cells like neutrophils, lymphocytes, monocytes, erythrocytes (RBC), etc., can only give an indication of biocompatibility and not really 'hemocompatibility'.

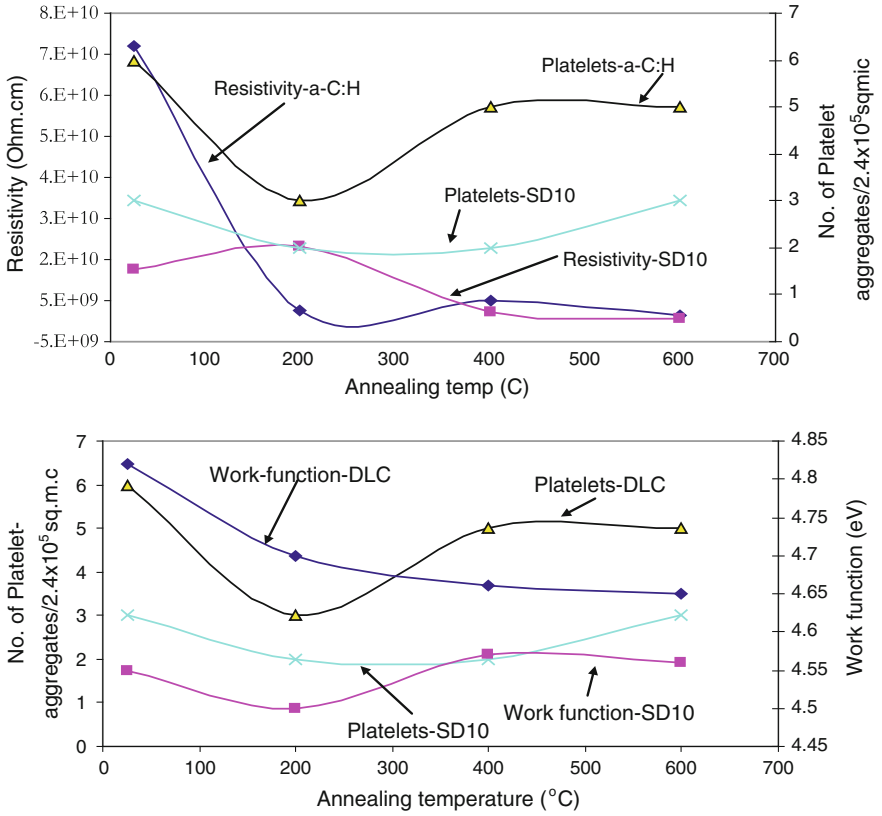

Fig. 11.13 Number of platelets aggregation (Seeded for 30 min) per 2.4 × 10^5 μ^2 as a function of resistivity and work function of a-C:H (DLC) and a-C:H:Si (SD10) thin films

11.11.10 DLC Interaction with Erythrocytes (Red Blood Cells, RBC)

Higson et al. [72, 73] examined the biocompatibility and substrate diffusion-limiting properties for a range of DLC (obtained from a saddle field source) coated porous polycarbonate membrane (nominal pore size of 0.01 μm) and hemodialysis membranes in whole blood. According to Higson et al. [72, 73] after 30 min exposure to unstirred whole blood, the uncoated polycarbonate did show red blood cells (and possibly other blood cells) adherent to the membrane surface, while in the DLC-coated membranes there was much reduced surface adherence of red blood cells and proteins, though some deposition of amorphous materials occurred. They also found that glucose sensors employing DLC-coated outer covering membranes were found to have suffered smaller losses of response following exposure to whole blood [72, 73].

Dion et al. [42] also evaluated the in vitro RBC retention of the new prosthetic heart valve that has been designed by FII Company and Pr. Baudet which is composed of Ti6Al4V titanium alloy coated with DLC (obtained by chemical vapour deposition technique). The retention/adhesion of RBC was evaluated by analysing radioactivity on the exposed wall of test or control tubes through which a blood cell suspension containing ^{99m}Tc-labelled red blood cells had circulated. According to Dion et al., the red cell retention, which may be due to either poor rinsing or morphological irregularities, leads to greater platelet retention; that mechanical entrapment accounted for only 0.07 % of red cell retention for silicone and 0.08 % for DLC/Ti6Al4V [42].

11.11.11 DLC Interaction with Human Haematopoietic Myeloblasts In Vitro

The haematopoietic myeloblasts are young blast cells derived from the progenitor cells in the bone marrow responsible for the generation of new white blood cells-granulocytes (neutophils, basophils and eosinophils).

ML-1 cells

ML-1 human haematopoietic myeloblasts were used in the study of **Lu et al**. [111] for assessing the biocompatibility of DLC. Using the hemacytometer for cell counting and Trypan Blue dye exclusion for determining cell viability, Lu et al. [111] found out that ML-1 cells cultured in DLC-coated P-35 dishes proliferated very well when compared to ML-1 cells growing in the uncoated control dishes and there was no sign to indicate cellular differentiation occurring among the ML-1 cells growing on the DLC-coating dishes [111].

11.11.12 DLC Interactions with Granulocytes (Neutrophils or Basophils or Eosinophils) In Vitro

Granulocytes are white blood cells containing granules (granules can either be acidic, basic or neutral thereby giving rise to different types of granulocytes, neutrophils, basophils and eosinophils, see Table 11.1), that are also responsible for combating infections. Neutrophils and eosinophils are also called microphages.

Neutrophils (polymorphonuclear leucocytes or PMNs, polymorphs)

Neutrophils are the most abundant white blood cells numbering an average of 4150 cells/μl (50–70 % of total number of white blood cells). They are round cells with a lobed nucleus (usually 2–5 lobes) that may resemble a string of beads and cytoplasm containing large pale inclusions, their granules being neutral and difficult to stain with either acidic or basic dyes. Their function is phagocytic, engulfing pathogens or debris in tissues and releasing cytotoxic enzymes and chemicals (lysosomal enzymes and bactericidal compounds). They measure about 12 μm in diameter and are the first of the WBCs to arrive at an injury site. High neutrophil adhesion produces negative effect on tissue biocompatibility.

Li et al. [157] reported based on their study of neutral granulocytes/neutrophils () interaction with DLC (obtained by ion beam assisted deposition, IBAD technique) coated polymethylmethacrylate (PMMA) intraoccular lens (IOLs), that DLC-coated PMMA-IOLs exhibit a lower neutophils adhesion compared to the uncoated PMMA-IOLs [157].

Eosinophils (acidophils)

Eosinophils are another type of granulocytes with cytoplasms that contain large granules that generally stain bright red with a red dye eosin, and can also stain with other acid dyes, hence also known as acidophils. The size of eosinophils is similar to that of neutrophils (∼12 μm). Eosinophils have bilobed nucleus and make up ∼2–4 % of the white blood cell population. They are phagocytic and engulf

Table 11.1 Operating conditions for SVTA RF plasma source for atomic nitrogen post-deposition doping of a-C:H thin films

Operating conditions	SVTA RF plasma source	PECVD
Power (W)	500	140
Reflected power (W)	25	5
Sweep plate voltage (V)	100–120	–
Bias voltage (V)	–	400
Deposition temperature (°C)	<100	25
Source temperature (°C)	300	–
Pressure (torr)	0.3	$\sim 7 \times 10^{-3}$
Atomic flux (atoms/s)	0.8×10^{18}	–
Exposure time (h)	1–2.5	∼0.1

antibody coated or marked foreign substances. Their primary mode of attack is the exocytosis of toxic compounds, including nitric oxide and cytotoxic enzymes, onto the surface of their targets. They are attracted to site of injury and so the increase in their number may indicate inflammation, allergy, etc.

Basophils

These are another type of granulocytes with numerous granules that stain darkly with basic dyes. They measure 8–10 μm in diameter and make up only about 1 % of the white blood cells. Basophils migrate to injury sites and cross the capillary endothelium to accumulate in the damage tissue where they discharge their granules which contain histamine (dilate blood vessels) and heparin (prevents clotting). They enhance local inflammation at the sites of injury and other chemicals that they release attract eosinophils and other basophils in the area of injury.

11.11.13 DLC Interaction with Monocytes (Macrophages) In Vitro

The monocytes also fall into the white blood cell category primarily produced in the bone marrow. The monocytes are 'agranular leucocytes' (agranulocytes), that is they lack abundant, deeply stained granules, though they also contain vesicles and lysosomes which are much smaller compared to those of the granulocytes [145]. They are very large cells ($\sim$15 μm in diameter, nearly about 2$\times$ the diameter of red blood cells) with kidney bean-shaped nucleus and abundant pale cytoplasm. They constitute about 2–8 % of the population of the circulating white blood cells. Monocytes move from the flowing blood to the tissues after 1–2 days. When monocytes enter the tissue they become to be known as macrophages and are responsible for fighting foreign bodies or pathogen and debris by engulfing and inactivating and digesting them in a process known as phagocytosis. They are aggressive phagocytes, often attempting to engulf as large or larger than their size. When activated they release chemicals that attract and stimulate neutrophils, monocytes and other phagocytic cells, as well as fibroblasts to the region of injury. The fibroblasts then begin producing scar tissues which walls off the injured area.

Linder et al. [158] studied the adhesion, cytoarchitecture and activation of primary human monocytes and their differentiated derivatives, macrophages, on DLC (obtained by radio frequency PACVD using methane/helium mixture: 1.5 vol.%/98.5 vol.%) coated glass coverslips using immunofluorescence technique. According to Linder et al. [158] the adhesion of primary monocytes to a DLC-coated coverslip is slightly, but not significantly, enhanced in comparison to uncoated coverslips, while the actin and microtubule cytoskeletons of mature macrophages show a normal development. The activation status of macrophages, as judged by polarisation of the cell body, was not affected by growth on a diamond-like carbon surface, thus DLC

shows good indications for biocompatibility to blood monocytes in vitro. It is therefore unlikely that contact with a DLC-coated surface in the human body could cause the cells to elicit inflammatory reaction [158].

Allen et al. [102] reported that DLC-coated polysterene (coating obtained by the low temperature dual ion beam technique using a saddle field source) culture plates produced good macrophage (murine macrophage cell line, IC-21) cell proliferation with a statistically significant faster growth rate (observed at the 48 and 72 h time points) when compared to the uncoated polysterene, and with no evidence of cytoplasmic vacuolation, membrane damage or excessive macrophage cell death [102]. Their LDH assay also indicates that there was no significant increase in LDH release from cells grown on DLC-coated surfaces as compared with cells grown on control surfaces, thus DLC has not caused any significant level of cell toxicity when compared to the uncoated samples [102].

Thomson et al. [108] by measuring the level of lysosomal enzymes *N*-acetyl-D-glucosaminidase released (enzyme is usually released as part of inflammatory reaction) in cell culture medium by macrophages (mouse peritoneal macrophage) after the cells interacted with DLC, reported that there was no significant difference in the amount of enzyme detected in the DLC-coated samples (using saddle field source and different source gases: acetylene, butane or propane) compared with the uncoated control tissue culture sample (24 well tissue culture plates) [108]. This implies that DLC is not cytotoxic and may not have elicited an inflammatory reaction. This was also corroborated by their lactate dehydrogenase, LDH assay which indicated that there was no statistically significant different level of LDH detected on the DLC-coated samples when compared to the non-coated samples.

11.11.14 DLC Interaction with Lymphocytes

The lymphocytes are also ‘agranular leucocytes’ (agranulocytes) lacking abundant and deeply stained granules. In a blood smear they are seen as a thin hallow of cytoplasm around a relatively large nucleus. In diameter they are slightly larger than the RBCs. Lymphocytes account 20–30 % of the WBC population of blood. Some lymphocytes are in circulation (small percentage) while others are in various tissues, organs and lymphatic system. Three classes of lymphocytes exist in the circulating blood, the T cells (responsible for cell-mediated immunity), the B cells (responsible for humoral immunity) and the NK cells (natural killer cells responsible for immune surveillance, are important in preventing cancer, sometimes known as large granular lymphocytes).

Plasma proteins and cell adhesion proteins/molecules (CAM)

Plasma, the fluid portion of the blood is a remarkable solution containing an immense number of ions, inorganic molecules, and organic molecules that are in transit to transport substances to various parts of the body. The plasma proteins

consist of albumin, globulin and fibrinogen fractions. Cells are attached to the basal lamina and to each other via the cell adhesion molecules (CAM) which are adhesion proteins. Many of these proteins pass through the cell membranes of the cells and are anchored to the cytoskeleton. Many CAMs have been characterised biochemically, and their functions are being investigated. Some of the CAMs bind to like molecules on other cells (homophilic binding) and the others to other molecules (heterophilic binding). Many CAMs bind to laminins, a family of large cross-shaped molecules with multiple receptor domains in the extracellular matrix. Nomenclature of CAM is still chaotic due partly of rapid growth in the field and also due to extensive use of acronyms in modern biology, however four broad families of CAM are known. The CAM categories are (1) the 'integrins' which are heterodimers that bind to various receptors; (2) the adhesion molecules of the 'IgG superfamily' of immunoglobulins, some of which bind to their molecules and some binding homophilically; (3) the 'cadherins', Ca^{2+}-dependent molecules that mediate cell-to-cell adhesion by homophilic reactions and (4) 'selectins', which have lectin-like domains that bind carbohydrates [145]. Goodman et al. [159] reported that since shape change responses of in vitro column-purified platelets to several polymeric biomaterials are very similar to those of circulating non-anticoagulated platelets and because column separation significantly reduces the protein content [160] of in vitro platelets, it appears that differences in platelet spreading on various materials are not entirely dependent on the preferential adsorption of plasma proteins from blood. They also observed that in vitro shape changes on Formvar and glass are the same in the presence and the absence of protein-containing buffer. Also cell spreading is similar in the presence and the absence of serum proteins [159, 161, 162]. A 'shine-through' hypothesis has been proposed to explain this biomaterial–protein–cellular interaction [163]. Additionally, fibroblasts and platelets appear to remove or move (sweep aside) adsorbed proteins [164–167], it is therefore conceivable that platelets alter adsorbed albumin layer(s) and adhere directly or via particular adhesion proteins on platelets surface to the material surface, if this occurs it would be expected that platelets would exhibit little differences in spreading on uncoated and albumin-coated surfaces, regardless of the thickness of an albumin layer. It has also been observed that initially adsorbed proteins tend to be more denatured than subsequent layers [168], and that the initial layer also appears to be more important in determining thrombotic responses [169]. Park et al., 1985 have also shown that platelet deposition in ex vivo circulation is determined by the first layer of adsorbed proteins and not subsequent layers, suggesting that platelets remove secondarily adsorbed layers of proteins. Another hypothesis is that platelets may not make direct contact with the substrate but are nonetheless influenced by surface character through an intervening layer of proteins, which is itself influenced by the surface. Different orientations or conformations of adsorbed proteins, as determined by the substrate, would then influence the behaviour of adherent platelets and other cells [159]. How these proteins may interact with DLC and DLC-like materials is yet to be explored.

Non-adhesive proteins: Albumin, Transferrin, like proteins

Albumin and tranferin like proteins with non-adhesive functions tend to decrease subsequent thromboembolic events [159, 170].

Dion et al. [42] have examined ^{131}I-labelled albumin plasma protein adhesion on DLC-coated Ti6Al4V and silicone elastomer and reported that DLC can adhere more albumin than the medical grade elastomer.

Adheisve proteins: Fibrinogen, Fibronectin, VWF and CAM

In general these plasma proteins with adhesive functions tend to increase thrombosis [159, 171]. Adhesive proteins and likely increased expression of CAM, e.g. ICAM-1, VCAM-1, ELAM-1, E-selectin, GMP-140 (P-selectins) and other molecules/ligands from the immunoglobulin and selectin superfamily have been shown to be important in cascade reactions like the platelet–leucocyte and leucocyte–endothelial cell adhesion and activation reactions [172–174]. When expressed on the cell surface the NH_2-terminal lectin-like domains of the selectins bind with their counter-receptors (specific carbohydrate ligands on white blood cells and platelets).

Dion et al. [42] have also examined ^{125}I-labelled fibrinogen plasma protein adhesion on DLC-coated Ti6Al4V and silicone elastomer and reported that DLC can adhere slightly more fibrinogen than the silicone elastomer.

Non-adhesive/Adhesive protein ratios: Albumin/Fibrinogen ratios

It has been shown that platelet adhesion depends on the albumin/fibrinogen ratio: the higher the albumin/fibrinogen ratio the lower the number of adhering platelets and hence less risk of platelet aggregation and less risk of thromboembolism. The albumin/fibrinogen ratio for DLC is 1.24 and 0.76 for silicone elastomer [42]. According to Dion et al. [42] these two ratios allow us to consider that platelet adhesion would be weaker on DLC than on silicone elastomer but, infact the opposite occurred, which they thought could be explained by the large dispersion of results in percentage of platelet retained due to the device concept itself they added [42].

Cui and Li [75] also studied the adhesion of plasma proteins on DLC-coated, CN-coated PMMA, and uncoated PMMA using radioactive targed proteins. They reported the albumin/fibrinogen ratio of 1.008 for DLC, 0.49 for CN and 0.39 for PMMA [75].

11.12 Endothelial Preseeding on Biomaterials for Tissue Engineering

Preliminary study on the platelet interaction with a-C:H:Si and a-C:H thin film samples preseeded with endothelial cells in vitro is reported in this section to corroborate the reported results in the other sections where a-C:H:Si and a-C:H

were interacting with endothelial cells and platelets separately. These joint interactions were investigated in order to confirm the reports in the literature on the opposing but complementary interactions of endothelial cells and platelets in blood coagulation/thrombus formation regulation in the body. The role of microvascular endothelial cell in preventing platelet aggregation and acting as a simple model in haemocompatibility assessment is hereby affirmed. This investigation also tries to demonstrate that since these interactions do not occur either separately or in sequence but, at about the same time, the microstructural finish of the biomaterial before implantation becomes crucial therefore in determining the fate of the biomaterial in vivo.

11.12.1 Endothelial Cell–Platelet Interactions on a-C:H and a-C:H:Si Thin Films

Human microvascular endothelial cells were seeded on a-C:H and a-C:H:Si thin films for about 6 h, washed with PBS twice, followed finally by seeding of human platelets for 30 min. This section of the study acts as an adjunct to the reports already presented in this chapter.

In the above micrograph (Fig. 11.14), there seems to be no platelet aggregation present on the as obtained a-C:H. Instead there seems to be endothelial cell activation, and or aggregation in response to potential platelet attachment and or aggregation. Also there seems to be some changes in the morphology of the endothelial cells. However, the exact relation of this change in morphology in the presence of platelets is not known to the author. That is whether the endothelial cells engulf the platelets and or by its secretions wall off platelets where ever they seem to appear is not really understood by the author. The other possibility could be that the endothelial cell do not allow the platelets to adhere at all, such that they could all be washed off by the PBS washing (to remove proteins) before samples were prepared for imaging.

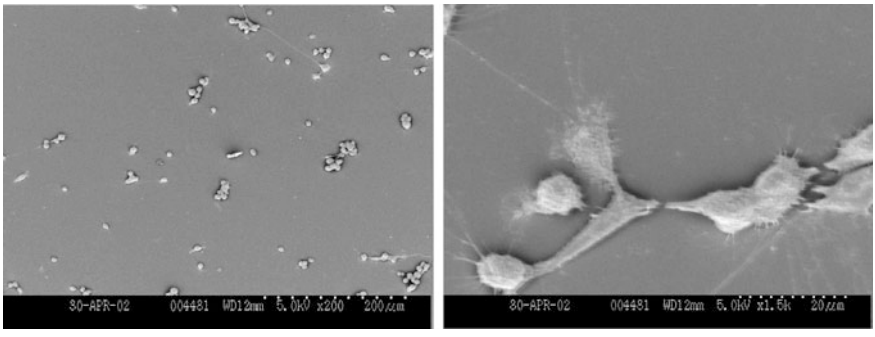

Fig. 11.14 Endothelial cell seeded on as obtained a-C:H for 6 h and followed by platelets seeding for 30 min; ×200 (*left*), ×1500 (*right*)

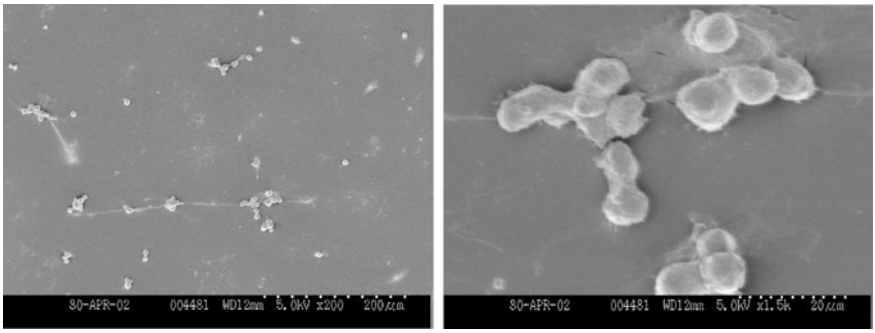

Fig. 11.15 Endothelial cell seeded on as obtained a-C:H:Si (SD10) for 6 h and followed by platelets seeding for 30 min; ×200 (*left*), ×1500 (*right*)

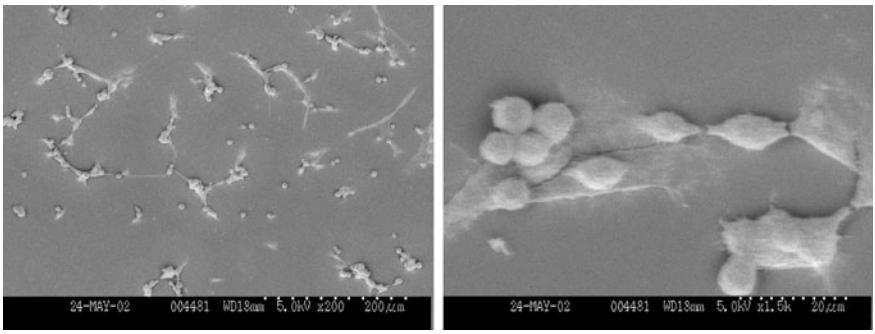

Fig. 11.16 Endothelial cell seeded on a-C:H (thermally annealed at 200 °C) for 6 h and followed by platelets seeding for 30 min; ×200 (*top*), ×1500 (*bottom*)

Under normal circumstances, platelets do not interact with the endothelial cells—that is platelet adhesion to the vessel wall and the formation of platelet aggregates do not normally take place except when required for haemostasis. Hence, the surface of endothelial cells does not promote platelet attachment [117]. The formation of platelet aggregates in close proximity to the endothelium is also rendered difficult by prostacyclin (PGI2), a powerful inhibitor of platelet aggregation secreted by the endothelial cells. Prostacyclin can be secreted by endothelial cells in culture as well as by isolated vascular tissue [118]. The vascular endothelium is now known to be a dynamic regulator of haemostasis and thrombosis with the endothelial cells playing multiple and active (rather than passive) roles in haemostasis and thrombosis [119, 120].

Figures 11.15, 11.16 and 11.17 show both the doped (Silicon, SD10) and non-doped DLC films, as deposited and thermally annealed (at low temperature, <400 °C) preseeded with endothelial cells (6 h) and then seeded with platelets. At both low (×200) and high magnifications (×1.5 K) the features seen are neither that of platelet aggregation nor individual platelet adhesion (Figs. 11.15, 11.16 and 11.17).

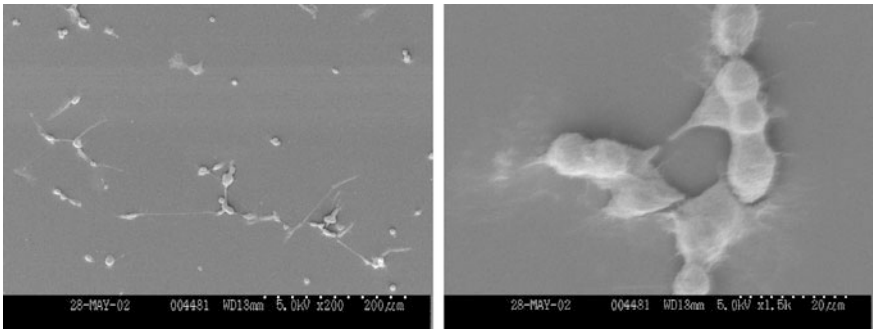

Fig. 11.17 Endothelial cell seeded on a-C:H:Si (SD10, thermally annealed at 200 °C) for 6 h and followed by platelets seeding for 30 min; ×200 (*left*), ×1500 (*right*)

Many of the functions of the endothelial cells appear to be antithrombotic in nature. Several of the 'natural anticoagulant mechanisms', including the heparin–antithrombin mechanism, the protein C-thrombomodulin mechanism, and the tissue plasminogin activator mechanism, are endothelial-associated. Among the proteins on the endothelial surface is antithrombin III [121] which catalyses the inactivation of thrombin by heparin. Endothelial cells also have heparan sulphate and dermatan sulphate (glycosaminoglycans) on their surfaces [122] which are known to have anticoagulant activity.

In this micrograph (Fig. 11.18) a bit strange star-shaped features that seemingly engulfing platelet aggregates are seen in this 400 °C thermally annealed a-C:H. These could possibly be endothelial cell(s) in 'extreme activation'. Based on the results from previous chapters, fewer endothelial cells combating with more platelet aggregations are expected in this supposedly graphitized film. This could possibly lead to extreme endothelial cell activation and extreme flattening/spreading of the few endothelial cells expected to be interacting with platelet aggregations.

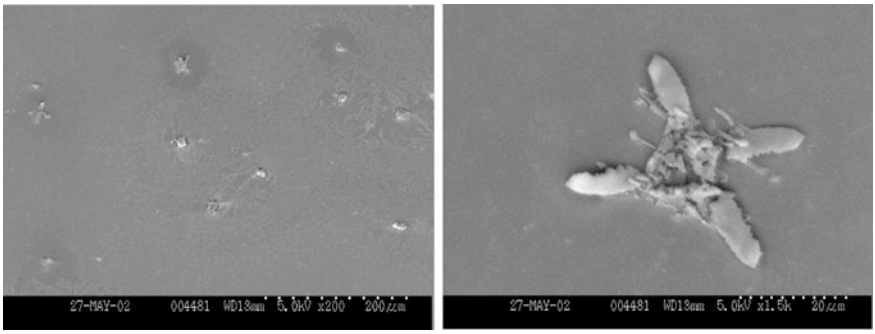

Fig. 11.18 Endothelial cell seeded on a-C:H (thermally annealed at 400 °C) for 6 h and followed by platelets seeding for 30 min; ×200 (*left*), ×1500 (*right*)

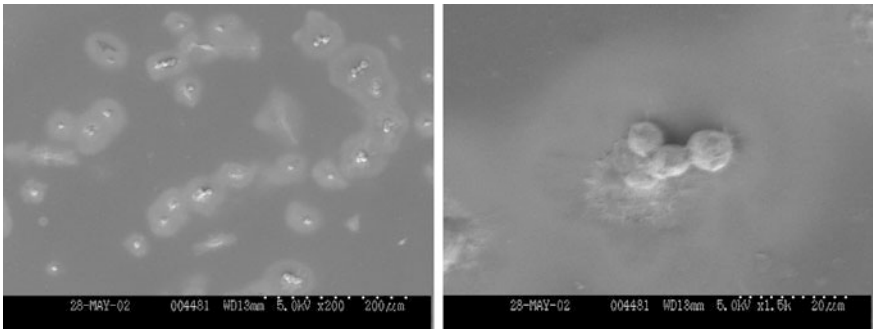

Fig. 11.19 Endothelial cell seeded on a-C:H:Si (SD10, thermally annealed at 400 °C) for 6 h and followed by platelets seeding for 30 min; ×200 (*left*), ×1500 (*right*)

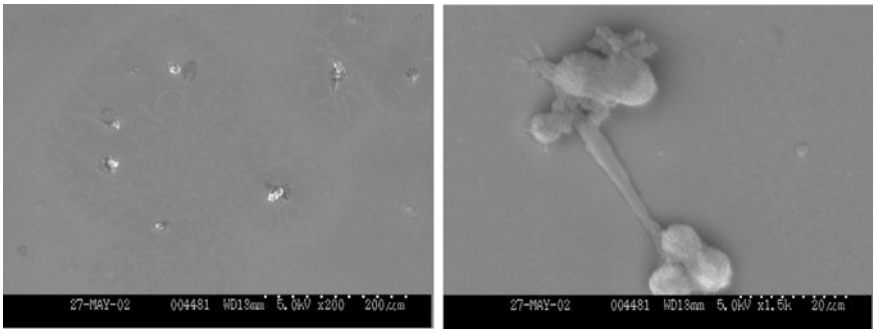

Fig. 11.20 Endothelial cell seeded on a-C:H (thermally annealed at 600 °C) for 6 h and followed by platelets seeding for 30 min; ×200 (*left*), ×1500 (*right*)

The clump seen above (Fig. 11.19) seems to be a platelet aggregate walled off by endothelial cell or endothelial secretions. No individual platelet or platelet aggregates are identifiable.

In this micrograph (Fig. 11.20) is seen also 'endothelial aggregates' and star-shaped endothelial cells in 'extreme activation'. This film is also expected to be graphitized.

The top left micrograph (Fig. 11.21) seems to show some platelet aggregates surrounded by a halo of what could be endothelial secretion. This preliminary study seems to show that in the presence of endothelial cells, platelet aggregation could be almost impossible. Therefore, any biomaterial with good surface properties suitable for endothelial cell adhesion could be confirmed as haemocompatible biomaterial until proven otherwise.

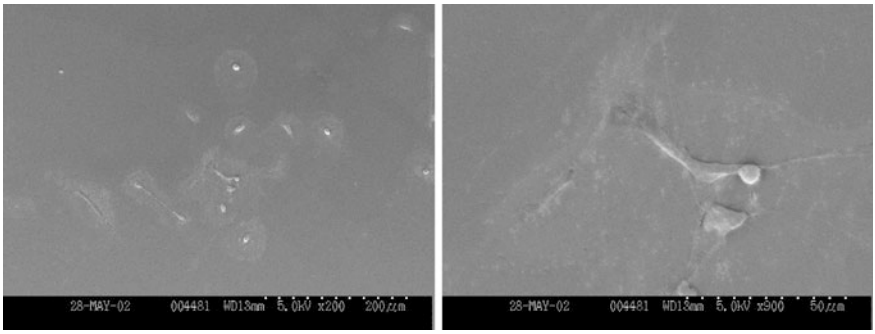

Fig. 11.21 Endothelial cell seeded on a-C:H:Si (SD10, thermally annealed at 600 °C) for 6 h and followed by seeding with platelets for 30 min

11.13 Bioassays and Assessment of Intracellular Activities

Bioassays are generally adopted biochemical protocols for assessing intracellular activities such as free ions concentration, radicals or even membrane potentials. These bioassays are based on the assumption that biomaterial–cellular interactions occurring over a reasonable length of time at the cell–biomaterials interfaces are able to triggers some intracellular event/processes via the cell mediators. Cell viability, cell proliferation, cell morphology and cytotoxicity are commonly determined and some live cell functions such as gene expression, apoptosis, level of protein phosphorylation, chemotaxis, endocytosis, cell secretions, cell transduction or production of cell signalling molecules such as nitric oxide or flux of Ca^{2+} and expression of CAM can be determined by some bioassays. The effect of the biomaterials surface features on first overlying protein biofilms and the morphological changes induced on these proteins result in some cellular events. Various bioassays exist and involve in most cases the use of various biochemical agents and reagents to assess some of the expressed biochemical mediators and/or enzymes (proteins). The results of the bioassays depend on the cell function being investigated and may be detected by microscopy, microplate (e.g. ELISA) readers and flow cytometry. There is some challenge in using bioassay to detect early biomaterial–cellular interactions occurring at the cell–material interface. Assessment of cell proliferation can be achieved by various bioassays: (a) the detection of proliferation associated antigens by immunohistochemical techniques, e.g. Ki-67 antigen [175], proliferating cell nuclear antigen, PCNA; (b) quantification of DNA synthesis by measuring tritiated thymidine, ^{3}H-thymidine or bromodeoxyuridine, BrdU uptake; (c) measurement of changes in total DNA content with DNA specific dyes (e.g. Hoechst 33258); (d) determination of intracellular metabolic activity or reduction state by Tetrazolium salts (MTT, XTT, MTS), or Alamar Blue reduction; (e) Determination of the optical absorbance of Neutral Red stained cells. Cell viability can be assessed by various methods: (a) Trypan Blue exclusion and Propidium iodide exclusion as these are excluded from the viable cells; (b) CFDA

staining, Crystal violet inclusion and Neutral red staining of viable cells; (c) Quantification of cell-mediated cytotoxicity by measurement of the LDH (lactate dehydrogenase) activity, measurement of the release of ^{51}Cr or Europium Titriplex V from labelled cells; (d) Alamar Blue reduction.

11.13.1 MTT Assay

MTT (3-(4,5-dimethylthiazol-2-yl)-2,5-diphenyl tetrazolium bromide; Sigma) was dissolved in PBS at 5 mg/ml concentration and filter sterilised inside the hood to remove a small amount of insoluble residues usually present in some batches of MTT. About 5 h before the end of the incubation period, 20 µl of MTT solution was added to each well including the blank wells (wells with added media, but no cells added). The plates were then transferred back to the incubator (37 °C) for 5 h. After the incubation period, the media were gently removed from all the wells with a syringe and 200 µl of DMSO were added to each of the wells (DMSO was handled in the dark, because it is unstable in the light). The plates were returned to the incubator for 5 min in order to dissolve air bubbles. These samples were then transferred to the Titertek+plus MS2 Microelisa reader and the optical density was read using a test wavelength of 550 nm and a reference wavelength of 660 nm. The plates were read within 1 hour of adding DMSO.

11.13.1.1 The Interaction of a-C:H and a-C:H:Si Thin Films with Bovine Retinal Pericytes

Another carefully selected cell in this study is the pericytes which are cells supporting the blood vessel walls. The bovine pericytes used in this study is from the eye compartment (retinal) which is a special compartment of the body. The pericytes and the other cells (human embryonic lung cells, L132, and Chinese hamster-V79 cell lines) used in this study were essentially used to examine the possible cytotoxicity/biocompatibility of the a-C:H:Si thin film biomaterial. The results (Fig. 11.22) show that when pericytes are seeded on 96-well plates coated with a-C:H and a-C:H:Si, the cells viability in these coated wells are comparable (and/or generally slightly better) to those in the non-coated TCPS (control) wells [37]. This is in agreement with reports in the literature using some other cell lines [74, 75]. a-C:H has also been reported to do well in both organ [74] and cell culture [75] when compared to the materials conventionally used for this purpose. It should be noted however that the MTT assay of different cell line could be different due to the origin, nature, function and rate of proliferation/metabolic activation state of the cells in culture. Growing pericytes on the surfaces of these as deposited thin films coated on silicon wafers are shown below, a-C:H (Fig. 11.23) and SD10 (Fig. 11.24).

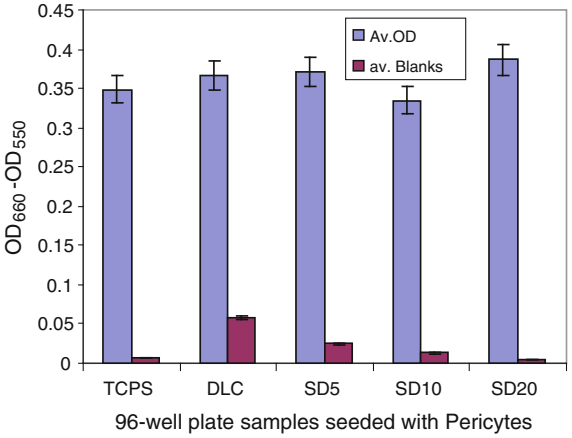

Fig. 11.22 MTT assay of pericytes seeded on standard tissue culture 96-well plates coated with a-C:H and a-C:H:Si (SD5-20), TCPS = control (uncoated) [37]

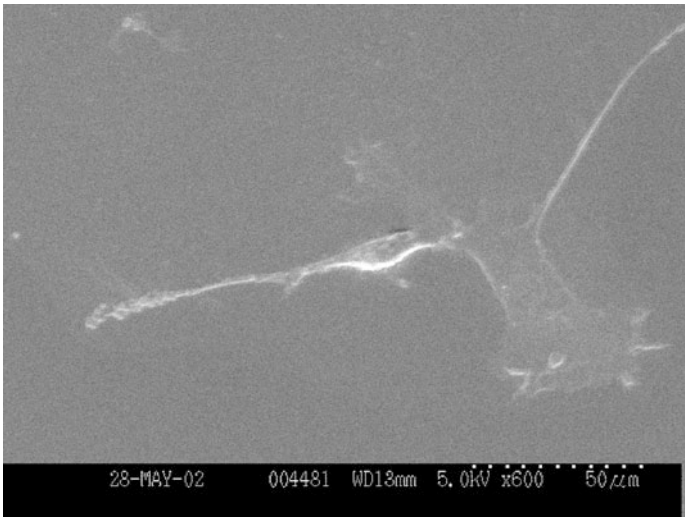

Fig. 11.23 Pericytes growing on the as deposited a-C:H after seeding for >12 h [37]

Pericytes are intimately associated with the vasculature and appear to be present in most tissues. They are generally considered to be restricted to the microvessels (arterioles, venules and capillaries where there are no smooth muscles) [176]. Pericytes embrace capillary, and their nuclei bulge outward rather than inward like endothelial nuclei. Pericytes are thought to contribute to endothelial cell proliferation, via selective inhibition of endothelial cell growth and lack of pericytes has lead to endothelial hyperplasia and abnormal vascular morphogenesis in the brain [177]. They exhibit small, oval cell body with multiple processes extending for

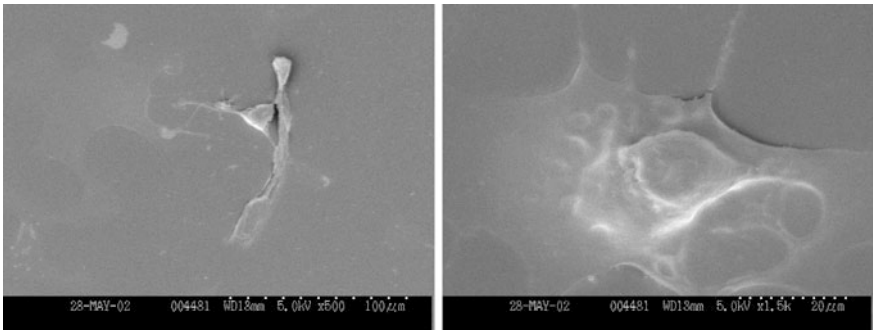

Fig. 11.24 Pericytes growing on the as deposited a-C:H:Si (SD10) after seeding for >12 h

some distances along the vessel axis and these primary processes then give rise to orthogonal secondary branches which encircle the vascular wall. They function as macrophages and have multiple suggested functions. Pericytes have a close physical association with the endothelium. Gap junction communication between pericyte and endothelial cells, as well as at endothelial–endothelial junctions, has been shown in vitro.

This SEM image (Fig. 11.24) shows that bovine retinal pericytes grow well in silicon-modified a-C:H thin films. On the whole these results show that bovine retinal pericytes grow well in both coated and uncoated TCPS tissue culture wells, thus the a-C:H and a-C:H:Si coatings are not toxic to these cells. Thus a-C:H and a-C:H:Si thin films could possibly function well in the eye compartment as materials for medical/optical prostheses. However, this study requires further investigation possibly with human pericytes and possibly to assess the differential cell attachment in relation to microstructural changes like the electrical properties, graphitisation and so on.

11.13.1.2 The Interaction of a-C:H and a-C:H:Si Thin Films with L132 Cell Line

The L132 cell line (human embryonic lung cells) originally purchased from ATCC (CCL-5), is epithelial and normal but with Hela characteristics. This cell line has Hela contamination and thus proliferates in a very rapid rate characteristic of Hela tumour cells. The results of MTT assay of L132 cell lines on 96-well TCPS plates coated with a-C:H and a-C:H:Si (Fig. 11.25) show that L132 cell lines proliferate well on both the uncoated TCPS (control) and the a-C:H, a-C:H:Si coated wells.

In this SEM images (Fig. 11.26), the L132 cell lines are seen growing on silicon wafer but, the morphology of these cells is not as good as those of the coated samples (Figs. 11.27, 11.28, 11.29 and 11.30), indicating possibly less proliferation in these samples. This could be attributed to high surface energy of this uncoated silicon wafer substrate.

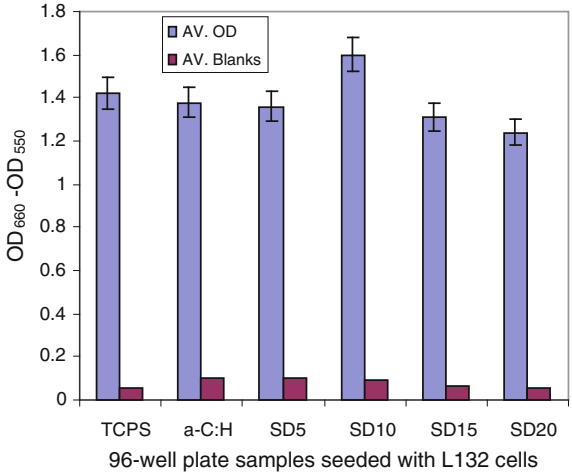

Fig. 11.25 MTT assay of L132 cells seeded on standard tissue culture 96-well plates coated with a-C:H and a-C:H:Si (SD5-20), TCPS = control

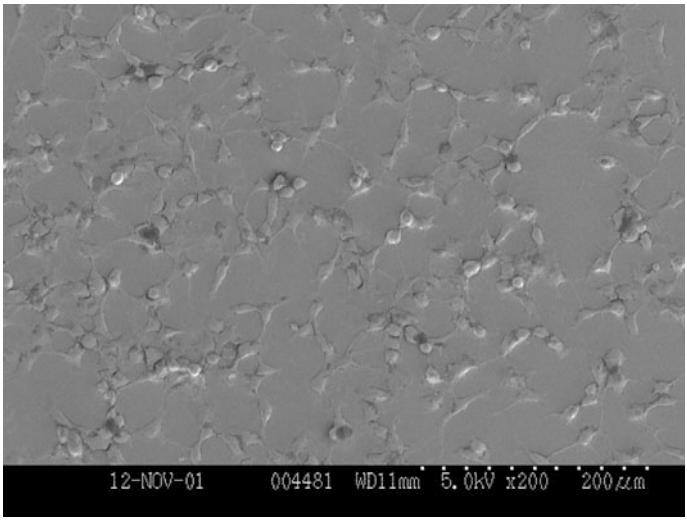

Fig. 11.26 SEM image of L132 cell lines seeded on uncoated silicon wafer samples

The L132 cell lines proliferate well on a-C:H samples as shown in Fig. 11.27. The morphology of these cells is clearly defined indicating a good proliferation in this sample.

Again the L132 cells are seen proliferating very well in this a-C:H:Si sample (Fig. 11.28). The morphology and spreading of these cells are better in this sample compared to the uncoated substrate. Compared to the a-C:H samples the morphology and spreading seem to be slightly better in these silicon-doped samples.

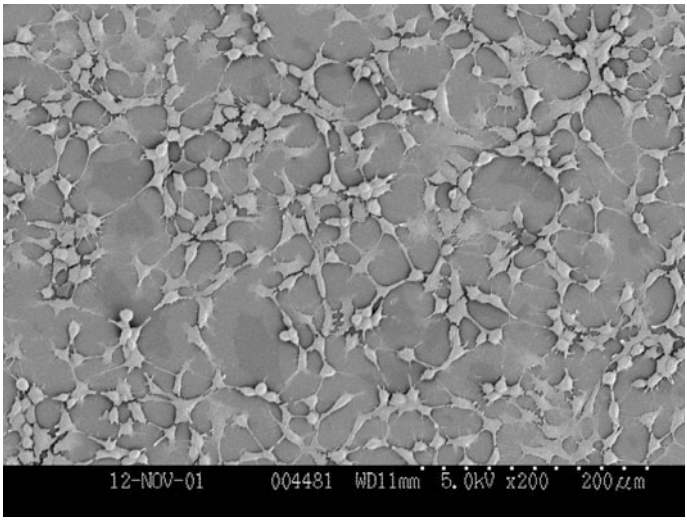

Fig. 11.27 SEM image of L132 cell lines seeded on as deposited a-C:H sample

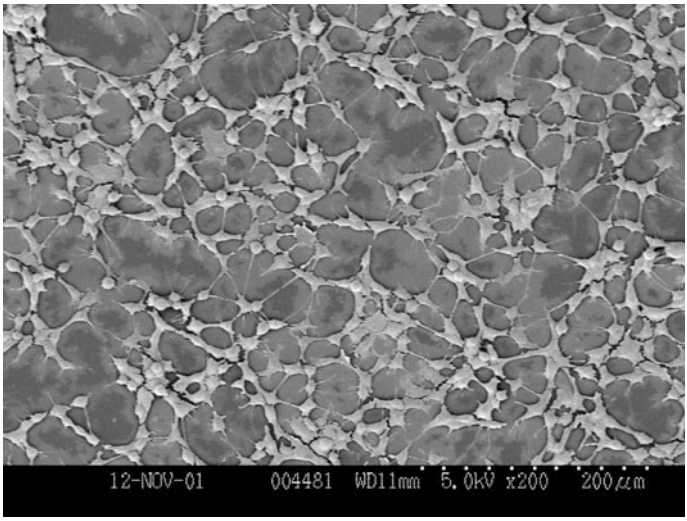

Fig. 11.28 SEM image of L132 cell lines seeded on as obtained a-C:H:Si (SD10) sample

In a-C:H (Fig. 11.29) and a-C:H:Si (Fig. 11.30) films thermally annealed at 400 °C the L132 cells are seen proliferating fairly well. Though the onset of graphitisation is expected at this temperature in the a-C:H film thermally annealed at 400 °C, the proliferation of L132 cells on these samples does not seem to reflect this. This could be attributed to the nature of this Hela-contaminated cell line. These cell lines are contaminated with Hela cells (high proliferation/cancerous) and are

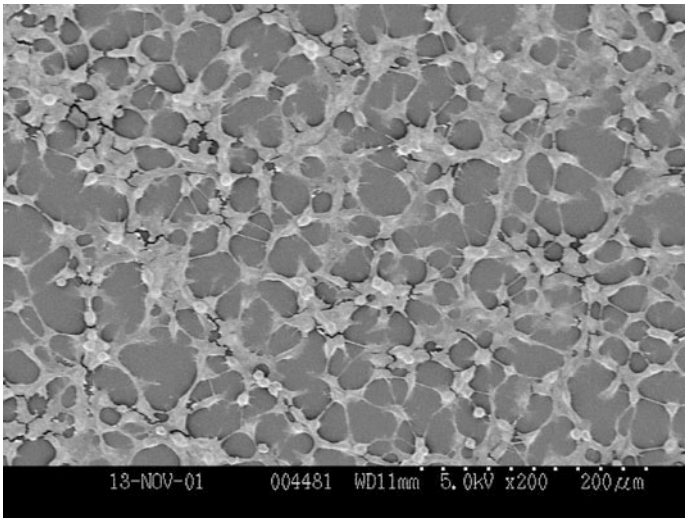

Fig. 11.29 SEM image of L132 cell lines seeded on a-C:H (thermally annealed at 400 °C)

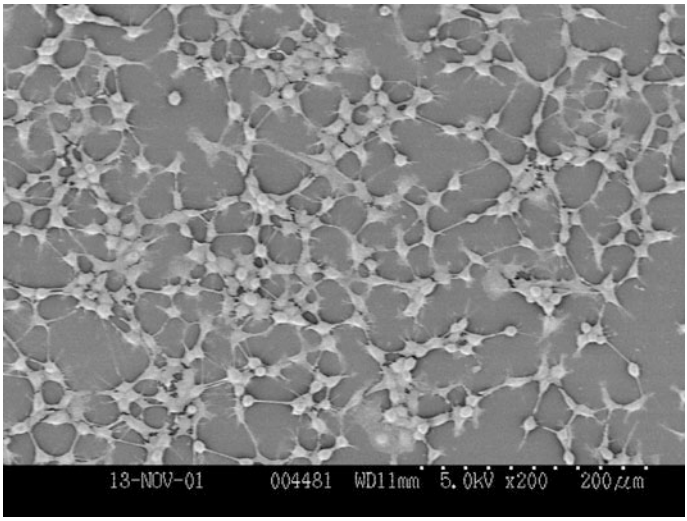

Fig. 11.30 SEM image of L132 cell lines seeded on a-C:H:Si (SD5, thermally annealed at 400 °C)

suitable for investigating cellular toxicity but may not be sensitive enough for assessing differential cell proliferation on closely varied sample surface properties due to this contamination on the original cell line.

However, thermal annealing at higher temperature 600 °C, thought to produce high graphitic films which does show a poor proliferating/spreading L 132 cell lines (Fig. 11.31). This a-C:H sample thermally annealed at 600 °C shows the L132 cells

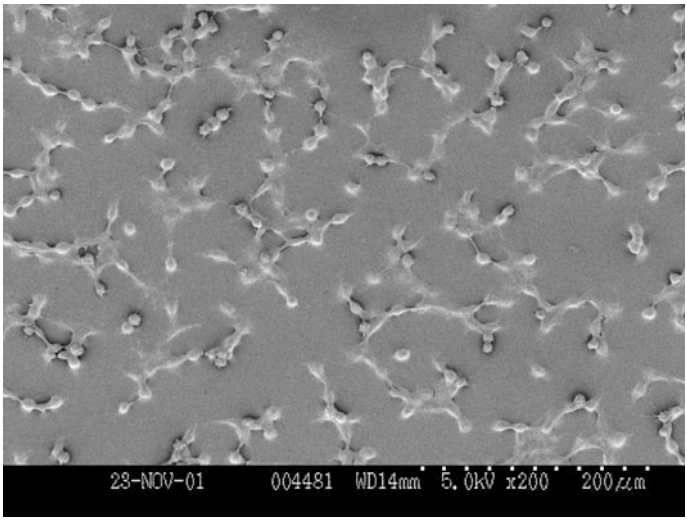

Fig. 11.31 SEM image of L132 cell lines seeded on a-C:H (thermally annealed at 600 °C)

growing on the sample but with poorly defined morphological features similar to that observed on the uncoated sample (Fig. 11.26). This poorly defined morphology could be attributable to graphitisation in this film. Thus low contact angle (high surface energy) and graphitisation may lead to impaired L132 cell spreading and morphology.

11.13.1.3 The Interaction of a-C:H and a-C:H:Si Thin Films with V79 Cell Line

Figure 11.32 shows the MTT assay of Chinese Hamster cell line (V79) on uncoated TCPS (control), a-C:H and a-C:H:Si coated 96-well plate standard tissue culture plates. The cells proliferate well on the coated and uncoated control plates, but generally the cells seem to proliferate slightly better on the coated samples. This could be attributed to the change in surface energy in these as obtained thin film coatings. This result also agrees with reports in the literature using some other cell lines [74, 75], a-C:H has been reported to do well in both organ [74] and cell culture [75] when compared to the materials conventionally used for this purpose.

In summary, it could therefore be inferred from this section that endothelial cells prevent platelet adhesion and aggregation. The a-C:H and a-C:H:Si thin films are not toxic to the bovine retinal pericytes, the L132 (human embryonic lung) cell line and the Chinese hamster (V79) cell lines. Based on these MTT assay results it seems that these cells seem to proliferate slightly better in the a-C:H and a-C:H:Si coated wells compared to uncoated TCPS conventionally used for cell culture.

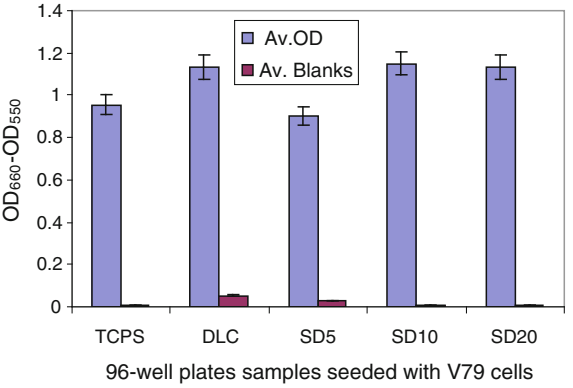

Fig. 11.32 MTT assay of V79 cells (Chinese hamster) seeded on standard tissue culture 96-well plates (*TCPS*) coated with a-C:H and a-C:H:Si (*SD*)

11.13.2 Other Bioassays Techniques

Alamar Blue Assay

The Alamar Blue dye contains a fluorometric/colorimetric growth indicator which detects metabolic activity in the cell. Cell growth causes a chemical reduction of the medium; this causes the Redox indicator to change from an oxidised, non-fluorescent blue colour, to a reduced, fluorescent red colour. The indicator has been shown to be minimally toxic to living cells and produces a clear, stable, distinct colour change. When the assay is completed the Alamar Blue dye can be removed and the cells can be used for further experiments.

See samples with 1×10^5 cells per well in a 6 well plate with 3 ml of the RPMI medium. Incubate cells in standard incubator (37 °C and 5 % CO_2). Perform test at chosen/different day/time points. Prepare 1:20 dilution of the stock solution of Alamar Blue dye by adding 1 ml of Alamar Blue and 19 ml of Hank's Balanced Salt Solution (HBSS). Wash cells twice with HBSS and add the Alamar Blue dye to each well in 2.5 ml volumes. Incubate at 37 °C and 5 % CO_2 for 90 min. Following incubation, volumes of 100 µl were taken from each well in duplicate and added to a black 96 well plate. Read the fluorescence on a fluorescence reader at excitation 530 nm and emission 590 nm.

DNA Assay

The DNA content of cell suspensions can be measured using the binding of bis-benzamide to DNA. Prepare a stock solution of (bis-benzamide) 33258 by the addition of 1 mg of the dye to 1 ml deionised water, covered in foil and stored at 4 °C. Prepare a 1:50 dilution of the 1 mg/ml bis-benzamide with TNE buffer, to give a working solution of 20 µg/ml. Lyse cells to release DNA, using a freeze thaw method by freezing at −80 °C and allowed to thaw; repeat procedure three times. Add sample volumes of 50–50 µl of TNE buffer and 100 µl of bis-benzamide 33258. Read plate on the plate reader at excitation wavelength of

360 nm and an emission wavelength of 460 nm. Determined values against a calf thymus DNA standard curve and displayed as µg/ml.

Hydrogen Peroxide Production: Dichlorofluorescein Diacetate Assay

The dichlorofluorescein diacetate assay was employed to measure the amount of H_2O_2 peroxide production from cells, e.g. monocytes following growth on materials. The generation of reactive oxygen intermediates, such as H_2O_2, is usually increased in inflammatory, injury and repair processes.

Prepare a 1 mM stock solution of dichlorofluorocein diacetate by the addition of 4.87 mg of dichlorofluorocein diacetate (DCFH-DA) to 10 ml of ethanol. Suspend monocytes in Hanks balanced salt solution without phenol red. Seed samples with 5×10^5 cells in a 6 well plate, with 2 ml of Hanks balanced salt solution. Incubated for 3–4 h in a standard incubator (37 °C and 5 % CO_2). As a positive control, 1 µg/ml PMA [178] should be added to cells to give a final concentration of 50 ng/ml. After incubation, add 10.2 µl of 1000 µM DCFH-DA to each well and incubated for 1 h at 37 °C and 5 % CO_2. After incubation, transfer 100 µl to a 96 well plate. Read plate on a fluorescence plate reader at an excitation wavelength of 485 nm and an emission wavelength of 528 nm.

11.14 In Vivo Studies of Carbon-Based Materials: Cell–Tissue Interactions In Situ

11.14.1 In Vivo Studies on the Biocompatibility and Hemocompatibility of DLC

Allen et al. [109] implanted DLC-coated cobalt-chromium cylinders in the intramuscular locations in rats and in transcortical sites in sheep and their histological analysis of specimens retrieved 90 days after surgery showed that the DLC-coated specimens were well tolerated in both sites [109].

Fournier et al. [179] has shown from their clinical and angiographic data that the ***hydrogenated silicon carbide coating*** of the Tenax coronary stent may indeed play a beneficial role in patient outcome, and should therefore be evaluated by prospective clinical trials. They implanted the prostheses (231 Tenax stents) in 206 patients (62 ± 5 years) in the patients left anterior descending (51 %) and right coronary arteries (36 %). Their results show that revascularization was complete in 70 %, elective in 80 %, and the implantation was direct in 25 % of the cases and that the procedure was successful in all the lesions, reducing stenosis from 62 ± 16 to 16 ± 10 % and increasing the minimal luminal diameter from 0.81 ± 0.40 to 2.61 ± 0.59 mm. Also the TIMI flow was reduced in 30 %, but normalised after the stent in all but one case. They also reported that the incidence of cardiac events was minimal: 1 acute thrombosis (0.5 %) resolved by a new angioplasty and 1 non-Q myocardial infarction (0.5 %) and finally at the 6-month clinical follow-up 10 % of the patients presented complaints of angina greater than class II [179].

De Scheerder et al. [180] investigated the in vivo biointeraction with one particular class of modified DLC coatings: diamond-like nanocomposite coatings (DLN or Dylyn, Bekaert, Kortrijk, Belgium). Either coated or non-coated stents were randomly implanted in two coronary arteries of 20 pigs so that each group contained 13 stented arteries. Pigs underwent a control angiogram at 6 weeks and were then sacrificed. They performed a quantitative coronary analysis before, immediately after stent implantation, and at 6 weeks using the semi-automated Polytron 1000 system (Siemens, Erlangen, Germany). They also performed a morphometry using a computerised morphometric program and their angiographic analysis showed similar baseline selected arteries and post-stenting diameters. At 6-week follow-up, they discovered no significant difference in minimal stent diameter and their histopathological investigation revealed a similar injury score in the three groups. According to De Scheerder et al. [180] inflammatory reactions were significantly increased in the DLN–DLC coating group, thrombus formation was significantly decreased in both coated stent groups and neointimal hyperplasia was decreased in both coated stent groups; however, the difference with the non-coated stents was not statistically significant; and also area stenosis was lower in the DLN-coated stent group than in the control group (41 ± 17 % vs. 54 ± 15 %; $p = 0.06$). in their conclusion they indicated that the diamond-like nanocomposite stent coatings are compatible, resulting in decreased thrombogenicity and decreased neointimal hyperplasia and covering this coating with another DLC film resulted in an increased inflammatory reaction and no additional advantage is compared to the single-layer diamond-like nanocomposite coating [180].

Tran et al. [181] reviewed the mechanical heart valves' (MHV) thrombogenicity and pointed out that the application of surface modification technology to reduce the incidence of thrombus formation on MHV is a novel undertaking requiring the collaboration within the bioengineering and cardiothoracic surgery fields. From reviewing results of recent and past investigations, and their own preliminary study with DLC coating and plasma or glow discharge treatment (GDT) of MHV, they identified and discussed several potentially beneficial effects that may reduce the extent of valve-related thrombogenesis by surface modification: DLC and GDT may affect the surfaces of MHV in many ways, including cleaning of organic and inorganic debris, generating reactive and functional groups on the surface layers without affecting their bulk properties, and making the surfaces more adherent to endothelial cells and albumin and less adherent to platelets; therefore these different effects of surface modification, separately or in combination, may transform the surfaces of MHV to be more thromboresistant in the vascular system [181].

Dowling et al. [69] implanted two DLC-coated and uncoated stainless steel cylinders into both cortical bone (femur) and muscle (femoral quadriceps) sites of six adult (>40 kg) sheeps, for a period of 4 weeks (three sheep) and the rest for 12 weeks. According to Dowling et al. [69] after explantation of the implants and the pathological/histological examination of the implanted cylinders, no macroscopic adverse effect was observed on both the bone and the muscles of the used sheep.

Yang et al. [9, 10] examined in vivo interactions of dics coated with TiN, DLC (deposited on SS316L disc using PVD) and or Pyrolytic carbon (PyC) films, implanted into the descending aorta of anaesthesized sheep (6 animals) for 2 h. They evaluated the three different samples simultaneously in each animal. After explantation they examined the thombus-free area on the disc with close-up photography and planimetry, and the test surfaces with SEM. Yang et al. [9, 10] found out that there were many leucocytes adherent, activated and spread onto PyC and DLC, but on TiN it was the erythrocytes that were mainly adherent [9, 10].

Patients using implanted prostheses are faced with life-threatening bleeding problems because they are kept under life-long anticoagulant therapies in order to reduce the risk of thromboembolism. In order to reduce the risk of platelet aggregation/thromboembolism and complications following the life-long course(s) of anticoagulants, the biomaterials need to be improved in order to achieve better haemocompatibility. Platelet aggregation in the surfaces of these prostheses is the key factor in thrombus formation. The platelets is known to play a crucial role in blood clotting/thrombus formation which is indicative of the ability of a foreign body to trigger off clot formation and or thrombosis which may impair free flow of blood and result in some damaging effect on the internal body organs.

11.14.2 Summary

In this chapter, the role of microstructure, electrical properties and surface energy of amorphous hydrogenated carbon (a-C:H) and silicon-modified a-C:H (a-C:H:Si) in relation to their biocompatibility/haemocompatibility interactions with human microvascular endothelial cells and human platelets have been investigated in full. Preliminary investigations on nitrogen modified films (a-C:H:N) and a-C:H, a-C:H:Si interactions with other cell lines have been carried out. The findings are summarised as follows:

Microstructure

- The microstructure was tailored by the films deposition parameters, silicon and nitrogen doping and thermal annealing.
- Surface roughness: a-C:H, a-C:H:Si and a-C:H:N are ultrasmooth thin films that can be used to improve the surface features necessary for improved biocompatibility in biomedical implants and devices made with conventionally rougher metals or polymers for example. Silicon incorporation seems to slightly increase the surface roughness. Thermal annealing also seems to increase slightly the surface roughness.
- Intrinsic Compressive stress: stress reduction in the film seems to be important in improving biocompatibility. Stress reduction was achieved by thermal annealing of the films. Silicon incorporation also seems to reduce the intrinsic stress in the film. Lowered intrinsic stress is associated with decreased surface energy.

- Graphitisation: excessive graphitisation seems to impair biocompatibility. Graphitisation occurs at annealing temperature greater than 400 °C in a-C:H thin films and may occur as well in a-C:H:Si film at a higher annealing temperatures of ~600 °C. Silicon seems to lower the rate and degree of graphitisation in a-C:H and thereby improving hemocompatibility.
- The sp^2/sp^3 ratio and the sp^2 cluster size in the sp^3 matrix and not the absolute sp^2 or sp^3 content play a role in hamocompatibility.
- Silicon doping of a-C:H thin films decreases the I_D/I_G ratio and on annealing the I_D/I_G ratio starts to increase above 300 °C of annealing temperature.

Electrical properties

- Conductivity/resistivity: silicon incorporation lowers the resistivity (Fig. 11.33) of a-C:H thin film from 6.7×10^{10} Ω cm (a-C:H) to 5.4×10^9 Ω cm (a-C:H:Si) and thereby increased the conductivity. Increased conductivity (without graphitisation) is associated with an improved haemocompatibility (Fig. 14.1). Resistivity behaviour is electric field dependent, and for high amount of silicon, the resistivity first increases and then later decreases as the field increases ($\geq$ 1.5–1.8×10^4 V/cm).
- Work Function: Lower work functions in the examined films seem to improve biocompatibility. Silicon doping and nitrogen doping seem to lower the WF. Silicon doping lowers the WF from 4.77 eV (a-C:H) to 4.56–4.34 eV (a-C:H:Si), a reduction of 0.21–0.43 eV. Silicon atomic percentage concentration of up to ~7.61 % (TMS = 10 sccm) led to a rapid jump in decrease of WF.
- Band gap: Optical band gap was determined by ellipsometry technique. Silicon addition seems to increase the optical band gap energy. The optical gap values depend on the type of transition assumed and the model used for the calculation.

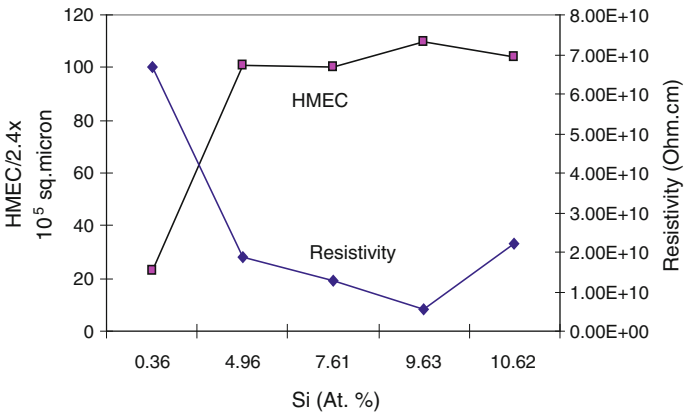

Fig. 11.33 HMEC adhesion related to resistivity as a function of percentage atomic concentration of silicon in a-C:H thin films

- The author suggests that the density of states (DOS) and charge carriers could play a greater role compared to the optical band gap energy. Moderate amount of silicon (≤ 10 at.%) seems to increase the DOS in the sp^2 cluster region even though silicon does not form π-bond. There is however the need to establish the exact DOS distribution, at the extended states, at the mobility edge, the band tail or the defect states in the valence and conduction band within the band structure; and for the band gap determination there is need to ascertain the degree (percentage) of different electrons in (assumed different) transitions (Fig. 11.34).

Surface energy/contact angle

- Contact angle: a higher contact angle seems to improve hemocompatibility. Silicon incorporation increases the contact angle (by up to $\sim 17°$) while nitrogen incorporation decreases it (Fig. 11.35).

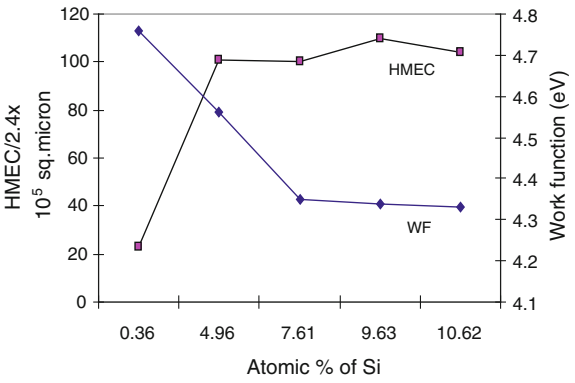

Fig. 11.34 HMEC adhesion related to the work function of a-C:H thin films as a function of percentage atomic concentration of silicon in the a-C:H thin films

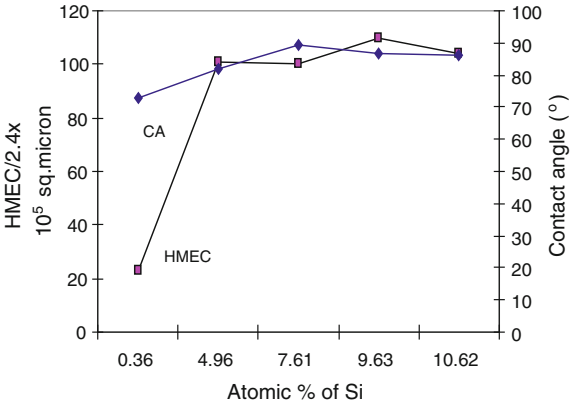

Fig. 11.35 HMEC adhesion related to the water contact angle of a-C:H films as a function of percentage atomic concentration of silicon in a-C:H thin films

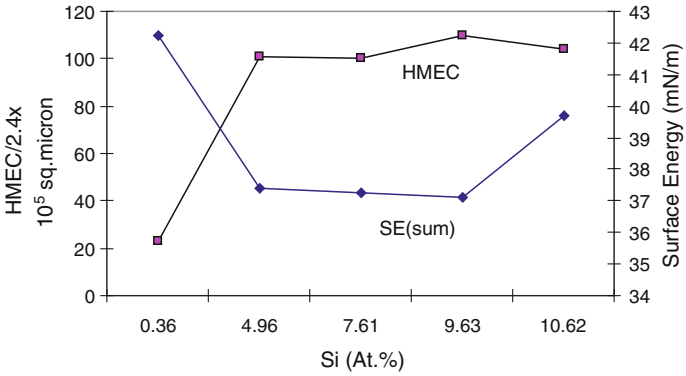

Fig. 11.36 HMEC adhesion related to the surface energy (sum) of a-C:H films as a function of percentage atomic concentration of silicon in a-C:H thin films

- Surface energy: About 99 % of the surface energy components of a-C:H:Si and a-C:H are dispersive and seem to be responsible for the biocompatibility of these thin films. Silicon addition decreased the surface energy by ~5–10 mN/m (Fig. 11.36).

Cellular interactions

- Cellular origin-specie differences: Human cells are relevant to biocompatibility studies for biomedical use in man and seem to be much more sensitive than cells from other species that may not be relevant to man.
- Cell specificity/function/sensitivity: Human cells should be carefully chosen from tissue of interest for biocompatibility studies in relation to those tissues for specific application in the particular tissue, organ and or system. Endothelial cells and platelets seem to be the most suitable cells in the blood compatibility studies.
- The results of these investigations have shown that microstructural changes in the films, especially the electrical conductivity, work functional changes, the contact angle/surface energy and the degree of graphitisation in these films play a key role in especially the haemocompatibility of these thin films. These physical changes are easily detected when these thin films interact with microvascular endothelial cells and human platelets in vitro. However, with other cell lines which may not be human and which may not play crucial roles like the endothelial cells and platelets, these changes may not easily be detected. Nevertheless these other cells may be good enough in investigations to say whether or not a material is just cytotoxic.
- MTT assay reveals that a-C:H and a-C:H:Si are generally not toxic to the cells, and may in some cases even encourage better cell proliferation when compared to tissue culture polystyrene (TCPS) conventionally used for cell culture.

Film adhesion in biological fluids

- Si-DLC-coated stainless steel substrates were also immersed in various biological fluids (Saliva, PBS and FCS) similar to human body fluids incubated at body temperature. The adhesion properties of the films were tested using both the four-point bend test and the pull tensile substrate plastic straining techniques. With the use of SEM the crack initiation strain and the saturation crack spacing were determined. Statistical analysis of the data using two-parameter Weibull, lognormal probability density function models as well as Gamma function suggests long-term reliability and good adhesion of Si-DLC to stainless steel and metallic substrates if used in biomedical implants and devices in continuous contact with body fluids.

Silicon doping of a-C:H lowers the WF, the resistivity, the surface energy of the films and the rate and degree of graphitisation in the films. Silicon doping also

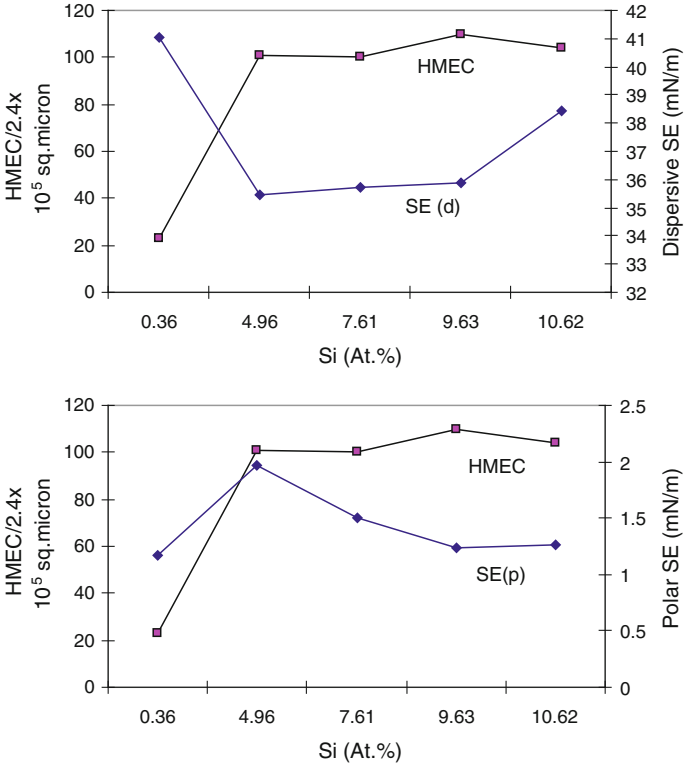

Fig. 11.37 HMEC adhesion related to the surface energy (dispersive and polar components) of a-C:H films as a function of percentage atomic concentration of silicon in a-C:H thin films

improves the adhesion of a-C:H thin films to its substrates. The a-C:H:Si thin films and conducting a-C:H thin films with less internal stress and less degree of graphitisation are good haemocompatible materials suitable for biomedical applications as in heart valve prostheses, stents, etc (Fig. 11.37).

Generally, a-C:H and a-C:H:Si are non-toxic to cells in vitro. Also a-C:H:Si coated stainless steel on immersion and incubation inside biological fluids have shown good shear strength and are therefore suitable for use for biomedical applications.

11.15 Ongoing and Future Investigations

- ^{13}C-NMR and the X-ray excited Auger electron spectroscopy studies of a-C:H:Si.
- Determination of exact amorphous–crystal structure, bond angles, bond angle disorders, number of and or distributions of dangling bonds, and dislocations in the films.
- Density of States (DOS) determination in a-C:H, a-C:H:Si, a-C:H:N and a-C:H:Me.
- Determination of the effective band gaps of the a-C:H:Si -Protein-Cellular system and to relate the interactions with the DOS and/or the band gap.
- The reported results and discussions termed 'preliminary investigations' are under further investigation.
- The interaction of a-C:H and a-C:H:Si with proteins with adhesive and non-adhesive functions needs to be investigated in order to see the exact role of these proteins in biocompatibility and haemocompatibility. The role and the mechanism interaction of CAM should be investigated. Surface Plasmon Resonance (SPR) technique is envisaged to be useful in monitoring these interacting proteins in situ.
- The effects of a-C:H, a-C:H:Si and a-C:H:N optical properties on cellular growth and interaction in situ.
- Optical techniques to monitor the underside of cells, the mechanism of cell attachment, cell proliferation and density of distribution over the attached surfaces of a-C:H, a-C:H:Si and a-C:H:N coated transparent/glass substrates. By measuring the refractive indices of the glass, the medium (protein layer without cells), the cells and how the refractive index changes, the cell density and the cell cytoskeleton and how they change when the cell attaches to the surface can be monitored (Fig. 11.38).

The relative intensity, R, of the reflected light at the interfaces of the glass and cell is given by

$$\mathrm{R} = \left(\frac{r_g - r_c}{r_g + r_c}\right)^2 \tag{1}$$

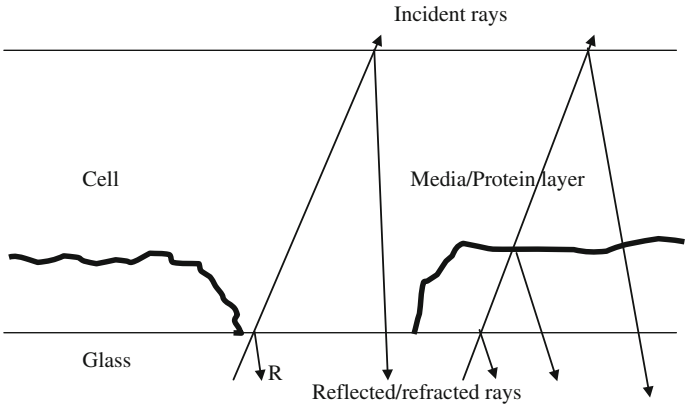

Fig. 11.38 Illustration of principles of optical method of cell characterization [182]

$$r_c = r_g \times \frac{1-\sqrt{R}}{1+\sqrt{R}}$$

where r_c = Refactive index of cell; r_g = refractive index of glass.

In this case, the refractive index of a-C:H, a-C:H:Si (SD) or a-C:H:N thin film coating has to be substituted in the above equation:

$$\mathrm{R} = \left(\frac{r_{SD}-r_c}{r_{SD}+r_c}\right)^2 \tag{2}$$

$$r_c = r_{SD} \times \frac{1-\sqrt{R}}{1+\sqrt{R}}$$

The cytoplasmic content of the cells follows the distribution of the cellular attachments on the substrates/samples. Therefore, regions of focal or more condensed cellular attachment imply heavy density of cytoplasm and a relatively higher refractive index. The cellular microfilaments and cytoskeleton are condensed in the region of attachment, thereby allowing less amount of light to pass through and thus a higher refraction occurring. Well spread cells on the other hand have more widely distributed cytoplasmic content since the volume of the cytoplasm is relatively the same (the larger the area, the lesser the thickness for the same volume of material inclusion). However, there has to be an assumption that the same thickness of protein interlayer exists between every cell and the substrate at the points of cell attachment, and at regions where there is no attached cells but just layer of protein/culture media. For further reading refer to [183, 184].

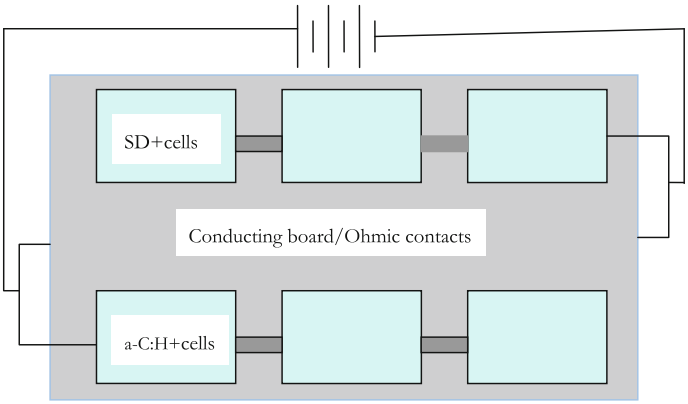

Fig. 11.39 Schematics of the layout for applying electric field on the coatings with seeded cells in culture

- Further investigation on the role of surface charges is needed. By applying a small electric field (not to affect the cells) through the film while the cells are growing in culture will help to redistribute the charges (11.39).
- Similarly, impedance spectroscopy can be used to monitor the cell growth and distribution on the a-C:H, a-C:H:Si and a-C:H:N thin film coatings in situ.
- For a-C:H, a-C:H:Si and a-C:H:N to find their way into routine use as biomedical prostheses, they need to be tested in vivo with animals with close physiological relation with the humans, e.g. the baboons.
- Extensive clinical trials of a-C:H, a-C:H:Si and a-C:H:N coated implant.

References

1. Bittl, J. A. (1996). Advances in coronary angioplasty. *New England Journal of Medicine, 335*, 1290–1302.
2. Gawaz, M., Neumann, F. J., Ott, I., May, A., & Schomig, A. (1996). *Circulation, 94*, 279–285.
3. Inoue, T., Sakai, Y., Fujito, T., Hoshi, K., Hayashi, T., Takayanagi, K., et al. (1996). *Circulation, 94*, 1518–1523.
4. Lahann, J., Klee, D., Thelen, H., Bienert, H., Vorwerk, D., & Hocker, H. (1999). *Journal of Materials Science: Materials in Medicine, 10*, 443–448.
5. Haycox, C. L., & Ratner, B. D. (1993). *Journal of Biomedical Materials Research, 27*, 1181–1193.
6. Courtney, J. M., Lamba, N. M. K., Sundaram, S., & Forbes, C. D. (1994). *Biomaterials, 15*, 737–744.
7. Klein, C. L., Nieder, P., Wagner, M., Kohler, H., Bittinger, F., Kirkpatrick, C. J., et al. (1994). *Journal of Pathophysiology, 5*, 798–807.
8. Gutensohn, K., Beythien, C., Koester, R., Bau, J., Fenner, T., Grewe, et al. (2000) *Infusionstherapie und Transfusionmedizin, 27*(4), 200–206.

9. Yang, Y. (1996). S. F Franzen, C.L Olin. *Cells and Materials, 6*(4), 339–354.
10. Yang, Y., Franzen, S. F., & Olin, C. L. (1996). *The Journal of Heart Valve Disease, 5*, 532–537.
11. Bittl, J. A. (1996). Subacute stent occlusion: Thrombus horribilis. *JACC, 28*, 368–370.
12. Mark, K., Belli, G., Ellis, S., & Moliterno, D. (1996). *Journal of the American College of Cardiology, 27*, 494–503.
13. Colombo, A., Hall, P., Nakamura, S., Almagor, Y., Maiello, L., Martini, G., et al. (1995). *Circulation, 91*, 1676–1688.
14. Gott, V. L., Koepke, D. E., Daggett, R. L., Zarnstorff, W., & Young, W. P. (1961). The coating of intravascular plastic prostheses with colloidal graphite. *Surgery, 50*, 382–389.
15. Haubold, A. (1977). *Annals of the New York Academy of Sciences, 283*, 383.
16. Goodman, S. L., Tweden, K. S., & Albrecht, R. M. (1996). Platelet interaction with pyrolytic carbon heart-valve leaflets. *Journal of Biomedical Materials Research, 32*, 249–258.
17. Baier, R. E. (1972). *The Bulletin of the New York Academy of Medicine, 48*, 273.
18. Williams, D. F. (1989). *Journal of Biomedical Engineering, 11*, 185.
19. Salzman, E. (Ed.). (1981). *Interaction of blood with natural and artificial surfaces*. New York: Marcel Dekker.
20. Gordon, J. L. (1986). In J. P. Cazenave, J. A. Davies, M. D. Kazatchkine, & W.G. van Aken (Eds.), *Blood-surface interactions: Biological principles underlying hemocompatibility with artificial materials* (p. 5). Amsterdam: Elsevier Science Publishers (Biomedical Division).
21. Cenni, E., Arciola, C. R., Ciapetti, G., Granchi, D., Savarino, L., Stea, S., et al. (1995). *Biomaterials, 16*, 973–976.
22. Herring, M. B., Gardner, A. & Gloves, J. A. (1978). *Surgery, 84*, 498.
23. Remy, M., Bordenave, L., Bareille, R., Rouais, F., Baquey, C., Gorodkov, A., et al. (1994). *Journal of Materials Science Materials in Medicine, 5*, 808.
24. Pesakova, V., Klezl, Z., Balik, K., & Adam, M. (2000). *Journal of Material Science: Materials in Medicine, 11*, p797.
25. Hallab, N. J., Bundy, K. J., O'Connor, K., Clark, R., & Moses, R. L. (1995) *Journal of Long-Term Effects of Medical Implants, 5*, 209.
26. Ahluwalia, A., Basta, G., Chiellini, F., Ricci, D., & Vozzi, G. (2001). *Journal of Material Science: Materials in Medicine, 12*, 613–619.
27. Bowlin, G. L., & Rittger, S. E. (1997). *Cell Transplantation, 6*, 623.
28. Altankov, G., & Grott, T. (1997). *Journal of Biomaterials Science, Polymer Edition, 8*, 299.
29. Grinnell, F. (1978). *International Review of Cytology, 53*, p65.
30. Van Wachem, P. B., Schakenraad, J. M., Feijen, J., Beugeling, T., van Aken, W. G., Blaauw, E. H., et al. (1989). *Biomaterials, 10*, 532–539.
31. Van Wachem, P. B., Beugeling, T., Feijen, J., Bantjes, A., Detmers, J. P., & van Aken, W. G. (1985). *Biomaterials, 6*, 403–408.
32. McLaughlin, J., Meenan, B., Maguire, P., & Jamieson, N. (1996). Properties of diamond like carbon thin film coatings on stainless steel medical guidewires. *Diamond and Related Materials, 8*, 486–491.
33. Jones, M. I., McColl, I. R., Grant, D. M., Parker, K. G., & Parker, T. L. (1999). Hemocompatibility of DLC and TiC-TiN interlayers in titanium. *Diamond and Related Materials, 8*, 457–462.
34. Okpalugo, T. I. T., Ogwu, A. A., Maguire, P., & McLaughlin, J. A. D. (2001). Technology and health care. *International Journal of Health Care Engineering, 9*(1–2), 80–82.
35. Okpalugo, T. I. T., Ogwu, A. A., Maguire, P. D., McLaughlin, J. A., & Hirst, D. G. (2004). In-vitro blood compatibility of a-C:H: Si and a-C: H thin films. *Diamond and Related Materials, 13*(4–8), 1088–1092.
36. Okpalugo, T. I. T., Ogwu, A. A., Maguire, P. D., & McLaughlin, J. A. (2004). Platelet adhesion on silicon modified hydrogenated amorphous carbon films. *Biomaterials, 25*(3), 239–245.
37. Okpalugo, T. I. T., McKenna, E., Magee, A. C., McLaughlin, J. A., & Brown, N. M. D. (2004). The MTT assays of bovine retinal pericytes and human microvascular endothelial

cells on DLC and Si-DLC-coated TCPS. *Journal of Biomedical Materials Research, Part A, 71A*(2), 201–208.
38. Okpalugo, T. I. T., Maguire, P. D., Ogwu, A. A., & McLaughlin, J. A. (2004). The effect of silicon doping and thermal annealing on the electrical and structural properties of hydrogenated amorphous carbon thin films. *Diamond and Related Materials, 13*(4–8), 1549–1552.
39. Okpalugo, T. I. T., Ogwu, A. A., Maguire, P. D., McLaughlin, J. A., & McCullough, R. W. (2006). Human micro-vascular endothelial cellular interaction with atomic N-doped compared to Si-doped DLC. *Journal of Biomedical Materials Research Part B: Applied Biomaterials, 78B*(2), 222–229.
40. Okpalugo, T. I. T. (2002). The hemocompatibility of ultra-smooth silicon and nitrogen doped hydrogenated amorphous carbon thin films—The role of the microstructure, electrical properties, and surface energy (G2c., Ph.D., Ulster, 53-4066). (BL: DXN062999).
41. Parker, T. L., Parker, K. L., McColl, I. R., Grant, D. M., & Wood, J. V. (1993). *Diamond and Related Materials, 93*, 118.
42. Dion, I., Roques, X., Baquey, C., Baudet, E., Basse Cathalinat, B., & More, N. (1999). *Biomedical Materials and Engineering, 3*, 51–55 (spring).
43. O'Leary, A., Bowling, D. P., Donnelly, K., O'Brien, T. P., Kelly, T. C., Weill, N., et al. (1995). *Key Engineering Materials, 99–100*, 301–308.
44. Freitas, R. A., IMM report number 12. http://www.imm.org/reports/rep012.html
45. Allen, M., Law, F. C., & Rushton, N. (1994). *Clinical Materials, 17*, p1–p10.
46. Allen, M. J., Myer, B. J., Law, F. C., & Rushton, N. (1995). *Transaction of Orthopaedic Research Society, 20*, 489.
47. Szent-Gyorgyi, A. (1957). *Bioenergetics*. New York: Academic Press.
48. Szent-Gyorgyi, A. (1946). *Nature, 157*, 875.
49. Eley, D. D., Parfitt, G. D., Perry, M. J., & Taysum, D. H. (1953). *Transactions of the Faraday Society, 49*, 79.
50. Postow, E., & Rosenberg, B. (1970). *Bioenergetics, 1*, 467.
51. Bruck, S. D. (1965). *Polymer, 6*, 319.
52. Bruck, S. D. (1967). *Journal of Polymer Science Part C, 17*, 169.
53. Bruck, S. D. (1973). Intrinsic semiconduction, electronic conduction of polymers and blood compatibility. *Nature, 243*, 416–417.
54. Bruck, S. D. (1975). The role of electrical conduction of macromolecules in certain biomedical problems. *Polymer, 16*, 25.
55. Van Oss, C. J. (1978). Phagocytosis as a surface phenomenon. *Annual Review of Microbiology, 32*, 19–39.
56. Kochwa, S., Litwak, R. S., Rosenfield, R. E., & Leonard, E. F. (1977). *Annals of New York Academy of Sciences, 283*, 37.
57. Lettington, A. H. (1991). Applications of diamond films and related materials. In Y. Tzeng, et al (Ed.), Materials *science monographs* (Vol. 73, p. 703). New York: Elsevier.
58. Evans, A. C., Franks, J., & Revell, P. J. (1991). *Surface and Coatings Technology, 47*, 662–667.
59. Grill, A. (1999). *Diamond and Related Materials, 8*, 428.
60. Gutensohn, K., Beythien, C., Bau, J., Fenner, T., Grewe, P., Koester, R., et al. (2000). *Thrombosis Research, 99*, 577–585.
61. Gutensohn, K., Beythien, C., Koester, R., Bau, J., Fenner, T., Grewe, P., et al. (2000). *Infusionstherapie und Transfusionmedizin, 27*(4), 200–206.
62. Zheng, C., Ran, J., Yin, G., & Lei, W. (1991). In Y. Tzeng, et al (Ed.), *Applications of diamond films and related materials, materials science monographs* (Vol. 73, p. 711). New York: Elsevier.
63. Jones, M. I., McColl, I. R., Grant, D. M., Parker, K. G., & Parker, T. L. (2000). *Journal of Biomedical Materials Research, 52*(2), 413–421.
64. Alanazi, A., Nojiri, C., Noguchi, T., et al. (2000). *ASAIO Journal, 46*(4), 440–443.

65. Alanazi, A., Nojiri, C., Noguchi, T., Ohgoe, Y., Matsuda, T., Hirakuri, K., et al. (2000). *Artificial Organs, 24*(8), 624–627.
66. Bangali, Z., & Shea, L. D. (2005). *MRS Bulletin, 30*(9), 659.
67. Morrison, M. L., Buchanan, R. A., Liaw, P. K., Berry, C. J., Brigmon, R. L., Riester, L., et al. (2006). Electrochemical and antimicrobial properties of diamond like carbon-metal composite films. *Diamond and Related Materials, 15*(1), 138–146.
68. Maizza, G., Saracco, G., & Abe, Y. (1999). Advances in science and technology. In Vincenzini, P. (Eds.), *9th Cimetec-World Forum on New Materials, Faenza* (pp. 75–82).
69. Dowling, D. P., Kola, P. V., Donnelly, K., Kelly, T. C., Brumitt, K., Lloyd, L., et al. (1997). *Diamond and Related Materials, 6*, 390–393.
70. Tiainen, V. M. (2001). *Diamond and Related Materials, 10*, 153–160.
71. Butter, R. S., & Lettington, A. H. (1995). DLC for biomedical applications (reviews). *Journal of Chemical Vapor Deposition, 3*, 182–192.
72. Higson, S. P. J., & Vadgama, P. M. (1995). *Analytica Chemica Acta, 300*, 77–83.
73. Higson, S. P. J., & Vadgama, P. M. (1995). *Biosensors and Bioelectronics, 10*(5), VIII.
74. Du, C., Su, X. W., Cui, F. Z., & Zhu, X. D. (1998). *Biomaterials, 19*, 651–658.
75. Cui, F. Z., & Li, D. J. (2000). *Surface Coatings Technology, 131*, 481–487.
76. Ivanov-Omskii, V. I., Panina, L. K., & Yastrebov, S. G. (2000). *Carbon, 38*, 495–499.
77. Dyuzhev, G. A., Ivanov-Omskii, V. I., Kuznetsova, E. K., Rumyantsev, V. D., et al (1996). *Journal of Molecular Materials, 8*, 103–106.
78. Ivanov-Omskii, V. I., Tolmatchev, A. V., & Yastrebov, S. G. (1996). *Philosophical Magazine Part B, 73*(4), 715–722.
79. Andrade, J. D. (Ed.). (1988). *Surface and interfacial aspect of biomedical polymers. Protein Adsorption* (Vol. 2). New York: Plenum.
80. William, D. F. (1985). Physiological and microbiological corrosion CRC Crit (review). *Biocompatibility, 1*, 1–30.
81. William, D. F. (Ed.) (1987). *Definitions in biomaterials*. Amsterdam: Elsevier.
82. William, D. F. (1981). *Systemic aspects of biocompatibility* (Vol. 1–2). Boca Raton: CRC Press.
83. Martini, F. C. (2001). *Fundamentals of anatomy and physiology* (5th ed.). New Jersey, USA: Prentice Hall.
84. Hoffman, A. S. (1982). *Advances in Chemistry Series, 199*, 3.
85. Vroman, L. (1977). *Annals of the New York Academy of Science, 283*, 65 (L. Vroman & E. F. Leonard (Eds.)).
86. National Heart, Lung, and Blood Institute (NHBLI), (1980). *Clinical Guidelines for Biocompatibility*. Washington D.C. USA.
87. Neumann, A. W., Absolom, D. R., Francis, D. W., Omenyi, S. N., Spelt, J. K., Policova, Z., et al. (1983). *Annals of the New York Academy of Sciences, 416*, 276.
88. Srinivasan, S., & Sawyer, P. N. (1970). *Journal of Colloid and Interface Science, 32*(3), 456.
89. Sawyer, P. N., & Pate, J. W. (1953). *American Journal of Physiology, 175*, 113.
90. Sawyer, P. N., & Srinavasan, S. (1967). *American Journal of Physiology, 114*, 42.
91. Srinivasan, S., & Sawyer, P. N. (1969). *JAAMI, 3*, 116.
92. Martin, J. G., Afshar, A., Kaplitt, M. J., Chopra, P. S., Srinivasan, S., & Sawyer, P. N. (1968). Implantation studies with some non-metallic prostheses. *Transaction of American Society for Artificial Internal Organ, 14*, 78.
93. Wilcox, C. D., Dove, S. B. McDavid, W. D., & Greer, D. B., Imagetool. http://ddsdx.uthscsa.edu/dig/itdesc
94. Baier, R. E. (1972). *The Bulletin of the New York Academy of Medicine, 48*, 273.
95. Baier, R. E., Loeb, G. I., & Wallace, G. T. (1971). *Federation Proceedings, 30*, 1523–1538.
96. Chen, J. Y., Leng, Y. X., Tian, X. B., Wang, L. P., Huang, N., Chu, P. K., et al. (2002). Antithrombogenic investigation of surface energy and optical bandgap and hemocompatibility mechanism of Ti (Ta + 5)O_2 thin films. *Biomaterials, 23*, 2545.
97. Curtis, A. (2004). Tutorial on the biology of nanotopography. *IEEE Transactions on Nanobioscience, 3*(4), 293–295.

98. Matsuda, T., & Kurumatani, H. (1990). Surface induced in vitro angiogenesis: Surface property is a determinant of angio-genesis. *ASAIO Transactions, 36*, M565–M568.
99. Hubbell, J. A., Massia, S. P., & Drumheller, P. D. (1992). Surface-grafted cell-binding peptides in tissue engineering of vascular graft. *Annals of the New York Academy of Sciences, 665*, 253–258.
100. Goodman, S. L., Lelah, M. D., Lambrecht, L. K., Cooper, S. L., & Albrecht, R. M. (1984). *Scanning Electron Microscopy, 1*, 279.
101. Dowling, D. P., Kola, P. V., Donnelly, K., Kelly, T. C., Brumitt, K., Lloyd, L., et al. (1997). *Diamond and Related Materials, 6*, 390–393.
102. Allen, M., Law, F. C., & Rushton, N. (1994). *Clinical Materials, 17*, p1–p10.
103. Hauert, R., Muller, U., Francz, G., Birchler, F., Schroeder, A., Mayer, J., et al. (1997). *Thin Solid Films, 308–309*, 191–194.
104. Allen, M., Butter, R., Chandra, L., Lettington, A., & Rushton, N. (1995). *Biomedical Materials and Engineering, 5*(3), 151–159.
105. McColl, I. R., Grant, D. M., Green, S. M., et al. (1993). *Diamond and Related Materials, 3*, 83.
106. Parker, T. L., Parker, K. L., McColl, I. R., Grant, D. M., & Wood, J. V. (1993). *Diamond and Related Materials, 93*, 118.
107. Parker, T. L., Parker, K. L., McColl, I. R., Grant, D. M., & Wood, J. V. (1994). *Diamond and Related Materials, 3*, 1120–1123.
108. Thomson, L. A., Law, F. C., Rushton, N., & Franks, J. (1991). *Biomaterials, 12*, 37–40.
109. Allen, M., Myer, B., & Rushton, N. J. (2001). *Journal of Biomedical Materials Research, 58* (3), 319–328.
110. Schroeder, A., Francz, G., Bruinink, A., Hauert, R., Mayer, J., & Wintermantel, E. (2000). *Biomaterials, 21*, 449–456.
111. Lu, L., Jones, M. W., & Wu, R. L. C. (1993). *Biomedical Materials and Engineering, 3*, 223.
112. Evans, A. C., Franks, J., & Revell, P. J. (1991). *Surface and Coatings Technology, 47*, 662–667.
113. Ames, B. N., McCann, J., & Yamasaki, E. (1975). *Mutation Research, 31*, 347–367.
114. Bruck, S. D. (1977). *Biomaterials, Medical Devices, and Artificial Organs, 5*(1).
115. McHargue, C. J. (1991). In: Y. Tzeng et al. (Eds.), *Application of diamond films and related materials, materials science monographs* (p. 113). New York: Elsevier.
116. Devlin, D., et al. (1997). In: B. Simons (Ed.), *Proceedings of the ASME International Mechanical Engineering Congress and Exposition* (p. 265), Fairfield, NJ, USA: Bioengineering Division.
117. Gordon, J. L. (1986). In J. P. Cazenave, J. A. Davies, M. D. Kazatchkine, van Aken, W. G. (Eds.), *Blood-surface interactions: Biological principles underlying hemocompatibility with artificial materials* (p. 5). Amsterdam: Elsevier Science Publishers (Biomedical Division).
118. Moncada, S., & Vane, J. R. (1982). The role of prostaglandins in platelet-vessel wall interactions. In H. L. Nossel & H. J. Vogel (Eds.), *Pathobiology of endothelial cells* (pp. 253–285). New York: Academic Press.
119. Gimbrone, M. A., Jr. (1986). In M. A. Gimbrone Jr. (Ed.), *Vascular endothelium in hemostasis and thrombosis* (pp.1–13). Edinburgh: Churchill Livingstone.
120. Gimbrone, M. A, Jr. (1987). *Annals of New York Acad. Sci., 516*, 5–11.
121. Chan, T. K., & Chan, V. (1981). Antithrombin III, the major modulator of intravascular coagulation is synthesised by human endothelial cells. *Thrombosis and Haemostasis, 46* (1981), 504–506.
122. Busch, C., Ljungman, C., Heldin, C.-M., Waskson, E., & Obrink, B. (1979). Surface properties of cultured endothelial cells. *Haemostasis, 8*(1979), 142–148.
123. Jaffe, E. A. (1982). Synthesis of factor VIII by endothelial cells. *Annals of New York Academy of Sciences, 401*(1982), 163–170.
124. Mosher, D. F., Doyle, M. J., & Jaffe, E. A. (1982). Secretion and synthesis of thrombospondin by cultured human endothelial cells. *Journal of Cell Biology, 93*(1982), 343.
125. Folkman, J., & Haudenschild, C. (1980). Angiogenesis in vitro. *Nature, 288*, 551–556.

126. Tonnesen, M. G., Smedly, L. A., & Henson, P. M. (1984). *The Journal of Clinical Investigation, 74*, 1581–1592.
127. Kubota, Y., Kleinman, H. K., Martin, G. R., & Lawley, T. J. (1988). *Journal of Cell Biology, 107*, 1589–1598.
128. Pauli, B., & Lee, C. (1988). *Laboratory Investigation, 58*, 379–387.
129. Picker, L. J., Nakache, M., & Butcher, E. C. (1989). Monoclonal antibodies to human lymphocyte homing receptors define a novel class of adhesion molecules on diverse cell types. *Journal of Cell Biology, 109*(2), 927–937.
130. Pober, J. (1988). *American Journal of Pathology, 133*, 426–433.
131. Berg, E. L., Goldstein, L. A., Jutila, M. A., Nakache, M., Picker, L. J., Streeter, P. R., et al. (1989). *Immunological Reviews, 108*, 1–18.
132. Rice, G. E., & Bevilacqua, M. P. (1989). *Science, 246*, 1303–1306.
133. Springer, T. (1990). *Nature, 346*, 425–433.
134. Hynes, R. (1992). *Cell, 69*, 11–25.
135. Folkman, J., Haudenschild, C., & Zetter, B. R. (1979). *Proceedings of the National Academy of Sciences of the United States of America, 76*, 5217.
136. Keegan, A., Hill, C., Kumar, S., Phillips, P., Schof, A., & Weiss, J. (1982). *Journal of Cell Science, 55*, 261.
137. Charo, I., Karasek, M. A., Davison, P. M., & Goldstein, I. M. (1984). *Journal of Clinical Investigation, 74*, 914.
138. Gerritsen, M. E. (1987). *Biochemical Pharmacology, 36*, 2701–2711.
139. Fujimoto, T., & Singer, S. J. (1988). *Journal of Histochemistry and Cytochemistry, 36*, 1309–1317.
140. Kubota, Y., Kleinman, H. K., Martin, G. R., & Lawley, T. J. (1988). *Journal of Cell Biology, 107*, 1589.
141. Ades, E. W., Candal, F., Swerlick, J., George, R. A., Summers Susan, V. G., Bosse, D. C., et al. (1992). *Journal of Investigative Dermatology, 99*, 683–690.
142. Van Wachem, P. B., Beugeling, T., Feijen, J., Bantjes, A., Detmers, J. P., & van Aken, W. G. (1985). *Biomaterials, 6*, 403–408.
143. Van Wachem, P. B., Schakenraad, J. M., Feijen, J., Beugeling, T., van Aken, W. G., Blaauw, E. H., et al. (1989). *Biomaterials, 10*, 532–539.
144. Kaukonen, M., Nieminen, R. M., Poykko, S., & Settsonen, A. (1999). Nitrogen doping of amorphous carbon surfaces. *Physical Review Letters, 83*(25), 5346–5349.
145. Ganong, W. F. (1995). *Ganong's review of medical physiology* (17th ed.). New York: Appleton & Lang.
146. Chen, J. Y., Wang, L. P., Fu, K. Y., Huang, N., Leng, Y., Leng, Y. X., et al. (2002). *Surface and Coatings Technology, 156*, 289–294.
147. Krishnan, L. K., Varghese, N., Muraleedharan, C.V., Bhuvaneshwar, G.S., Derangere, F., Sampeur, Y., et al. (2002). *Biomolecular Engineering, 1–3*.
148. Gutensohn, K., Beythien, C., Bau, J., Fenner, T., Grewe, P., Koester, R., et al. (2000). *Thrombosis Research, 99*, 577–585.
149. Ogwu, A. A., Lamberton, R. W., McLaughlin, J. A., & Maguire, P. D. (1999). *Journal of Physics Part D. Applied Physics, 32*, 981.
150. Jiu, J. T., Wang, H., Cao, C. B., & Zhu, H. S. (1999). *Journal Materials Science, 34*, 5205–5209.
151. Dementjev, A. P., Petukhov, M. N., & Baranov, A. M. (1998). *Diamond and Related Materials, 7*, 1534–1538.
152. Dementjev, A. P., & Petukhov, M. N. (1997). *Diamond and Related Materials, 6*, 486.
153. Grill, A., Meyerson, B., Patel, V., Reimer, J. A., & Petrich, M. A. (1987). *Journal of Applied Physics, 61*, 2874.
154. Miyake, S., Kaneko, R., Kikuya, Y., & Sugimoto, I. (1991). *Transactions of the ASME Journal of Tribology, 113*, 384.
155. Baker, M. A., & Hammer, P. (1997). *Surface and Interface Analysis, 25*, 629–642.

156. Demichelis, F., Pirri, C. F., & Tagliaferro, A. (1992). *Materials Science and Engineering B, 11*, 313–316.
157. Li, D. J., Cui, F. Z., Gu, H. Q., & Adhesion, J. (1999). *Sci. Technol., 13*, 169.
158. Linder, S., Pinkowski, W., & Aepfelbacher, M. (2002). *Biomaterials, 23*, 767–773.
159. Goodman, S. L., Cooper, S. L., & Albrecht, R. M. (1991). *Journal of Biomaterials Science, Polymer Edition, 2*(2), 147–159.
160. Tangen, D., Berman, H. J., & Marfey, P. (1971). *Thrombosis et Diathesis Haemorrhagica, 25*, 268.
161. Schakenraad, J. M., Busscher, H. J., Wildevuur, C. R. H., & Arends, J. (1988). *Cell Biophysics, 13*, 75.
162. Goodman, S. L., Cooper, S. L., & Albrecht, R. M. (1985). In Y. Nose, C. Kjellstrand, & P. Ivanovich (Eds.) *Progress in artificial organs* (pp. 1050–1055). Cleveland, OH: ISAO Press.
163. Schakenraad, J. M., Busscher, H. J., Wildevuur, C. R. H., & Arends, J. (1986). *Journal of Biomedical Materials Research, 20*, 773.
164. Grinnell, F. (1987). *Annals of the New York Academy of Sciences, 516*, 280.
165. Grinnell, F. (1986). *Journal of Cell Biology, 103*, 2697.
166. Feuerstein, I. A. (1987). *Annals of the New York Academy of Sciences, 516*, 484
167. Park, K., & Park, H. (1989). *Scanning Microscopy, 3*(Suppl), 137.
168. Pitt, W. G., Spiegelberg, S. H., & Cooper, S. L. (1987). *Transactions of the Society for Biomaterials, 10*, 59.
169. Park, K., Mosher, D. F., & Cooper, S. L. (1985). *Journal of Biomedical Materials Research, 20*, 589.
170. Brash, J. L. (1985). *Macromolecular Chemistry, 9*(Suppl), 69.
171. Lambrecht, L. K., Young, B. R., Stafford, R. E., Park, K., Albrecht, R. M., Mosher, D. F., et al. (1986). *Thrombosis Research, 41*, 99.
172. Wildner, O., Lipkow, T., & Knop, J. (1992). Increased expression of ICAM-1, E-selectin and V-CAM-1 by cultured endothelial cells upon exposure to haptens. *Experimental Dermatology, 1*, 191.
173. Klein, C. L., Nieder, P., Wagner, M., Kohler, H., Bittinger, F., Kirkpatrick, C. J., et al. (1994). *Journal of Pathophysiology, 5*, 798–807.
174. Albelda, S., Smith, C., & Ward, P. (1994). Adhesion molecules and inflammatory injury. *FASEB Journal, 8*, 504–512.
175. Gerdes, J., Schwab, U., Lemke, H., & Stein, H. (1983). Production of a mouse monoclonal antibody reactive with a human nuclear antigen associated with cell proliferation. *International Journal of Cancer, 31*(1), 13–20.
176. Thomas, W. E. (1999). *Brain Research Reviews, 31*(1), 42–57.
177. http://users.ahsc.arizona.edu/davis/bbbpericytes.htm
178. Chen, X., & Zuckerman, S. T. (2005). Weiyuan John Kao. Intracellular protein phosphorylation in adherent U937 monocytes mediated by various culture conditions and fibronectin-derived surface ligands. *Biomaterials, 26*(8), 873–882.
179. Fournier, J. A., Calabuig, J., Merchán, A., Augé, J. M., Melgares, R., Colman, T., et al. (2001). *Revista Espanola de Cardiologia, 54*(5), 567–572.
180. De Scheerder, I., Szilard, M., Yanming, H., Ping, X. B., Verbeken, E., Neerinck, D., et al. (2000). *The Journal of Invasive Cardiology, 12*(8), 389–394.
181. Tran, H. S., Puc, M. M., Hewitt, C. W., Soll, D. B., Marra, S. W., Simonetti, V. A., et al. (1999). *Journal of Investigative Surgery: The Official Journal of the Academy of Surgical Research, 12*(3), 133–140.
182. http://www.tiem.utk.edu/~gross/bioed/webmodules/cellattach.htm
183. Izzard, C. S., & Lochner, L. R. (1976). Cell-to-substrate contacts in living fibroblasts: An interference reflection study with an evaluation of the technique. *Journal of Cell Science, 21*, 129.
184. Bereiter-Hahn, J., Fox, C. H., & Thorell, B. (1979). Quantitative reflection contrast microscopy of living cells. *Journal of Cell Biology, 82*, 767–779.